(including HE, PAS and Trichrome stains). Using Dako Autostainer, representative renal sections were immunohistochemically stained for CD3 and CD68 to identify T lymphocytes and monocytes, respectively. Results: Statistically, cases with grade Ib or higher rejection (n = 11) had a significantly higher percentage of CD68 positive monocytes (66.9 ± 6.4 %∗) than the cases with Ia rejection (n = 11, 40.0 ± 5.2 %, ∗p<0.05 vs Ia rejection, using student t test), regardless of the status of Campath-1H induction.   Conversely, the percent of CD3 positive T lymphocytes from the cases with grade Ib or higher rejection was significantly lower (27.2 ± 7.1 %∗), when compared to the cases with Ia rejection (56.4 ± 5.8 %). Furthermore cases of acute rejection, following Campath-1H induction, appear to demonstrate a "pure form" of monocytic acute rejection, whereas monocytes were mixed with many other types of inflammatory cells in the cases of acute rejection in the absence of Campath-1H induction. In addition with Campath-1H induction, the cases of monocyte-predominant acute rejection were found to uniformly exhibit a good response to corticosteroid treatment. Conclusion: Our findings suggest that monocyte-predominate acute rejection is often a severe form of acute rejection either with or without Campath-1H induction, although monocytic acute rejection, following Campath-1H induction, appears to be more obvious on the CD68 stained section.

Liver & Pancreas

1258   Histologic Abnormalities Are Common in Protocol Liver Allograft Biopsies from Patients with Normal Liver Function Tests
SC Abraham, AM Krasinskas. Mayo Clinic, Rochester, MN; University of Pittsburgh, Pittsburgh, PA.
Background: The utility of protocol liver allograft biopsies remains controversial, particularly in patients with normal liver function tests (LFTs). However, evaluation of these biopsies provides an opportunity to examine the types and severity of liver disease that occur in livers with normal clinical and laboratory function.
Design: We studied 165 protocol allograft biopsies taken from 100 liver transplant patients at the time of normal LFTs at 3-8 mos (n=36), 1 yr (n=52), 2-3 yrs (n=54), and 4-5 yrs (n=23). Biopsies were classified as normal, minimal/nonspecific changes (e.g., nonaggressive portal or lobular inflammation, steatosis <10%), mild steatosis (10-33%), fatty liver disease (steatosis >33% or active steatohepatitis), recurrent primary liver disease, and transplant-related disease (portal-based rejection or central venulitis, an inflammatory pattern encompassing perivenular hepatocyte dropout, mononuclear inflammation, and pigment-laden macrophages).
Results: In these 100 patients, 165 (42%) of a total of 394 protocol biopsies were performed at the time of normal LFTs. 121 (73%) biopsies were normal or showed minimal changes. 44 (27%) showed histologic abnormalities that included mild steatosis (n=9), fatty liver disease (n=10; steatosis range 25-50%, grade 1/3 steatohepatitis in 7, stage 1/4 fibrosis in 1), recurrent primary biliary cirrhosis (n=8; all stage 1/4), recurrent hepatitis C (n=6; grade 0/4 in 1, grade 1/4 in 5, stage 0/4 in 4, stage 1/4 in 1, and stage 2/4 in 1), recurrent sarcoidosis (n=1), Ito cell hyperplasia (n=3), central venulitis (n=10; with mild zone 3 fibrosis or central vein obliteration in 5 and central-portal bridging fibrosis in 1), and mild acute portal rejection (n=2). We judged the histologic changes to be of clinical significance in 19 (11.5%) cases.
Conclusions: Despite normal clinical and laboratory liver function, a significant fraction of protocol allograft biopsies show histologic (27%) and clinically significant (11.5%) abnormalities. Common liver diseases that occur in the absence of clinical or laboratory dysfunction include steatohepatitic liver disease, low-grade/low-stage hepatitis C and primary biliary cirrhosis, and central venulitis (including cases with early or advanced fibrosis). These results 1) support the performance of protocol biopsies to assess the status of the allograft, and 2) provide insight into the types and severity of liver disease that can smolder in transplant (and probably also native) livers with apparent normal function.

1259   Will the Real Mucinous Carcinoma of the Pancreas Please Stand Up?: A Reappraisal of the Terminology, Classification and Differential Diagnosis of "Mucinous" Carcinomas in the Ampullo-Pancreatobiliary Region
VN Adsay, F Khanani, O Basturk, A Andea, JD Cheng. Wayne State University, MI.
Background: The definition of "mucinous carcinoma" varies from organ to organ. In the pancreas, most tumor types are of ductal nature, and thereby form mucin. This study investigates the types of tumors of the ampullo-pancreatobiliary region that are referred to as mucinous by pathologists, and attempts to formulate an approach for a more accurate conceptualization of these neoplasms.
Design: Pathology material from 65 pancreatic specimens with 1° or 2° carcinomas, which had been designated as "mucinous" in a database of 908 cases, was reviewed. The cases were classified by an algorithmic approach based on the distribution of mucin and presence or absence of invasion (inv). Each case was designated a specific clinicopathologic entity according to current concepts.
Results: I. Inv ca with intracellular and/or intraluminal mucin (n=33). A. Without a pre-inv mass. 1. Inv ductal. (n=11). 2. Inv ductal: morphologic variants (8 foamy gland, and 2 signet ring). 3. CBD ca (n=2). 4. Secondary from GI-tract (n=3), and ovary (n=1). *These were all highly aggressive neoplasia.* **B. With a pre-invasive mass.** 5. Inv ductal associated with IPMN (n=3), or MCN (=2). 6. Intestinal type of ampulla/duodenum (n=1) with adenoma. *These were relatively less aggressive.* **II. Inv ca with stromal mucin deposition (n=25). A. Cells confined to (floating within) mucin** 7. Colloid ca (n=8), 4 with IPMNs. *These had indolent behavior.* **B. Non-mucinous type inv present.** 8. Mixed mucinous (n=7): Colloid admixed with intestinal type. *This group had moderately aggressive behavior.* 9. Mucinous ductal (n=10):Usual ductal ca with abundant stromal mucin deposition. *These were highly*

aggressive. **III. Intraductal and cystic (non-invasive) ca with intraluminal (and cytoplasmic) mucin (n=7). A. Without ovarian stroma.** 10. IPM ca (in-situ), n=5: *4 intestinal and 1 pancreatobiliary type papillae.* **B. With ovarian stroma.** 11. Mucinous non-invasive cystadenoca (in-situ), n=2. *These were indolent, although 1 from each behaved aggressively.*
Conclusions: In the pancreas, the term "mucinous carcinoma" has been applied to a plethora of neoplastic entities, ranging from in-situ to inv to secondary tumors. Pancreatic carcinomas with mucin formation should be classified as one of the specific entities described above, as each has different clinicopathologic characteristics and outcomes. An algorithmic approach based on the distribution of mucin and invasiveness of the tumor is useful in the differential diagnosis.

1260   Ampullary Carcinoma: Role of DNA Mismatch Repair Gene Defects in Pathogenesis
NP Agaram, J Shia, DS Klimstra. Memorial Sloan-Kettering Cancer Center, New York, NY.
Background: While microsatellite instability (MSI) secondary to DNA mismatch repair (MMR) gene abnormality is known to be the underlying molecular defect in about 15% colorectal carcinomas, the frequency and significance of MSI in ampullary carcinomas remain to be defined. We and others have previously shown that immunohistochemistry (IHC) using antibodies against the MLH1 and MSH2 proteins is a simple and specific method for detecting MMR defects, and in the case of colorectal carcinoma, certain morphological features, such as tumor infiltrating lymphocytes (TIL), poor differentiation, and medullary type and mucinous histology, also carry a significant predictive value in identifying MMR abnormalities. The purpose of this study was therefore to evaluate the frequency of MMR abnormality in ampullary carcinomas using IHC, and to investigate the presence or absence of any association of morphological features with MMR defects in these tumors.
Design: Pathologic review and IHC with anti-MLH1 (clone G168-728, PharMingen) and anti-MSH2(clone FE11, Oncogene Research Products) antibodies were performed on a series of 60 ampullary carcinomas treated at Memorial Sloan-Kettering Cancer Center from 1986 to 1994. Morphological features analyzed included tumor differentiation, histological subtypes (medullary, mucinous and signet ring cell), and number of TILs per 10 high power field.
Results: All 60 tumors were adenocarcinomas, 45 moderately differentiated, 8 poorly differentiated and 7 mucinous. No tumors showed typical medullary carcinoma morphology. Focal presence of signet ring cells was noted in only 1 tumor. TILs were noted in 39 tumors, ranging from 1/10 hpf to 62/10 hpf. All 54 cases that were tested by IHC showed positive staining for MSH2, and 53 of 54 showed positive staining for MLH1. Of the positive cases, the staining intensity was scored as weak for MSH2 in 5 tumors and for MLH1 in 18 tumors, whereas the remaining positive cases showed moderate to strong intensity. No significant correlation was detected between any of the morphologic features and the staining intensity. The one MLH1-negative tumor was a moderately differentiated adenocarcinoma with no apparent TILs.
Conclusions: DNA mismatch repair gene defect does not appear to play a significant role in the pathogenesis of ampullary carcinoma, and morphological features that are shown to be associated with microsatellite instability in colorectal tumors do not carry the same implication in ampullary carcinomas.

1261   p53, Ki-67, VEGF and EGFR Expression in Liver Transplant Patients with Hepatocellular Carcinoma (HCC) with and without Subsequent HCC Recurrence
V Alagiozian-Angelova, S Cotler, D Mehta, A Kajdacsy-Balla, G Guzman. Univ. of Illinois at Chicago, Chicago, IL.
Background: Recurrence is the main factor influencing the prognosis of HCC. The aim of this study is to determine the expression of p53, Ki-67, VEGF, and EGFR in explanted livers with HCC and correlate the expression pattern with tumor recurrence.
Design: The study population consisted of 23 liver transplant recipients at UICMC who had HCC of the liver explant. The subjects were divided into two groups: 1. Non-recurrent: HCC patients with at least 1 year recurrence-free survival (n=14), and 2. Recurrent: HCC patients with known recurrence within the first year post-transplant (n=9). We performed standard immunohistochemical staining for p53, Ki-67, VEGF and EGFR on the cirrhotic liver and the tumor. Results were independently analyzed by two observers. Nuclear staining for p53 was interpreted as positive. Ki-67 was interpreted as percent positive nuclear stain per 100 cells. A diffuse cytoplasmic staining for VEGF was interpreted as positive. A membranous staining for EGFR was interpreted as positive. For both VEGF and EGFR, the percentage of positive cells were multiplied by the intensity of staining (grade 0=no staining to 3+=strongest intensity of staining) to provide an index.
Results: While p53 expression in the tumor of the non-recurrent vs. recurrent group did not show any significant difference (χ^2 test), a negative p53 in the cirrhotic liver correlated significantly with absence of HCC recurrence (p≤0.05 χ^2 test). High percentage of Ki-67 expression (>10%) correlated significantly with HCC recurrence when observed both in the tumor (p≤0.05 χ^2 test) or the cirrhotic liver (p≤0.025 χ^2 test). A high VEGF index in the cirrhotic liver was not seen in any of the cases that recurred. While VEGF index was stronger in the tumor compared to the cirrhotic liver in the recurrent group (p≤0.008 Wilcoxon paired test), there was no difference in the VEGF index of the cirrhotic liver compared to tumor in the non-recurrent group (p≤0.25 Wilcoxon paired test). EGFR indices were higher in the tumor compared to the cirrhotic liver in both the recurrent (p≤ 0.008 Wilcoxon matched-pairs signed-ranks test) and non-recurrent group (p≤0.014 Wilcoxon matched-pairs signed-ranks test).

Conclusions: Our results suggest that P-53, Ki-67, VEGF and EGFR expression in adjacent cirrhotic livers and HCC may provide a means to identify patients who are high risk for recurrence and therefore may need more aggressive antineoplastic therapy at the initial diagnosis.

1262 Intestinal and Oncocytic Variants of Pancreatic Intraepithelial Neoplasia (PanIN): A Morphologic and Immunohistochemical Study
J Albores-Saavedra, J Wu, T Crook, RH Amirkhan, L Jones, RH Hruban. LSUHSC, Shreveport, LA; Dallas Veterans Affairs Medical Center, Dallas, TX; The Johns Hopkins Medical Institutions, Baltimore, MD.
Background: PanIN is currently considered the precursor of the ordinary invasive ductal carcinoma of the pancreas. Data in favor of this conclusion include: a) high grade Pan-IN is found in up to 60% of pancreata harboring invasive ductal carcinoma; b) Both PanIN and invasive ductal carcinoma share many genetic alterations; c) The cytologic features of high grade PanIN lesions are similar to those of invasive ductal carcinoma; d) PanIN, like invasive ductal carcinoma, expresses MUC-1 and is MUC-2 negative. PanIN lesions with intestinal or oncocytic phenotype have not been described.
Design: Two pancreatic mucinous carcinomas and three intraductal papillary oncocytic carcinomas (IPOC) that showed foci of stromal invasion were examined histologically and by immunohistochemistry. Immunostains for MUC-1, MUC-2, MIB-1, P53 and DPC4 were also evaluated.
Results: The pancreas adjacent to the mucinous carcinomas showed small ducts (< 5mm) with PanIN lesions. The ducts were lined by pseudostratified columnar cells with intestinal phenotype and variable degrees of dysplasia. These PanIN lesions expressed both membranous and cytoplasmic MUC-2, but were MUC-1 and P53 negative. Approximately 35% of PanIN intestinal cells labeled with MIB-1 and nearly all expressed DPC4. The pancreas adjacent to the three IOPCs showed small ducts with Pan-IN lesions that vary from conventional PanIN-1 to PanIN-3 with oncocytic features. Some small ducts were lined by dysplastic goblet cells. Oncocytic PanIN lesions labeled focally with MUC-2 and MUC-1. They expressed DPC4, were P53 negative and showed a low MIB-1 labeling index (< 5% of cells). Similar MUC-2 and MUC-1 reactivities were observed in the IOPCs.
Conclusions: PanIN-3 lesions cytologically similar to colonic tubular adenomas and with an immunophenotype (MUC-2 positive and MUC-1 negative) different from that of conventional PanIN were seen in association with pancreatic mucinous carcinomas that arose in the tail of the pancreas of two adult men. PanIN oncocytic lesions associated with IOPCs showed an immunophenotype (focal co-expression of MUC-2 and MUC-1 mucin) different from that of conventional PanIN. We believe that these intestinal and oncocytic PanIN lesions are unusual but distinctive variants of PanIN, which may represent cancer precursors.

1263 Papillary Carcinomas of the Gallbladder: Analysis of Non-Invasive and Invasive Types
J Albores-Saavedra, M Tuck, KS Carrick, DE Henson. LSUHSC, Shreveport, LA; UT Southwestern Medical Center, Dallas, TX; George Washington University Cancer Institute, Washington, DC.
Background: Although papillary carcinomas have been recognized as distinct morphological variants of gallbladder neoplasms they have been categorized as a single group despite the recognition of non-invasive and invasive types. As a result the biologic behavior of each type is unknown.
Design: The clinical and morphologic features of 16 non-invasive papillary carcinomas (> 1 cm) of the gallbladder were analyzed and their clinical behavior compared with that of 370 invasive papillary carcinomas recorded in the Survey Epidemiology and End Results (SEER) Program of the National Cancer Institute from 1973 to 2001. Hematoxylin-eosin stained sections were available for review in the 16 non-invasive papillary carcinomas. The number of slides examined varied form 3 to 16 with an average of 7.
Results: The 16 patients with non-invasive papillary carcinomas included 11 women and 5 men from 34 to 83 years (mean age 61 years). Thirteen patients had cholelithiasis. Laparoscopic cholecystectomy was performed on 12 patients and open cholecystectomy in 4. The tumors measured from 1.3 to 8.6 cm and were well to moderately differentiated. Fourteen non-invasive papillary carcinomas showed biliary phenotype and two intestinal phenotype. Follow-up was obtained in 11 patients, 6 were asymptomatic, 5 to 11 years after surgery; two were symptom free, 9 months to 4 years following cholecystectomy and 3 died of unrelated causes, 2 to 3 years after surgery. There were 370 cases of invasive papillary carcinomas recorded in SEER. The ten year relative survival rate for 225 patients with papillary carcinomas confined to the gallbladder wall was 50%, while the ten year relative survival rate for 83 patients with papillary carcinomas that had spread to the lymph nodes was 10 %. The stage for the remaining 62 cases was unknown.
Conclusions: Non-invasive papillary carcinomas of the gallbladder, regardless of size, cell phenotype and degree of differentiation do not metastasize and a simple cholecystectomy appears to be a curative procedure. In contrast, invasive papillary carcinomas metastasize and are associated with poor prognosis (ten year relative survival rate for tumors confined to the wall was 50 %, while the ten year relative survival rate for tumors with lymph node metastasis was 10 %). The separation of papillary carcinomas into non-invasive and invasive types is fully justified.

1264 Immunohistochemistry as a Helpful Adjunct in the Differential Diagnosis of Intraabdominal Carcinomatosis Originating from the Pancreas Versus Ovary
R Ali-Fehmi, O Basturk, JD Cheng, I Khalifeh, S Bandyopadhyay, E Silva, H Nassar, NV Adsay. Wayne State University, MI; MD Anderson Cancer Center, TX.
Background: Ovarian surface-epithelial (OV) and pancreatobiliary (PB) carcinomas are similar in their propensity for abdominal carcinomatosis. Our recent study disclosed the high number of misdiagnoses in distinguishing these tumors on biopsies from the omentum or peritoneum. Although the application of morphologic criteria established in our previous study appeared to improve the diagnostic accuracy, it still needs to be complemented by other diagnostic studies.
Design: Immunohistochemical stains for WT1, CDX2, MUC5AC, CK7 and CK20 were performed on confirmed examples of OV (n=21) and PB (n=21) adenocarcinomas metastatic to omentum or peritoneum, in order to determine their applicability in distinguishing these two tumor types in these locations.
Results: The percentage of cases that showed labeling with these markers is shown in the table.
In addition to the individual markers, when they were analyzed in combination, WT1-/MUC5AC+ phenotype had 100% specificity for PB *while* WT1+/MUC5AC- had 96% specificity for OV.
Conclusions: Immunohistochemistry can be a valuable adjunct to the morphologic criteria we recently identified as useful in distinguishing OV from PB carcinomas in omental or peritoneal biopsies, which often proves to be a challenging differential diagnosis. While expression of WT1 is highly in favor of OV over PB, the positivity of MUC5AC would point towards PB. These two markers are highly specific especially if used in combination. If present, CK20, and less reliably, CDX2 would also be more compatible with a diagnosis of PB. Based on these findings, a panel composed of WT1, MUC5AC and CK20 would be advisable in this differential diagnosis.

	WT1	MUC5AC	CK20	CDX2	CK7
PB	10	76	33	24	100
OV	90	10	0	5	95

1265 Adenocarcinoma Progression Analysis in Pancreatic Intraductal Papillary Mucinous Neoplasms Using Tissue Microarrays
A Andea, L Tang, A Suriawinata, A Hoos, C Ferrone, J Metcalf, D Klimstra. Medical University of South Carolina, Charleston, SC; Memorial Sloan-Kettering Cancer Center, New York, NY.
Background: Intraductal papillary mucinous neoplasms (IPMN) appear to progress from IPM adenoma (IPMA) to borderline IPMN (IPMB) to carcinoma in situ (IPMC) and eventually to invasive carcinoma, either tubular (TA) or colloid (CC) types. The genetic events associated with IPMN progression have not been entirely established but are thought to differ from those involved in the development of DA from PanIN lesions.
Design: We analyzed by immunohistochemistry the expression pattern of 13 proteins implicated in pancreatic carcinogenesis in IMPN lesions of different grades as well as in IPMNs associated with invasive carcinoma (TA and CC) and compared these to the expression profile of conventional DAs in an attempt to identify molecular markers associated with progression and invasive phenotype in IPMNs. The markers analyzed were epithelial apomucins (MUC1, MUC2, MUC5, MUC6), tumor suppressor genes (p53, DPC4, CDX-2), inhibitors of apoptosis (BCL2, survivin), cell adhesion proteins (mesothelin, galectin-3), maspin and B72.3. Three tissue microarray blocks were constructed containing IPMN lesions of various grades, some with associated TA and CC as well as conventional DA lesions (343 cores).
Results: There was a gradual increase in the expression of MUC1, MUC2, MUC5, maspin, mesothelin, B72.3, p53, survivin and CDX2 along the adenoma-carcinoma axis. This was associated with a progressive decrease in staining for MUC6, DPC4 and BCL2. Some abnormalities appeared to occur early, at the IPMA stage (e.g. MUC5 expression) whereas others manifested at IPMC or TA level (e.g. expression of MUC1, MUC2, mesothelin, and p53 or loss of DPC4 and MUC6). A significant difference was found between non-invasive IPMCs (increased expression of MUC2; decreased expression of MUC1, MUC6, mesothelin, and p53; retained DPC4) and IPMCs associated with invasive TA (increased expression of MUC1, MUC6, and mesothelin; decreased expression of MUC2; some gain in p53 expression and loss of DPC4), the latter being similar to the expression profile of conventional DA.
Conclusions: The results provide further evidence of an adenoma-carcinoma progression pathway in IPMNs. Moreover, the phenotypic difference between IPMC associated with TA (that has a profile similar to conventional DA in the non-invasive component) and non-invasive IPMC supports the existence of 2 separate pathways of carcinogenesis in IPMNs and could provide a tool to predict their behavior.

1266 Preneoplasia and Neoplasia in Hepatitis C Cirrhosis-A Study of Liver Explants
A Arslan, M Facciuto, G Ramaswamy. Westchester Medical Center, Valhalla, NY.
Background: 200 million people world wide including 3 million in the U.S. are infected with the hepatitis C virus. It is responsible for 40% of end stage liver disease, 60% of hepatocellular carcinomas and 30% of all liver transplants in the U.S.
The aim of our study was to specifically analyse explanted livers due to hepatitis C cirrhosis and evaluate these explants for the presence of clinically/radiologically undetected (incidental) hepatocellular carcinoma (HCC); as well preneoplastic changes including macroregenerative nodules (MRN), small cell change (SCC)and large cell change(LgCC) .
We did a comparative analyses of preneoplastic changes in the hepatitis C positive explants having HCC and those without tumor.

Design: A retrospective examination of all liver explants (195 cases) performed at Westchester Medical Center (WMC) from January 1996 to April 2004 was performed of which there were 50 cases of Hepatitis C end stage liver disease.

About 20 glass slides per case (~1000 slides) were examined by a single pathologist and resident by light microscopy. The slides were stained with Hematoxylin and Eosin, Trichrome, Reticulin and Iron stains .

The slides were studied for presence of preneoplastic changes: MRN, SCC and LgCC.

The minimum size to identify a nodule as a MRN was 10mm and for foci of liver cell change (SCC and LgCC) was 1 mm.

Results: 50/195; 26% of all explants at WMC (Jan 96-Apr 04) were of hepatitis C etiology.

HCC was present in 12/50; (24%) of cases of hepatitis C explants.

38/50; (76%) of the explants did not have HCC.

PRENEOPLASTIC CHANGES IN HEPATITIS C CIRRHOSIS

	Hepatitis C explants, 50cases	Hepatitis C with HCC, 12 cases	Hepatitis C without HCC, 38 cases
Macrorenegerative nodules	21/50; 42%	6/12; 50%	15/38; 39%
Small cell change	21/50; 42%	7/12; 58%	14/38; 37%
Large cell change	38/50; 76%	7/12; 58%	31/38; 82%

Conclusions: 26% of all liver explants were of hepatitis C etiology.

24% of end stage livers with hepatitis C harboured incidental HCC (average size =1.7 cm) .

Macroregenerative nodules and small cell change occured in 42% of explanted livers with hepatitis C.

Macroregenerative nodules and small cell change can be considered as precursors of HCC as they both occured more frequently in the livers with incidental HCC

Large cell change occured in 76% of explanted livers with hepatitis C.

Large cell change was present more often in hepatitis C explants without HCC than with tumor and therefore may not represent a premalignant change.

1267   Incidental Hepatocellular Carcinomas Arising in Hepatitis C Cirrhosis—A Study of Liver Explants

A Arslan, M Facciuto, G Ramaswamy. Westchester Medical Center, Valhalla, NY.

Background: Hepatocellular carcinomas (HCC) comprise 80% of the primary liver tumors. Hepatitis C is an important cause of HCC. The aim of our study is to analyse liver explants with hepatitis C cirrhosis for the presence of clinically/radiologically undetected (incidental) HCC and to study its charctersitcs.

Design: A retrospective study of all liver explants (195) at Westchester Medical Center from January 1996-April 2004 was performed, of which there were 50 cases of hepatitis C cirrhosis.

About 20 slides per case were examined by light microscopy by a single resident and pathologist .

The slides were stained for Hematoxylin and Eosin, Trichrome, Iron and Reticulin stains.

The parameters used to analyse the HCC were age and sex of the patients, tumor size, multiplicity, histological pattern, differentiation, cell plate thickness, mitosis, vascular invasion, nodule in nodule change and desmoplasia.

Results: 12/50, (24%) of the explanted livers with hepatitis C had HCC

There were 4 females and 8 males; mean age=53.7 years.

Mean tumor size= 1.7cm ; 8/12, (67%) were solitary and 4/12, (33%) were multiple.

7/12, (58%) were moderate-poorly differentiated and 5/12, (42%)were well differentiated.

HCC IN HEPATITIS C CIRRHOSIS

		TOTAL NO. OF HCC (12 CASES)	MODERATE-POORLY DIFFERENTIATED HCC (7 CASES)	WELL DIFFERENETIATED HCC (5 CASES)
1.	SIZE ,<2CM	8/12, 66%	7/7, 100%	1/5, 20%
	=or >2cm	4/12, 33%		4/5, 80%
2.	MULTIPLE TUMORS	4/12, 33%	4/7, 57%	0/5, 0%
3.	HISTOLOGY PATTERN TRABECULAR	4/12, 33%	2/7, 29%	2/5, 40% -
	-TRABECULAR/ ACINAR	5/12, 42%	3/7, 43%	2/5, 40%
	COMPACT	3/12, 25%	2/7, 29%	1/5, 20%
4.	PLATE THICKNESS -<5 cells thick	7/12, 58%	3/7, 43%	4/5, 80%
	= or >5 cells thick	5/12, 42%	4/7, 57%	1/5, 20%
5.	MITOSIS- <5/10hpf	10/12, 83%	6/7, 86%	4/5, 80%
	=or >5/10hpf	2/12,17%	1/7, 14%	1/5, 20%
6.	NODULE IN NODULE	6/12, 50%	5/7, 73%	1/5, 20%
7.	VASCULAR INVASION	5/12, 42%	4/7, 57%	1/5, 20%
8.	DESMOPLASIA	7/12, 58%	4/7, 57%	3/5, 71%

Conclusions: 24% of the explanted hepatitis C livers had incidental HCC.

Moderate-poorly differentiated HCC 7/12, (58%): predominantly with sizes <2 cm, trabecular/acinar pattern, cell plate thickness >5 cells, occurance of multiple tumors, vascular invasion and nodule in nodule formation.

Well differentiated HCC 5/12, (42%): predominantly solitary, with size >2cm, tabecular pattern and plate thickness <5 cells thick.

There was no significant difference in the mitotic rates and desmoplasia in both groups.

1268   Correlation of Hepatitis B Surface Antigen and Hepatitis B Core Antigen Immunohistochemical Stains with Serum HBV DNA and ALT in Patients with Chronic HBV

A Auerbach, A Mehrotra, Z Goodman, D Apelian, R Wilber. The Armed Forces Institute of Pathology, Washington, DC; Bristol-Myers Squibb Pharmaceutical Research Institute, Wallingford, CT.

Background: This is the largest study to compare immunohistochemistry (HBsAg, HBcAg) to pathology (Knodell Score, Ishak Score), and to clinical tests (serum HBV DNA, ALT) in patients with hepatitis B. The entecavir phase III program contains the largest HBV biopsy dataset to date (treated= 1633), with 3 cohorts of patients: (1) Nucleoside naive HBeAg+ (treated=709): mean serum HBV DNA by PCR = 9.7 $\log_{10}$ c/mL; ALT = 143 U/L; (2) Lamivudine refractory HBeAg+ (persistent viremia while on lamivudine with or without documented YMDD mutation) (treated 286): mean serum HBV DNA = 9.4 $\log_{10}$ c/mL; ALT = 128; (3) Nucleoside naive HBeAg negative: mean serum HBV DNA = 7.6 $\log_{10}$ c/mL; ALT = 142.

Design: Pearson cross-sectional correlations were performed at baseline for hepatic markers of HBV with serum HBV DNA and liver histology with serum ALT in three study cohorts. Viral antigen immunostaining was scored on a 5-point ordinal scale.

Results: HBeAg negative patients had less hepatic HBsAg and HBcAg (nuclear and cytoplasmic) than either HBeAg+ cohort (p<0.05), and mean cccDNA was lower (-0.48 log10 c/HGE vs. 0.35 log10 c/HGE in naïve HBeAg+ and 0.20 log10 c/HGE in lamivudine refractory; p<0.0001). There were positive correlations in all three cohorts for serum HBV DNA with cytoplasmic HBcAg, nuclear HBcAg, HBsAg, cccDNA and total hepatic HBV DNA. Positive correlations were also seen in all three cohorts for ALT with Knodell inflammatory score (p<0.0001). Serum ALT showed positive correlations with Ishak fibrosis score in both HBeAg + cohorts, but not in the HBeAg- cohort.

Conclusions: This is the largest study to compare the immunohistochemistry with pathology, and clinical tests in patients with Chronic Hepatitis B. Serum HBV DNA and ALT levels show significant positive correlations with hepatic HBV immunostains. Nucleoside naive HBeAg negative subjects had significantly lower cccDNA, cytoplasmic HBcAg, and nuclear HBcAg compared to nucleoside naive HBeAg+ and lamivudine refractory subjects.

Correlation of Hepatic Markers with Serum HBV DNA (*p<0.0001), #p<0.05)

	cccDNA	total DNA	Nuclear HBc	Cytoplasmic HBc	HBsAg
Naïve HBeAg+	0.39*	0.16#	0.38*	0.42*	0.18*
LVD refractory	0.19#	0.31#	0.20#	0.32*	0.20#
Naïve HBeAg-	0.15#	0.43*	0.26*	0.28*	0.14#

1269   Impact of MELD (Model for End-Stage Liver Disease) Scoring System on Findings at and after Liver Transplantation (LT)

G Azabdaftari, M Simpson, E Pomfret, J Pomposelli, W Lewis, F Gordon, R Jenkins, U Khettry. Brigham and Women's Hosp, Harvard Med Sch, Boston, MA; Lahey Clinic Med Ctr, Tufts Univ Sch of Med, Burlington, MA.

Background: The MELD scoring system, a validated objective liver disease severity scale calculated using values of serum bilirubin, creatinine, and INR, was adopted in 2/2002 to allocate cadaveric organs for LT. To improve transplantability before succumbing to advanced disease, patients with stage I and II hepatocellular carcinoma (HCC) are given extra points in this system. Our aims were to determine: 1) any differences in native liver histology following the implementation of this system, and 2) the impact of scoring advantage given to early stage HCC.

Design: Clinicopathological evaluation was performed in recipients of first cadaveric LT before (Pre-MELD, n=87) and after (MELD, n=58) the introduction of the MELD system. The findings in the two groups were compared using the Chi-Square test.

Results:

Table1: Comparison of Selected Findings in the Two Groups

	Pre-MELD (n=87)	MELD (n=58)	P value
Hepatitis C (HCV) ± Alcoholic Disease	39/87 (44.8%)	30/58 (51.7%)	0.02
Autoimmune Liver Disease	4/87 (4.6%)	6/58 (10.3%)	0.04
Inflammation grade ≥ 2	38/87 (43.7%)	28/58 (48.3%)	0.03
HCC	24/87 (27.5%)	27/58 (46.5%)	0.001
Portal vein thrombosis	10/87 (11.5%)	15/58 (25.9%)	0.002
HCV with lymphoid aggregates	10/39 (25.6%)	17/30 (57.5%)	0.014
HCV with hyperplastic hilar nodes	3/39 (7.7%)	10/30 (33.3%)	0.03
HCV with grade ≥ 2	23/39 (58.9%)	18/30 (60%)	NS
HCC > stage 2	5/24 (20.8%)	2/27 (7.4%)	NS

Post-LT HCC recurrence was seen in 3/24 (12.5%) and 1/27 (3.7%) patients in the Pre-MELD and MELD groups (p=NS) respectively. The 3 Pre-MELD cases had multiple/diffuse HCCs with vascular invasion while the 1 MELD patient had a resection for HCC with recurrence pre-LT.

Conclusions: 1) Overall, native livers had significantly increased incidence of grade ≥2 inflammation and portal vein thrombosis in the MELD group which may correlate with patients' increased clinical disease severity at LT.

2) Significantly more HCV patients underwent LT in the MELD group and their native livers had increased incidence of lymphoid aggregates and hyperplastic hilar lymph nodes possibly representing a subgroup with increased immune activity.

3) The scoring advantage given to early stage HCC did result in a significantly increased incidence of HCC among the MELD group but it did not adversely effect the post-LT outcome.

1270 Two Major Types of Intraductal Papillary Mucinous Neoplasm (IPMN) of the Pancreas: Their Distinct Histological and Mucin Phenotypic Features
S Ban, Y Naitoh, T Sakurai, M Kuroda, M Shimizu. Saitama Medical School, Iruma, Saitama, Japan; Kyoto University Hospital, Kyoto, Japan; Fujita Health University School of Medicine, Toyoake, Aichi, Japan.
Background: IPMNs have been recognized as a distinct clinicopathological entity for the last two decades. Some histologic variations are observed in the type of epithelium of IPMNs, and several kinds of categorization of IPMNs have been proposed by different researchers. However, this issue has not been fully determined until now.
Design: Sixty cases of surgically resected IPMNs from three institutions between 1983 and 2003 were included in this study. Histological assessment and mucin immunohistochemistry for MUC1, MUC2, MUC5AC, and MUC6 were performed for each lesion to establish a major categorization of IPMNs. The results of immunohistochemistry were evaluated semi-quantitatively (score 0 to 5).
Results: Two major types of IPMNs were noted on the basis of the histological features of epithelium, one showing a feature similar to gastric foveolar epithelium (Gastric type, 38 cases) and the other with a feature similar to that of colorectal villous adenoma (Intestinal type, 15 cases). Other minor types included 2 cases with both Gastric type and Intestinal type areas, and 5 cases showing an oncocytic feature. These two major types were distinct in several respects. Compared to the Gastric type, the Intestinal type showed the following features: 1) they mostly expressed MUC2 as well as MUC5AC (mean score of MUC2: Intestinal type 4.20 ± 1.37 vs. Gastric type 0.39 ± 1.05, $p<0.05$); 2) they more frequently involved the main pancreatic duct, causing severe atrophy of the surrounding pancreatic tissue ($p<0.05$); 3) they had a higher histologic grade ($p<0.05$); 4) they were frequently associated with nodular growth ($p<0.05$) and mucous lake formation ($p<0.05$); 5) they were less frequently associated with pyloric gland-like structures ($p<0.05$) and PanIN-like complex lesions ($p<0.05$); and 6) they were accompanied with mucinous carcinoma (2 cases).
Conclusions: Our results indicate that the classification of IPMNs into the Gastric type and Intestinal type is regarded as a reasonable major categorization from the histological and mucin phenotypical point of view. This categorization suggests that at least two different forms of histogenesis and behavior are present in IPMNs.

1271 Intraductal and Papillary Variants of Pancreatic Acinar Cell Carcinoma: A New Addition to the Challenging Differential Diagnosis of Intraductal Neoplasms
O Basturk, G Zamboni, D Klimstra, A Andea, NS Kamel, P Capelli, JD Cheng, NV Adsay. Wayne State University, MI; Verona University, Italy; Memorial Sloan Kettering Cancer Center, NY.
Background: The recognition and differential diagnosis of pancreatic intraductal neoplasms (IN) have gained importance in the past few years, as the incidence of these tumors (especially IPMNs) have risen to >10% of pancreatic resections, and their significance as precursors of invasive cancer is better appreciated. Acinar cell carcinomas (ACCs) are typically solid tumors; however, we have recently encountered several examples that fall in the differential diagnosis of IN.
Design: 7 ACCs with either intraductal growth and/or a papillary/papillocystic pattern that could be mistaken for IN were identified in the authors' files, and their clinicopathologic features were studied.
Results: *Clinical:* M/F=4/3; mean age=59; mean tm size= 4.8 cm (as opposed to 10 cm in conventional ACCs). Only 1 patient had metastasis at the time of diagnosis (as opposed to 50% in usual ACCs). *Pathology:* In 5 cases, the tumors had nodular growth of sheet-forming acinar cells, some of which were within ducts, as evidenced by the polypoid nature of the process, partial ductal lining, and presence of small tributary ducts in the walls. In 3 cases, the tumor had papillary and/or papillocystic patterns, at least focally. All had cystic dilatation of the ducts. No mucin was identified. All expressed trypsin. Markers of ductal differentiation were either absent or very focal. A minor endocrine component was present in 3. The main histologic findings that distinguished these tumors from IPMNs were: more compact nature of the nodules (rather than villous or arborizing papillae); cuboidal cells; prominent nucleoli, overall basophilia of the cytoplasm, apical granules; intraluminal crystals or pale, acidophilic secretions (enzymatic condensations); and lack of mucin.
Conclusions: Some ACCs show intraductal growth or exhibit papillary patterns, which can mimic IN, especially IPMNs. In such cases, attention to morphologic details described above, and immunohistochemistry are helpful. An endocrine component was present in 3/7 cases. The tumors were relatively small and, metastasis at presentation was less common than typically seen in ACCs (1/7 *vs* 50%).

1272 Pathologic Findings in Gallbladders Resected during Morbid Obesity Operations
O Basturk, G Altinok, L Budev, A Hildebrandt, JD Cheng, NV Adsay. Wayne State University, MI.
Background: Pathologic changes in the gallbladder (GB) are highly population-dependent. The differential findings aid in understanding the pathogenesis of gallbladder disease and potentially, in developing preventive strategies. Elective cholecystectomies performed during bypass or banding operations for morbid obesity help expose another population that has not been studied previously.
Design: 58 elective cholecystectomies performed during bypass or banding operations were reviewed. 30 of these were obtained after the initiation of this study, and from these, 3 blocks each containing 3 different sections were submitted. In the remaining 28, only one block per case, each with 3 sections was available. Pathology reports were reviewed for stones or any other macroscopic findings. The slides were evaluated for chronic changes (inflammation/fibrosis), cholesterolosis, metaplasia (pyloric and intestinal), Aschoff-Rokitansky (A-R) sinuses, and dysplasia. Each parameter was graded none, minimal, mild, moderate or marked. The findings were contrasted with the ranges presented in the literature for other risk groups.
Results: Most patients were female (55/58) and the mean age was 40 (range, 26-58). Cholelithiasis was very common (87.9% *vs 10-40%*). Chronic changes (inflammation/fibrosis) of mild or higher degree were seen in 72% (*vs 90% of gallstone cases*). A-R sinuses, however, were prominent in only 10% of the cases. Cholesterolosis was detected in 34% (*vs 8-39%*); adenomyomatous changes in 3% (*vs 0.6-8.7%*); pyloric-type metaplasia in 55% (*vs 50-75%*); intestinal metaplasia in 9% (*2-25%*). Dysplastic changes were seen in 13.7% (*vs 3.3 in Australia and 13-16% in cancer endemic areas such as Chili and Mexico*). One patient had porcelain gallbladder.
Conclusions: Morbidly obese patients undergoing elective cholecystectomy form a relevant group in which to study GB pathology. Not surprisingly, the frequency of cholelithiasis is very high (87%) in this group, as compared to other risk groups (highest reported, 40%). Most appear to be cholesterol stones, as expected. Some of the chronic changes associated with gallstones such as A-R sinuses, however, may not be as high as anticipated, possibly because of the relatively younger age group. The frequency of dysplasia noted in this group may be as high as the incidence reported in cancer-endemic areas; however, such comparison is difficult because of the possible differences in the criteria applied.

1273 The Immunohistochemical Characterization of EGFR Expression in Pancreatic Adenocarcinoma- A Tissue Microarray Based Study
A Bhardwaj, JW Nash, C Barbacioru, WM Smith, WL Frankel. Ohio State University, Columbus, OH.
Background: Over-expression of epidermal growth factor receptor (EGFR) has been demonstrated in pancreatic carcinoma. Therapies targeted at EGFR have been shown to inhibit the growth of pancreatic carcinoma either alone or in combination with chemotherapy and radiation. We evaluated EGFR expression in pancreatic tissue microarrays. Additionally, we studied the correlation between EGFR expression and tumor size, grade and lymph node status in the patients with pancreatic adenocarcinoma.
Design: Seventy-two cases of pancreatic adenocarcinoma and 18 cases of chronic pancreatitis were retrieved from the archival files. Carcinomas were graded as well, moderately, or poorly differentiated using WHO criteria and the tumor size and lymph node status (positive or negative) were noted in each tumor case. Tissue cores from formalin-fixed, paraffin embedded donor blocks (2 cores per block) were arrayed to create a tissue microarray of cores measuring 2.0 mm each. Sections were stained with EGFR (Dakocytomation California, Inc) and 2 pathologists determined intensity of membranous staining and percentage of tumor cells showing immunoreactivity. Staining was considered positive in cases with greater than or equal to 1% membranous staining. Positive and negative controls stained appropriately.
Results: EGFR expression was present in 48 of 72 (67%) cases of pancreatic adenocarcinoma and 7 of 18 (39%) cases of chronic pancreatitis. We did not find a statistically significant correlation between the intensity or extent of EGFR expression and tumor size, tumor grade or the lymph node status of the patients.
Conclusions: EGFR targeted therapies may be useful for the treatment of advanced pancreatic carcinoma, and the immunohistochemical analysis of EGFR staining may have a role in identifying pancreatic cancer patients who can benefit from EGFR inhibitors. EGFR expression did not correlate with the commonly used prognostic indicators for pancreatic carcinoma that were evaluated in this study. Long term follow-up is necessary to determine if EGFR expression correlates with patient outcome and whether patients with tumors expressing EGFR benefit from EGFR inhibitors.

1274 Comparison of Cytokeratin 7 and 20 Staining in Whole Tissue Block and Mock-Radiologically Obtained Needle Cores Biopsies: A Potential Cause of False-Positive Results Due to Limited Tissue Samples
D Bosler, NS Goldstein. William Beaumont Hospital, Royal Oak, MI.
Background: Radiologically obtained thin-needle core biopsies are frequently used to evaluate the primary site of metastatic adenocarcinoma. Cytokeratin 7 and 20 are two antibodies that are commonly used for this purpose. Most authors have used 1% - 10% staining cut-point for a positive result. We evaluated the effect of limited tissue samples on CK 7/20 positive/ negative results by comparing staining of metastatic colorectal adenocarcinoma in whole tissue blocks and simulated needle core biopsy specimens.
Design: One tissue block with ample adenocarcinoma from 25 metastatic colorectal adenocarcinoma hepatic resection specimens was stained with CK 7 and CK 20. Extent of staining was scored 0%, 1= 1%-5%, 2= 6%-25%, 3= 26%-50%, 4= 51%-75%,5= >75%. Two paper cut-outs (6 mm and 8 mm) of radiologic needle core biopsies were overlaid over the slide and the proportion of stained cells in the mock-needle core was evaluated. Length of viable adenocarcinoma in each mock needle core was recorded.
Results: The mean percentage of CK 7/CK 20 staining in whole tissue blocks was 1.0/ 4.2. [CK 7 (-)/ CK 20 (+)]. For CK 7, mean staining in the mock needle cores increased 1.2 over the corresponding whole block staining in 13 cases (52%), shifting them from CK 7 (-) to CK 7 (+). For CK 20, staining in needle cores decreased a mean of 1.7 in 11 cases. The mean length of viable, non-necrotic adenocarcinoma in the mock needle cores was 1.2 mm (range, 0.6 mm 2.9 mm).
Conclusions: The limited tissue in needle cores shifted the proportion of CK 7 stained cells sufficiently to reclassify 52% of the cases from CK 7 (-) to CK 7 (+) which would alter the differential diagnosis list of primary sites to include pancreaticobiliary and gastric as more likely sites than the colon. No CK 7 (-) to (+) shifts would have occurred if a 25%-50% staining positivity cut-point was used. Positive/ negative staining cut-points should be increased to 25%-50% stained cells in needle core biopsies to avoid false-positive interpretations due to limited tissue samples. Focal staining with CK 7

or 20 occurs in most neoplasms. Extent of staining should be interpreted in the context of the amount of tissue available for evaluation, and higher thresholds should be considered for smaller specimens. Scoring the extent of staining in needle core biopsies is further hampered by the limited length (mean 1.2 mm) of viable adenocarcinoma in the needle core.

1275 EGFR Expression and Gene Copy Number in Fibrolamellar Hepatocellular Carcinoma
AF Buckley, LJ Burgart, S Kakar. UCSF Medical Center, San Francisco, CA; Mayo Clinic, Rochester, MN.
Background: Increased expression of epidermal growth factor receptor (EGFR), a transmembrane tyrosine kinase, is associated with tumor progression in many carcinomas. Both small-molecule tyrosine kinase inhibitors and anti-EGFR antibodies have shown promise in treating some of these tumors. Fibrolamellar hepatocellular carcinoma (FL-HCC) is a potentially aggressive neoplasm that occurs in young patients with no history of cirrhosis. This study examines the expression and gene copy number of EGFR in FL-HCC, with a view to using EGFR antagonists to treat advanced tumors.
Design: Formalin-fixed, paraffin-embedded FL-HCC (n=13) sections were stained with a monoclonal antibody against EGFR (Clone 2-18C9) according to manufacturer's instructions, using the EGFR pharmDx kit (DAKO, Carpinteria, CA). Cell membrane staining was recorded as absent, 1+ (weak), 2+ (moderate) or 3+ (strong). For fluorescence in situ hybridization (FISH) analysis, Spectrum Orange- labeled EGFR probe (Vysis, Downer's Grove, IL) and Spectrum Green-labeled probe against the centromeric region of chromosome 7 (CEP 7) were hybridized to 5 µm sections, and counterstained with 2'-6'-diamidino-2'-phenylindole (DAPI). EGFR and CEP 7 signals were counted in 50 tumor nuclei per case as well as 300 normal hepatocyte nuclei. The EGFR to CEP 7 signal ratio was calculated for each case.
Results: All cases had typical FL-HCC features including polygonal cells with granular cytoplasm, prominent nucleoli and lamellar fibrosis. 12/13 (92%) FL-HCC tumors stained diffusely positive (3+) with anti-EGFR antibody. Normal hepatocytes were negative or showed 1+ staining. FISH was informative in 10 cases, all of which showed extra EGFR gene copy numbers (mean 3.69; range 3.13-5.0). EGFR was overexpressed in all these cases. The mean number of EGFR signals per cell in FL-HCC was double that of normal hepatocytes (3.69 vs. 1.80); the mean EGFR:CEP 7 ratio in tumor cells was 1.05.
Conclusions: EGFR is strongly overexpressed on the cell membrane in almost all cases of FL-HCC. EGFR gene copy number in FL-HCC is double that of normal hepatocytes. Similar gains are observed in chromosome 7, indicating that the extra EGFR gene copies are due to aneuploidy rather than gene amplification. The strong expression of EGFR in FL-HCC tumors suggests that they may respond to treatment with EGFR anatagonists. Since FL-HCC arises in young patients with non-cirrhotic livers, a response to treatment could have a significant impact on patient survival.

1276 Hepatocellular Carcinoma: Therapeutic Intervention and Outcome - A Pathology Perspective
N Buza, F Regenstein, S Dash, S Haque. National Institute of Oncology, Budapest, Hungary; Tulane University Health Sciences Center, New Orleans, LA.
Background: Hepatocellular carcinoma (HCC) is a fatal disease unless detected and treated early. Unfortunately only occasional cases are detected early enough for curative surgical resection, vast majority of tumors are unresectable. Recently local ablative (LA) techniques (transarterial chemoembolization , percutaneous ethanol injection and radiofrequency ablation) are being used in selected cases as an adjunct therapy preceding resection or orthotopic liver transplantation (OLT) in an attempt at cure or longer survival. The purpose of our study was to correlate therapeutic interventions (OLT and LA), histologic findings and outcome.
Design: From the files of Tulane University Health Sciences Center between 1999 and 2004, 37 patients with HCC were identified who had undergone either 1) ablative procedure prior to resection or while awaiting OLT and 2) HCC found in explanted livers after OLT. Two pathologists graded histologic parameters. Review was made of records.
Results: 29 males and 8 females, all with cirrhosis due to: 26 HCV, 1HBV, 1 hemochromatosis, 9 steatohepatitis. At time of study 23 patients were alive without recurrent HCC. Two patients treated with ablation alone died soon after therapy.

	Resection	OLT	Ablation + OLT	Ablation only
Total # of cases	8	15	12	2
Age (mean, range)	54 (42-71)	55 (47-66)	52 (47-63)	59 (49-69)
# of tumor / case (mean, range)	2 (1->5)	2.1 (1->5)	2.8 (1->5)	5.5 (1-10)
Tumor size cm (mean, range)	3.6(0.3-9.0)	2.1(0.2-4.5)	2.8(0.7-8.8)	15.5 (11-20)
Histologic grade (mean)	2.4	2.6	2.3	3
VASCULAR INVASION (# of cases) Absent	3	8	5	0
Occasional	3	4	5	0
Extensive	2	3	2	2
Area of necrosis (mean, range)	14% (0-85%)	18,6% (0-90%)	46% (0-100%)	27,5% (25-30%)
OUTCOME Alive (# of patients)	3	12	8	0
Survival in mth (mean, range)	14 (9-23)	35.6 (2-68)	25.2 (1-61)	
DOD (# of patients)	5	3	4	2
Survival in mth (mean, range)	12 (0-38)	22 (0-42)	8.25 (2-21)	1.5 (1-2)

Conclusions: In our series of patients 1) OLT with or without ablation appeared to be the best therapeutic option for HCC. We found that patients treated with OLT had significantly better survival than those treated with resection. 2) Ablation alone did not improve survival. 3) Long term follow up is needed to see if ablation prior to OLT offers further survival benefits.

1277 Differential Expression of Mucins, MIB-1 and p53 in Mucinous Tumors of the Pancreas
G Cai, A Simsir, H Yee, L Chiriboga, P Kefalides, J Cangiarella. New York University - Bellevue Hospital Center, New York, NY; New York University School of Medicine, New York, NY.
Background: Mucins are high molecular weight glycoproteins that are produced by various epithelial cells including those found in the pancreas. Previous studies have demonstrated differential expression of mucin subtypes in pancreatic and gastrointestinal neoplasms. Although pancreatic tumors display overt histological heterogeneity, many share a common feature, extracellular mucin accumulation. The mucin-producing tumors in the pancreas include ductal adenocarcinoma (DCA), mucinous cystic neoplasm (MCN) and intraductal papillary mucinous tumor (IPMT). The aim of this study is to investigate expression of different subtypes of mucins in pancreatic mucinous tumors, in conjunction with the expression of MIB-1, a proliferation marker, and p53, a tumor suppressor gene to explore their potential diagnostic value in distinguishing these entities.
Design: Thirty-six cases including DCA (n = 6), serous cystadenoma (SCA, n = 8), mucinous cystadenoma (MCA, n = 6), mucinous cystic adenocarcinoma (MCCA, n = 6), IPMT (n = 5) and solid pseudopapillary tumor (SPT, n = 5) were retrieved. Representative foci from each case were combined to make a tissue microarray. Immunohistochemical studies were performed on microarray sections using the antibodies against MUC1, MUC2, MUC5AC, MUC6, MIB-1 and p53. Membranous staining for mucins, and nuclear staining for MIB-1 and p53 were quantitated as a percentage of immunoreactive neoplastic epithelial cells /total # neoplastic epithelial cells.
Results:

Expression pattern of mucins, MIB-1 and P53 in mucinous pancreatic neoplasms

	MUC1	MUC2	MUC5AC	MUC6	MIB-1	P53
SCA, n=8	54±28	0	0	57±24	1.5±1.0	0
MCA, n=6	17±28	0	58±42	25±27	4.2±4.5	0
MCCA, n=6	40±31	6±10	35±31	27±22	30±13	25±29
IPMT, n=5	4±10	66±43	54±33	26±36	13±8	0.3±0.6
DCA, n=6	91±2	0	15±8	7.5±4.2	37±8	58±12
SPT, n=5	0	0	0	4.8±3.3	14±8	1.4±2.1

Conclusions: SCA showed immunostaining for MUC1 and MUC6 but not for MUC2 and MUC5AC. All mucins except MUC2 were expressed in MCN. Only IPMT displayed significant immunoreactivity for MUC2. DCA predominantly expressed MUC1. No mucins were detected in SPT. MCCA differed from MCA in higher MIB-1 and p53 immunoreactivity. DCA also showed increased MIB-1 and p53 expression. These results indicate that mucins were expressed differentially in pancreatic neoplasms and combining expression of mucin with MIB-1 and p53 may be helpful in the differential diagnoses of pancreatic neoplasms.

1278 Expression of Two Novel Tumor Markers, Maspin and Tubulin beta Polypeptide (TUBB), in Biliary Cancers
D Cao, K Kassaui, P Argani, C Neumann, L Ho, JL Abbruzzese, M Ouellette, A Maitra. The Johns Hopkins Hospital, Baltimore, MD; MD Anderson Cancer Center, Houston, TX.
Background: Biliary tract cancers (BTCs) are uncommon neoplasms, usually associated with a dismal prognosis. Identification of novel tumor markers in BTCs is a prerequisite for the development of effective diagnostic and therapeutic strategies. Maspin, a serine protease inhibitor, is upregulated in pancreatic and breast cancers, and detection of circulating maspin mRNA or protein is reported to be a valuable adjunct for early detection and relapse monitoring protocols. Tubulin beta polypeptide (TUBB) is a cytoskeletal constituent that is also overexpressed in many solid cancers, and is associated with chemoresistance to microtubule stabilizing agents like paclitaxel. A recently developed TUBB immunohistochemical assay permits identification of TUBB-negative cases that might benefit from paclitaxel therapy. Here, we examine the expression of maspin and TUBB, two novel tumor markers with diagnostic and therapeutic potential, respectively, in BTCs.
Design: Tissue microarrays (TMAs) were generated from archival specimens of 34 BTCs, including 19 gallbladder, 4 intrahepatic, and 11 extrahepatic cancers. Each case was represented by 4 cores on the TMAs, to exclude tissue heterogeneity. Both maspin and TUBB are expressed in the cytoplasmic compartment, and immunolabeling was scored as negative (expression in < 5% neoplastic cells), focal (5-25% expression) and diffusely positive (>25% expression).
Results: Normal biliary epithelial cores did not label with either maspin or TUBB. Expression of maspin and TUBB in biliary tract cancers stratified by site is summarized in Table 1.
Conclusions: Both maspin and TUBB are frequently overexpressed in BTCs, although there are site-specific variations. Maspin overexpression supports the use of circulating maspin mRNA or protein as a diagnostic tool in BTCs. TUBB overexpression suggests a possible explanation for resistance to microtubule-stabilizing agents in these cancers, and immunolabeling for TUBB can be used as guide for selection of patients who might benefit from this form of therapy.

Site	Maspin Negative	Focally +	Diffusely +	TUBB Negative	Focally +	Diffusely +
Gallbladder (N =19)	6(32%)	1(5%)	12 (63%)	5 (26%)	4 (21%)	10(53%)
Intrahepatic bile duct (N=4)	0	0	4(100%)	0	1(25%)	3(75%)
Extrahepatic bile duct (N=11)	1(9%)	0	10(91%)	0	2(18%)	9(82%)
Total (N =34)	7 (21%)	1(3%)	26 (76%)	5(15%)	7(21%)	22(64%)

1279 Ultrasensitive Detection of *KRAS* Mutations in Bile and Serum from Patients with Biliary Cancer Using LigAmp Technology

A Chandrasekharan, C Shi, PJ Thuluvath, II Wistuba, CA Karikari, P Argani, MG Goggins, JR Eshleman, A Maitra. Johns Hopkins University, Baltimore, MD; UT MD Anderson Cancer Center, Houston, TX.

Background: Biliary cancer is a lethal disease, and early detection efforts are needed to ameliorate the dismal prognosis. Mutations of the *KRAS* gene, specifically at codon 12, are one of the most common genetic aberrations in this cancer. An ultra-sensitive technology – LigAmp - has been described (Shi et al, *Nature Methods*, 2004) for the detection of single base pair mutations in clinical samples. LigAmp has a sensitivity of detecting a mutant population with a sensitivity of 1:10,000 wild-type cells. We utilized LigAmp to detect $KRAS^{G12D}$ mutations in patients with a variety of neoplastic and non-neoplastic biliary diseases.

Design: In LigAmp, a mutation specific 5' oligonucleotide and a generic 3' oligonucleotide (both tagged with M13 "tails") are ligated using *Pfu ligase*, followed by amplification using M13 primers. The 5' oligonucleotide also has an upstream unrelated bacterial gene sequence (e.g., *lacZ*), and a specific flurophor-labeled probe to the latter can be utilized to generate cycle threshold (Ct) values for the mutant DNA of interest in the sample. Serially diluted positive control and negative control cell lines in each run provide relative quantification of mutant *KRAS* levels. Oligonucleotides specific to the $KRAS^{G12D}$ mutation were designed. DNA was extracted from 119 samples, including 10 biliary cancer xenografts, 54 archival biliary cancers, 44 bile samples, and 11 serum samples. Of the 44 bile samples, 16 were from patients with biliary cancers, and 28 from a variety of non-neoplastic pancreato-biliary disorders; all 11 serum samples were from patients with biliary cancer.

Results: $KRAS^{G12D}$ mutations were detected in 10/10 (100%) biliary xenografts and 52/54 (96%) archival cancers. 13/16 (81%) neoplastic bile samples and only 6/28 (21%) non-neoplastic bile samples harbored mutant *KRAS* DNA (*P*=0.0003); the latter included chronic pancreatitis and primary sclerosing cholangitis, both conditions where this mutation has been reported. $KRAS^{G12D}$ mutations were also detected in 6/11 (55%) serum samples from biliary cancer patients.

Conclusions: $KRAS^{G12D}$ mutations are present in the majority of biliary cancers, and are detectable in bile and serum using LigAmp. This technology has the potential for early detection of biliary cancer as well as for disease monitoring post-therapy.

1280 Under-Expression of *JUNB* Gene in Hepatocellular Carcinoma

JH Chang, YS Chang, KT Yeh, JG Chang. Chang-Hua Christian Hospital, Chang-Hua, Taiwan; China Medical College, Taichung, Taiwan.

Background: *JUNB* is a major component of Activator Protein-1 (AP-1) transcriptional factor complex, which consists of *JUN* (*JUNB*, *C-JUN*, and *JUND*), *FOS* (*C-FOS*, *FOSB*, *FRA-1*and *FRA-2*), and *ATF* families. The *JUNB* gene is an immediate early transcriptional factor, which can be activated by polypeptide growth factors, cytokines and various chemical agents in a variety of cell types (including myeloid, lymphoid, liver, neuron, fibroblast, and epidermal lineages). JUNB has also been implicated in the activation of *P16* gene expression during cell cycle control and cell senescence. Targeted disruption of the *JUNB* locus in mice caused early embryonic demise. Promoter methylation leading to *JUNB* under-expression has been reported in chronic myelocytic leukemia. This study is to determine the molecular profile of *JUNB* in human HCC and explore its role in the tumorigenesis of HCC.

Design: Thirty cases of resected primary hepatocellular carcinoma and paired non-cancerous tissue were collected. The molecular profile of *JUNB* was analyzed by real-time quantitative reverse transcription-polymerase chain reaction (RT-PCR), mutational analysis and methylation specific PCR. Immunohistochemical study for JUNB, P16 and cyclin D1 expression was accompanied.

Results: RT-PCR revealed a significant down-regulation of *JUNB* in all HCC cases (p<0.001). The mutational analysis demonstrated no mutation in the coding region in any of the HCC. Methylation specific PCR disclosed no promoter methylation of *JUNB*. Immunohistochemical study showed under-expression of JUNB in most of HCC, correlated well with decreased expression of P16, but was inversely proportional to the expression of cyclin D1.

Conclusions: Down-regulation of *JUNB* in HCC was not caused by genomic mutation or epigenetic silencing (promoter methylation). The under-expression of JUNB coincided with under-expression of P16. The mechanisms of under-expression of *JUNB* and its potential role in the development of HCC remain to be explored.

1281 Identification of a Gene Expression Signature That Differentiates Hepatocellular Adenoma from Well Differentiated Hepatocellular Carcinoma

ZE Chen, KG Crone, MA Watson, JD Pfeifer, HL Wang. Washington University, St. Louis, MO.

Background: It is often difficult to distinguish hepatocellular adenoma (HCA) from well differentiated hepatocellular carcinoma (WDHCC) when limited needle biopsy tissue is microscopically evaluated. The aim of this study was to identify differentiating gene expression patterns that may lead to the discovery of useful diagnostic markers.

Design: Gene expression profile analysis using Affymetrix U133Plus2 GeneChip microarrays was performed on 6 HCA and 8 WDHCC specimens. The Significance Analysis of Microarrays (SAM) algorithm was utilized to identify genes whose expression differed significantly between these two types of tumors. Patterns of gene expression were validated by quantitative RT-PCR on an independent set of 9 HCA and 9 HCC RNAs. Immunohistochemistry was performed on additional 28 HCAs and 32 HCCs using commercially available antibodies against 5 proteins.

Results: We identified 79 genes whose expression levels were significantly different between HCA and WDHCC. These included 73 genes overexpressed by HCAs and 6 overexpressed by WDHCCs. The identity of 8 genes chosen for further analysis is shown in the Table. By RT-PCR, 7 of them (with the exception of PRX1) demonstrated concordant average expression differences between HCAs and HCCs. The expression pattern of these genes correctly classified an independent set of 18 tumors using unsupervised cluster analysis. Immunostains confirmed that HCAs expressed significantly higher levels of IGF-II, TMOD1, CLU and ER proteins and a lower level of PCNA protein comparing to HCCs.

Gene (Abbreviation)	Microarray*	RT-PCR*
Insulin-like growth factor-II (IGF-II)	17.0	32.8 (P<0.0001)
Tropomodulin 1 (TMOD1)	9.5	1.7 (P=0.0493)
Hsp40 homolog, member C1 (DNAJ)	8.7	4.5 (P<0.0001)
Clusterin (CLU)	4.9	3.6 (P<0.0001)
Estrogen receptor (ER)	3.8	2.9 (P<0.0001)
Paired related homeobox 1 (PRX1)	-4.0	2.2 (P=0.0899)
Epithelial V-like antigen 1 (EVA1)	-2.4	-2.0 (P=0.0332)
Proliferating cell nuclear antigen (PCNA)	-2.3	-1.7 (P=0.0151)

*Fold change comparing HCA with HCC.

Conclusions: Our results demonstrate significant molecular differences between HCA and WDHCC, despite morphological similarities. Furthermore, we have identified a unique set of genes whose expression pattern can differentiate between these two entities, suggesting the possibility of future development of ancillary molecular or immunohistochemical diagnostic methods.

1282 Plasma Cell Infiltrate May Predict the Severity of Acute Cellular Rejection in Liver Allografts

W Chu, PE Swanson, MP Upton, MM Yeh. University of Washington Medical Center, Seattle, WA.

Background: Acute cellular rejection is one of the most common complications in allograft livers. Multiple episodes of acute cellular rejection may lead to chronic rejection and eventual graft failure. Typical inflammatory cells in acute cellular liver allograft rejection include a mixture of lymphocytes, neutrophils, and eosinophils. Increased plasma cells have been observed in renal allografts (plasma cell-rich allograft rejection) and are associated with poor graft survival, but it is not known if the amount of plasma cells are associated with the severity of acute cellular rejection in allograft livers.

Design: We studied 61 cases of acute cellular rejection from 2000 to 2004, and compared plasma cell numbers in the portal regions in four groups, including focal mild, mild, moderate, and severe acute cellular rejection. Histopathologic grading of acute cellular rejection is based on Banff criteria. In order to standardize the assessment of plasma cells in portal areas with variable intensities of inflammation, the number of plasma cells as a percentage of total inflammatory infiltrate was calculated: total number of plasma cells and total number of portal inflammatory cells including mononuclear cells, neutrophils and eosinophils were serially counted in the 5 most cellular portal areas; the mean percentage of plasma cells from those 5 portal areas is shown in table.

Results: The percentage of plasma cells in portal infiltrate increases with severity of rejection. Most cases of focal mild rejection do not contain a single plasma cell in the portal infiltrate (0-2.5%), while all severe rejection cases have plasma cells (2-30%). The difference in average percentage of plasma cells in the portal areas among the four groups is statistically significant by Anova analysis (p<0.0001). Plasma cell infiltration can occur either early (9 days post OLT) or late (3 years post OLT).

Conclusions: Plasma cells are seen in acute cellular rejection of liver allografts, and the relative number of plasma cells increase when the severity of rejection increases. This finding suggests an important role for plasma cells in the immunological response of liver allograft rejection, and indicates that their presence in the portal areas may be a reliable histologic indicator for more severe acute cellular rejection.

Mean percentage of plasma cells in portal infiltrate of liver allograft rejection

Groups	Mean Percentage
Focal mild (n=15)	0.33
Mild (n=25)	0.79
Moderate (n=17)	5.56
Severe (n=4)	14.00

P<0.0001 by ANOVA

1283 Analysis of Molecular Alterations and Differentiation Pathways in Intraductal Oncocytic Papillary Neoplasm of the Pancreas

SM Chung, RH Hruban, C Iacobuzio-Donahue, NV Adsay, SY Zee, DS Klimstra. Memorial Sloan-Kettering Cancer Center, New York, NY; Johns Hopkins Universtiy Hospitals, Baltimore, MD; Karmanos Cancer Institute and Wayne State University, Detroit, MI; Albert Einstein School of Medicine, New York, NY.

Background: Intraductal oncocytic papillary neoplasms (IOPNs) and intraductal papillary mucinous neoplasms (IPMNs) of the pancreas share features such as intraductal papillary growth, mucin secretion, and indolent behavior compared to pancreatic ductal adenocarcinoma (DA). IPMNs have different morphologic types of papillae, including gastric (IPMN-G), intestinal (IPMN-I) and pancreatobiliary (IPMN-PB). However, IOPNs are distinct, with granular, oncocytic cytoplasm containing intraepithelial lumina and cytoplasmic mucin vacuoles. The molecular and differentiation patterns of IOPNs have not been well studied.

Design: Immunohistochemical stains were performed (Table 1) on 19 IOPNs and 7 IPMN-G, 7 IPMN-I and 6 IPMN-PB. Ligase detection reaction was used to detect mutations in codons 12 and 13 of the K-ras gene in 8 IOPNs and 26 IPMNs.
Results:
Table 1: # of cases and staining result

Stain	IOPNs (19)	IPMN-G (7)	IPMN-I (7)	IPMN-PB (6)
p53[1]	4 P	0 P	2 P	3 P
p16[2]	12 A	5 A	5 A	3 A
Smad4[2]	0 A	0 A	0 A	0 A
ß catenin[1]	0 P	0 P	0 P	0 P
mesothelin[1]	16 P	0 P	1 P, 1 FP	3 P
claudin4[1]	0 P	1 P	6 P	1 P
MUC1[1]	11 P	0 P	1 P	4 P
MUC2[1]	4 P	1 P	6 P	1 P, 1 FP
HepPar1[1]	12 P	0 P	4 P	1 FP
CDX2[1]	0 P	1 P	6 P	1 FP

[1] P = >25% staining, FP = 10-25% staining, [2] A= absence of staining in neoplasm with expression in normal tissue
K-ras mutation detection: 0/8 IOPNs, 18/26 IPMNs.
Conclusions: 21% of IOPNs and 25% of IPMNs showed p53 staining, 78% of which showed high grade dysplasia. No cases showed evidence of Smad4 or ß catenin abnormalities. 63% of IOPNs and 65% of IPMNs lacked p16 staining. Thus IOPNs and IPMNs have similar changes in these genetic markers. However, IOPNs lacked K-ras mutations, unlike IPMNs and DA. In addition, 84% of IOPNs versus 25% of IPMNs expressed mesothelin. Only IPMN-I consistently expressed claudin4. IOPNs also showed distinct differentiation patterns from IPMNs, such as expression of MUC1, a marker of an aggressive phenotype, and less expression of MUC2, a marker of a more indolent pathway. Most IOPNs showed no intestinal differentiation (CDX2 negative), in contrast to IPMN-I. HepPar1 staining in IOPNs is interesting but unexplained. Thus, IOPNs and IPMNs are related tumors, but these data support divergent differentiation.

1284 Expression of ZO-1 in Pancreatic Intraepithelial Neoplasia (PanIN)
T Cibull, S Badve, A Thomas, R Saxena. Indiana University, Indianapolis, IN.
Background: Zonula occludens-1 (ZO-1) is a member of the MAGUK (membrane-associated guanylate kinase homologue) protein family found in the cytoplasmic plaques of tight junctions; these are the most apical junctions between adjacent cells and they divide the cell membrane into apical and baso-lateral domains. ZO-1 plays an important role in organization of proteins within the tight junctional complex and is thus an important marker of polarity. Since increasing grades of epithelial dysplasia are characterised by loss of polarity, we studied expression of ZO-1 in PanIN to elucidate whether this expression changes with grade of dysplasia.
Design: We searched the database of the Department of Pathology to identify specimens of Whipple's resection with adenocarcinoma. The slides from these cases were examined to identify and classify PanIN lesions by already published criteria (Hruban, 2001). Four micron thick sections were cut and stained for ZO-1 (prediluted, Zymed) by a standard immunohistochemical protocol following digestion by proteinase K for 5 minutes. The staining pattern in the lesions was characterised as apical (dot-like positivity at the apical portion of the cell membrane between adjacent cells) or cytoplasmic (with or concurrent apical staining). The intensity was graded as 1+ (weak/absent), 2+ or 3+ (positive).
Results: There were 19 cases of Whipple's resection for pancreatic adenocarcinoma (12 men, 7 women; age 40 - 79 years, mean 56 years). There were 11 lesions of PanIN 1A, 14 of PanIN 1B, 8 of PanIN 2 and 9 of PanIN 3. The staining pattern is shown in
[Table1]: ZO-1 staining in PanIN

PanIN Grade	No of lesions	Apical Posivity	Cytoplasmic positivity
PanIN 1A	11	11	1
PanIN 1B	14	14	1
PanIN 2	8	6	5
PanIN 3	9	4	9

Cytoplasmic staining in the 2 PanIN 1 lesions was of 2+ intensity. Cytoplasmic staining in PanIN2 lesions was 3+ in 4 lesions and 2+ in 1 lesion. Cytoplasmic staining in PanIN 3 was 3+ in 8 lesions and 2+ in 1 lesion.
Conclusions: 1. Apical staining of ZO-1 was maintained in PanIN 1, but was lost in higher grades of PanIn, being absent in 25% of PanIN 2 and 60% of PanIN 3.
2. Cytoplasmic localization of ZO-1 was rare in PanIN1A and PanIN1B but common in higher grades of PanIN, with 60% incidence in PanIN 2 and 100% incidence in PanIN 3.
3. Abnormal localization of ZO-1 to the cytoplasm occurs in high grade PanINs, and may be helpful in the diagnosis of high grade lesions.
Reference: Hruban RH et al. Intraepithelial neoplasia: A new nomenclature and classification system for pancreatic duct lesions. Am J Surg Pathol 2001; 25: 579.

1285 The Expression of Proxisome Proliferator Activated Receptor Gamma (PPAR γ) in Ductal Pancreatic Carcinoma: A Correlative Study with Angiogenic Factors (VEGF and CD 34)
Y Dancer, C Heard, R Shi, J Albores-Saavedra. Louisiana State University Health Science Center, Shreveport, LA.
Background: PPARs are ligand-activated transcription factors belonging to the nuclear receptor superfamily. Ligand activation of PPARγ decreases VEGF production by tumor cells. In ductal pancreatic carcinoma, the VEGF expression and the microvessel density (MVD) are closely correlated, and both are markers of prognostic relevance. It has been reported that ligand activation of PPARγ results in growth inhibition and differentiation of pancreatic cancer cell lines.
Design: In this study, we analyzed PPARγ expression in ductal pancreatic carcinomas and correlated it with tumor size, tumor grade and angiogenetic factors such as VEGF and microvessel density (MVD). Histologic sections from 28 pancreatic ductal

carcinomas were stained with antibodies against PPARγ, VEGF (Santa Cruz, CA) and CD 34 (Ventana). Interpretation of the results was done by three pathologists as follows: The expression of PPARγ was graded as positive when there was more than 5 percent of nuclear staining. The scores of the extent (0-3) and the intensity of staining (0-4) with VEGF antibodies were summed. Intratumoral microvessel density (MVD) was recorded by counting CD-34-positive vessels in the highest vascularized area in four high power fields. Cases were analyzed according to PPARγ expression: positive vs. negative groups. Chi -Square and Student T Tests were used for statistical analysis.
Results: Of twenty-eight carcinomas, sixteen (57.2%) stained for PPARγ, and showed moderate to strong nuclear staining. The mean ages were 63 ± 8.39 vs. 64.14 ± 15.37 (p>0.05). Tumor sizes were 3.56 ±1.01 vs. 2.64 ±1.00 (p>0.05). Twenty-six (92 %) carcinomas stained for VEGF, and showed moderate to strong diffuse cytoplasmic staining in tumor cells. All of the PPARγ positive cases showed less VEGF expression than tumors with negative PPARγ expression (2.31±0.47 vs. 2.91±1.16, p =0.012). Tumors with positive PPARγ showed significantly less MVD than tumors with negative PPARγ expression (43.62±13.25 vs. 134.66±47.7, p<0.0001).
Conclusions: The expression of PPARγ correlates inversely with expression of VEGF and MVD. There was no significant correlation between PPARγ expression and clinicopathologic data. Our findings suggest that the PPARγ signaling pathway may be responsible for tumor angiogenesis in human ductal pancreatic carcinoma. Ligand activation of PPARγ appears to decrease VEGF production by tumor cells and have both direct and indirect antiangiogenic effects.

1286 Comparison of PPAR-alpha Immunostaining in Steatohepatitis and Normal Liver Biopsies
RD DeHaan, SO Sanderson. Mayo Clinic, Rochester, MN.
Background: Peroxisome proliferator-activated receptor-α (PPARα) is a member of the nuclear hormone receptor superfamily and is a key transcriptional regulator of the genes involved in hepatic β-oxidation of fatty acids (FA). Recently, studies in rodent models have shown that PPARα may play a role in the pathogenesis of non-alcoholic fatty liver disease (NALFD). Mice deficient in PPARα and those deficient in both PPARα and PPARα-regulated FA oxidation enzymes exhibit severe steatosis and steatohepatitis under fasting conditions. Reduced PPARα expression has been demonstrated in mouse models of NAFLD and administration of PPARα agonists to such mice has been shown to both prevent the development of, and reverse existing steatohepatitis. It remains to be established if abnormalities in PPARα levels contribute to steatohepatitis in humans. In the present study, we compared the staining pattern of PPARα in normal liver biopsies to that of liver biopsies showing steatohepatitis.
Design: 22 cases of steatohepatitis and 28 cases of normal liver were selected. Formalin-fixed paraffin embedded biopsies were stained with antibodies against PPARα (Santa Cruz, clone H-98) using a biotin free detection system (DakoCytomation EnVision+ System, HRP). The character and distribution of PPARα staining was recorded for each case. The presence of steatosis and any associated necroinflammatory activity was evaluated on H&E stained sections. Medical records were reviewed to confirm the clinical diagnosis.
Results: All cases showed similar mild, homogeneous, cytoplasmic and nuclear staining for PPARα. Additional coarse granular cytoplasmic staining was present in 31 cases in a predominantly zone 3 distribution. 27 of these 31 cases showed no histologic necroinflammatory activity and absent to mild steatosis. Of the 22 cases with confirmed steatohepatitis, 18 lacked coarse granular cytoplasmic staining. In regards to steatohepatitis, the absence of coarse granular cytoplasmic PPARα staining had a positive predictive value of 95%, with an overall sensitivity and specificity of 82% and 96% respectively.
Conclusions: In our series, nearly all normal liver biopsies showed coarse cytoplasmic PPARα staining in a predominantly zone 3 distribution. This pattern of staining was typically not observed in confirmed cases of steatohepatitis. The apparent difference observed in PPARα immunostaining may reflect a lower quantity or altered nature of human PPARα in cases of steatohepatitis and may offer some insight into the overall pathogenesis of fatty liver disease.

1287 Demonstration of Metallothionein in Hepatocellular Carcinomas and Hepatocellular Adenomas - A Molecular and Immunohistochemical Analysis
CC Gable, K Ghoshal, S Majumder, ST Jacob, ML Prasad, WL Frankel. The Ohio State University, Columbus, OH.
Background: The metallothioneins (MT) are a family of cysteine-rich, low molecular weight proteins that exist as 4 different, yet highly homologous isoforms within the human body. Among their most important roles are those of detoxification of heavy metals and the scavenging of hydroxyl free radicals. MT-I and MT-IIA are the 2 isoforms induced in a variety of stresses in all cell types. MT are down-regulated in hepatocellular carcinomas (HCC). We examined the differential expression of MT in HCC and hepatocellular adenomas (HA) at the RNA level and analyzed immunohistochemical expression to confirm the molecular findings.
Design: Ten fresh frozen human HCC and 2 HA and matched controls (adjacent non-tumor liver) were analyzed for expression of MT-I (in HCC cases only) and MT-IIA at the RNA level by RT-PCR with primers specific for MT-IIA and common to all five variants (MT-I). In addition, 34 HCC and 7 HA were retrieved from the archival files. All cases were reviewed for confirmation of the diagnosis. Formalin-fixed, paraffin-embedded sections were cut and stained with antibodies against MT. MT staining was graded 0 to 2+ and the percentage of cells expressing MT in the tumor and adjacent non-tumor liver was scored by two pathologists.
Results: Tissue RNA levels of MT-I and MT-IIA were significantly decreased in all 10 HCC and MT-IIA was decreased in HA compared to the matched controls. Immunohistochemical analysis showed that of the 27 cases of HCC with adjacent control liver, 24 (89%) showed a decrease in MT expression (and 10 of these cases showed no

expression). Of the 7 cases of HCC without matched controls, 6 (86%) showed no MT expression. Overall, the majority of the adjacent control livers showed 2+ or diffuse 1+ expression while HCC showed 0, or focal 1 or 2+ staining with no expression in 16 of the 34 cases. Of the 5 HA with adjacent control liver, 4 (80%) displayed a decrease in either the intensity or percentage of MT expression when compared to the adjacent liver. All but one of the control adjacent livers showed 2+ staining in nearly 100% of cells while the HA showed 1+ staining or a decreased percentage of cells with 2+ staining.

Conclusions: The decreased RNA levels of MT-I and MT-IIA in HCC and HA indicate transcriptional downregulation of MTs in the tumors. We confirmed a significant decrease in MT at the protein level using immunohistochemistry.

1288 Association of E-Cadherin, Matrix Metalloproteinases, and Tissue Inhibitors of Metalloproteinases in the Progression of Hepatocellular Carcinoma

Z Gao, M Tretiakova, W Liu, J Hart. University of Calgary, Calgary, AB, Canada; University of Chicago, Chicago, IL.

Background: Molecular markers can provide additional information to traditional histomorphological evaluation for the assessment of tumor progression and predicting the likelihood of invasion and metastasis in various types of malignancies. We studied the association of E-Cadherin (E-C), matrix metalloproteinases (MMPs), and the tissue inhibitors of metalloproteinases (TIMPs) with the development and progression of hepatocellular carcinoma.

Design: Tissue arrays including 6 normal liver (NL), 13 cirrhotic liver (CL), 39 macro-regenerative nodule (MRN), 15 dysplastic nodule (DN), 22 grade I hepatocellular carcinoma (HCC-I), 42 grade II HCC (HCC-II), 6 grade III HCC (HCC-III) and 9 metastatic HCC (HCC-M) were stained immnuohistochemically with antibodies against MMP1, MMP2, MMP3, MMP6, MMP7, MMP9, TIMP1, TIMP2, TIMP3 and E-C. The intensity of staining for each antibody was scored manually by two pathologists as well as automatically using the Chromavision Automated Cellular Imaging System (ACIS).

Results: (1) Compared with NL, CL had lower E-C and TIMP1, but significantly higher MMP3 and MMP7; MRN had lower E-C and MMP6; DN had significantly higher MMP3 and TIMP2; (2) The histomorphological progression from HCC-I to HCC-III is associated with gradual decrease of MMP2, MMP3, MMP7, E-C, TIMP2 and TIMP3, but gradual increase of MMP9; (3) HCC-M is associated with significantly lower tissue expression of MMP2, MMP3, TIMP1, 2, 3 and E-C.

Conclusions: E-Cadherin over expression and lower level of MMPs in HCC-I and HCC-II explains the rarity of extrahepatic metastasis in low grade HCC. MMPs 2, 3, 7 and E-C can be used as markers for tumor progression. TIMP1, 2, 3, E-C and MMP9 are markers useful in predicting metastatic potential.

1289 C-Kit Expression in Hepatoblastoma - Evidence of Stem – Like Cell in Histogenesis?

A Gupta, PM Chou. Northwestern University, Feinberg School of Medicine, Chicago, IL; Childrens Memorial Hospital, Feinberg School of Medicine, Chicago, IL.

Background: Hepatoblastomas are the most common pediatric liver tumor. Due to the wide range of epithelial or mesenchymal differentiation, these tumors have been suggested to arise from pluripotent stem cells. The hepatic stem cells or stem-like cells have been shown to express C-Kit among various markers. Due to the implication that these stem-like cells are involved in the histogenesis of hepatoblastomas, we hypothesized that C-Kit may be expressed in various types of hepatoblastomas.

Design: Selected paraffin blocks from hepatoblastomas were obtained from 20 patients from our surgical pathology files. These sections were evaluated for expression of C-Kit using routine immunohistochemical analysis with a polyclonal rabbit antiserum (A4502, Dako, California). Tumor cells were evaluated for membrane and cytoplasmic immunoreactivity

Results: Histologically, all twenty hepatoblastomas were typed into either an embryonal, fetal, or mixed component. C- Kit expression was strongly positive in thirteen of the twenty cases (65%). This immunoreactivity was specifically present in the membrane of the fetal and the cytoplasm of the embryonal component of these tumors. In contrast to the this, the mesenchymal component and adjacent normal liver in all twenty cases were negative.

Conclusions: In conclusion, to our knowledge this is the first study identifiying the prevalence of C-Kit expression in hepatoblastomas supporting the hypothesis that these tumors arise from pluripotent stem-like cells. These findings may have therapeutic implications with a Kit-selective tyrosine kinase inhibitor(Glivec) in the future. More cases should be studied to confirm our findings.

1290 Analysis of Expression of CDX2 Protein in Metastatic Colorectal Carcinoma in the Liver and Primary Cholangiocarcinomas

R Gupta, M Abecassis, P Kashireddy, MS Rao. The Feinberg School of Medicine, Northwestern University, Chicago, IL.

Background: CDX2 is a transcription factor and plays an important role in the development and maintenance of the differentiated state of intestinal epithelium. CDX2 protein is considered as colon-specific marker. CDX2 protein expression is increasingly used in the diagnosis of primary and metastatic colorectal carcinoma since this protein is expressed in more than 90% of colorectal carcinomas. However, we, and others have shown that CDX2 protein is also expressed in adenocarcinomas arising in Barrett's esophagus and in the stomach arising in the background of intestinal metaplasia. One of the common sites that colorectal carcinomas metastasize is the liver and these tumors can histologically mimic cholangiocarcinomas and the distinction between these two types of tumors may be difficult. Commonly used cytokeratin markers (7, 19 and 20) are not often helpful in differentiating cholangiocarcinomas from metastatic colorectal carcinomas.

Design: Formalin-fixed, paraffin embedded sections from 15 metastatic colorectal carcinomas and 10 cholangiocarcinomas were stained immunohistochemically for CDX2 protein using monoclonal antibodies after antigen retreival in citrate buffer. Immunostain was evaluated based on the percentage of cells showing nuclear stain.

Results: Normal bile ducts (inter lobular and septal) were negative for CDX2 protein. One hundred percent of metastatic colorectal carcinomas showed strong nuclear stain in more than 50% of tumor cells. Three of ten cholangiocarcinomas showed CDX2 immunoreactivity. However the staining was strong and diffuse in only one tumor and in the other two tumors the nuclear staining was focal (15 to 20% of cells).

Conclusions: Results of this study indicate that CDX2 protein expression can be seen in a small percentage of cholangiocarcinomas. One should exercise caution when using CDX2 stain in small liver biopsies for differentiating cholangiocarcinomas from metastatic colorectal carcinomas.

1291 Oncocytic Pancreatic Endocrine Neoplasms: A Clinicopathologic and Immunohistochemical Analysis of 21 Cases

S Hussain, A Arwini, R Chetty, DS Klimstra. Memorial Sloan-Kettering Cancer Center, New York, NY; University Health Network, University of Toronto, Toronto, ON, Canada.

Background: Pancreatic endocrine neoplasms (PEN) are rare tumors that can exhibit unusual growth patterns, one of which is the oncocytic variant. They can mimic hepatocellular carcinoma histologically, especially when metastatic to the liver. We describe the clinical, pathological, and immunohistochemical features of 21 cases.

Design: 16 cases of PEN with oncocytic features were retrieved out of 237 PEN cases from the pathology files at Memorial Sloan-Kettering Cancer Center (1968-2003) and five additional cases came from the University of Toronto. Pathological data were taken from the slides and the pathology reports. Immunohistochemical stains were performed on selected paraffin blocks. Follow-up information was obtained from a prospective clinical database and from patients' charts. Electron microscopy was performed on three cases. Comparison and survival analysis were done using the Kaplan-Meier method between the oncocytic PENs and conventional PENs, which have been previously reported.

Results: There were 11 females and 10 males between 37-70 yrs (mean = 54). The tumors were 2.5-12.5 cm, with 13 cases in the tail of the pancreas, 7 in the head of the pancreas, and one unknown (liver metastasis only). Histologic examination showed >20% of the tumor cells were polygonal, with abundant granular eosinophilic cytoplasm, round vesicular nuclei, and occasionally prominent nucleoli. The cells were arranged in trabecular, gyriform and nested patterns. 8/17 evaluable cases had lymph node metastases. At follow-up, five patients (5/16) died of disease after a mean of 38 mos. Three patients (3/16) had no evidence of disease after a mean of 19 mos . Immunohistochemical results were as follows:

IHC Stain	Number of cases positive	%
111.3 (mitochondrial antigen)	16/16	100
Synaptophysin	18/19	95
Chromogranin	17/20	85
CEA (polyclonal)*	16/21	76
CK19	16/21	76
CD10	8/21	38
Hepatocyte paraffin 1	2/21	10
Trypsin	1/16	5
Chymotrypsin	1/16	5
AFP	0/21	0

*cell surface, "pseudocanalicular" pattern in 48%

The nuclear proliferative activity, determined by positive reaction for Ki-67, was low($<=5\%$)

Conclusions: Oncocytic PENs are important to recognize to avoid misdiagnosis. They may be confused for hepatocellular carcinomas due to a pseudocanalicular pattern of staining for pCEA. The clinical outcome of these tumors is not significantly different from that of the conventional PENs.

1292 Concordant Loss MTAP and p16/CDKN2A Expression in Pancreatic Intraepithelial Neoplasia: Evidence of Homozygous Deletion in a Non-Invasive Precursor Lesion
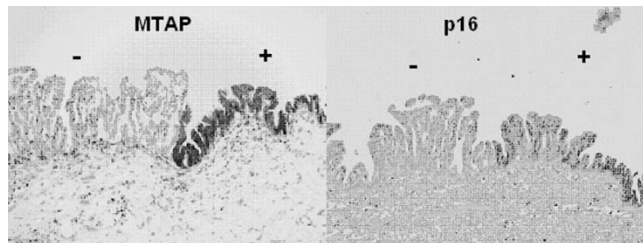
S Hustinx, A Maitra, LM Leoni, R Ashfaq, MG Goggins, C Iacobuzio-Donahue, SE Kern, RH Hruban. Johns Hopkins University, Baltimore, MD; Academic Medical Center, Amsterdam, Netherlands; Salmedix, Inc, San Diego, CA; University of Texas Southwestern Medical Center, Dallas, TX.

Background: The *p16INK4A* gene on chromosome 9p21 is inactivated in >90% of invasive pancreatic cancers, either by homozygous deletion (40%), intragenic mutation (40%), or promoter methylation (10-15%). Immunohistochemical loss of p16 expression does not provide information on the mechanism of *p16INK4A* gene inactivation. The methylthioadenosine phosphorylase gene (*MTAP*) gene resides on chromosome 9p21, and is frequently contained within *p16INK4A* homozygous deletions. Concordant loss of both *p16INK4A* and *MTAP* gene expression can therefore be used as a surrogate marker for *p16INK4A* homozygous deletion.

Design: We immunolabeled a series of 27 pancreatic intraepithelial neoplasia (PanIN) lesions and four infiltrating adenocarcinomas using monoclonal anti-p16 (clone 16P07, Neomarkers, Inc) and anti-MTAP (clone 6.9, Salmedix, Inc.) antibodies. Complete loss of labeling (nuclear for p16, cytoplasmic for MTAP) was considered negative, while any labeling was considered positive

Results: 1/9 (11%) PanIN-3 lesions and 1/4 (25%) invasive ductal adenocarcinomas did not label for the MTAP protein (the negative PanIN-3 and cancer were from the same specimen). The loss of MTAP labeling was diffuse in the infiltrating adenocarcinoma, and focal in the PanIN-3. MTAP labeling was lost in most of the epithelium, with an abrupt transition to a region with intact expression that precisely coincided with loss of p16 (*Figure*). The morphology of MTAP negative epithelium was similar to that with intact MTAP expression.

Conclusions: Immunolabeling for p16 and MTAP expression provides a tool to evaluate tissues with intact morphology for the mechanism of *p16INK4A* gene inactivation. The concordant loss of both proteins in a PanIN-3 lesion demonstrates that homozygous deletions of the *p16INK4A* tumor suppressor gene can also occur in non-invasive precursor lesions.

1293 Differentially Expressed Genes in Pancreatic Ductal Adenocarcinomas Identified through Serial Analysis of Gene Expression: An Update

SR Hustinx, D Cao, RH Hruban, N Sato, ST Martin, D Sudhir, C Iacobuzio-Donahue, SE Kern, MG Goggins, A Pandey, A Maitra. Johns Hopkins University, Baltimore, MD; Academic Medical Center, Amsterdam, Netherlands; Institute of Bioinformatics, Barcelona, India.

Background: Global gene expression platforms, such as serial analysis of gene expression (SAGE), are powerful tools for the discovery of novel tumor markers for pancreatic adenocarcinoma. The publicly available on-line SAGE libraries of normal and neoplastic tissues (*http://www.ncbi.nlm.nih.gov/SAGE/*). have recently been expanded; in addition, a more complete annotation of the human genome and better bicomputational techniques have substantially enhanced the assignment of differentially expressed SAGE "tags" to human genes.

Design: SAGE libraries generated from 6 pancreatic cancers were compared to SAGE libraries generated from 11 non-neoplastic tissues, and differentially expressed tags identified using X-Profiler program.

Results: Compared to normal tissue libraries, we identified 453 SAGE tags as differentially expressed in pancreatic cancer, including 395 that mapped to known genes and 58 "uncharacterized" tags. Of the 395 SAGE tags assigned to known genes, 223 were overexpressed in pancreatic cancer, and 172 were underexpressed. In order to map the 58 uncharacterized differentially expressed SAGE tags onto the human genome, we used a novel biocomputational tool, TAGmapper (*http://www.ibioinformatics.org/tagmapper*), and identified 16 additional differentially expressed genes. The differential expression of 7 of the genes, involved in multiple cellular processes such as signal transduction (*MIC-1*), differentiation (*DMBT1* and *Neugrin*), immune response (*CD74*), inflammation (*CXCL2*), cell cycle (*CEB1*) and enzymatic activity (*Kallikrein 6*), was confirmed by either immunohistochemical labeling of tissue microarrays (*Kallikrein 6, CD74, DMBT1*) or by RT-PCR (*CEB1, Neugrin, MIC1, CXCL2*). Neugrin was one of the genes whose previously uncharacterized SAGE tag was correctly assigned using TAGMapper, validating its utility.

Conclusions: Our results indicate that revisiting updated and expanded SAGE databases can be used to identify additional differentially expressed genes in pancreatic cancer. The new bioinformatic technique TAGmapper is a potential power tool to discover tumor markers through assigning uncharacterized SAGE tags.

1294 Homozygous Deletion of the *MTAP* Gene in Invasive Adenocarcinoma of the Pancreas and in Periampullary Cancer: A Potential New Target for Therapy

SR Hustinx, RH Hruban, LM Leoni, P Argani, R Ashfaq, MG Goggins, SE Kern, A Maitra. Johns Hopkins University, Baltimore, MD; Academic Medical Center, Amsterdam, Netherlands; Salmedix, Inc., San Diego, CA; University of Texas Southwestern Medical Center, Dallas, TX.

Background: Methylthioadenosine phosphorylase (MTAP) plays an important role in the salvage pathway for the synthesis of adenosine. Novel chemotherapeutic strategies exploiting the selective loss of MTAP function in cancers have been proposed. The *MTAP* gene, on chromosome 9p21, is frequently included within homozygous deletions of the *p16INK4A/CDKN2A* gene. Biallelic deletions of the *p16INK4A/CDKN2A* gene are found in 40 % of pancreatic cancers, suggesting that the *MTAP* gene may be frequently inactivated in pancreatic cancer and that selected patients may benefit from therapies targeting this loss.

Design: We immunolabeled six pancreatic cancer xenografts with known *p16INK4A/CDKN2A* and *MTAP* deletion status, and a series of 320 microarrayed archival infiltrating pancreatic adenocarcinomas, 35 biliary adenocarcinomas, 54 ampullary cancers, and 35 non-invasive intraductal papillary mucinous neoplasms using a monoclonal antibody against MTAP protein (clone 6.9, Salmedix, Inc) and two separate antibodies against p16 (Clone 16P07, Neomarkers, and Clone 16P04, Cell Marque Corp). Complete loss of labeling was considered "negative," while any labeling (p16: nuclear; MTAP: cytoplasmic) was considered "positive".

Results: There was complete concordance between the two p16 antibodies. Loss of expression of both MTAP and p16 was observed in 3/6 xenografted pancreatic cancers with homozygous deletions that encompassed *both* the *MTAP* and *p16INK4A/CDKN2A* genes; loss of only p16 was seen in the other three xenografts. Immunolabeling for MTAP was lost in 91 of the 300 (30%) evaluable pancreatic cancers, 9 of 54 (17%) ampullary cancers, 4 of 33 (12%) biliary cancers, and in 1 of 35 (3%) IPMNs. All neoplasms with loss of MTAP labeling also demonstrated loss of p16 labeling.

Conclusions: These results suggest that MTAP expression is lost in ~30% of infiltrating pancreatic cancers and in a lower percentage of other periampullary neoplasms, that this loss is the result of homozygous deletions encompassing both the *MTAP* and *p16INK4A/CDKN2A* genes. Thus, pancreatic cancer is a promising cancer type in which to explore novel chemotherapeutic strategies to exploit the selective loss of MTAP function.

1295 Histologic Variation of Grade and Stage of Non-Alcoholic Fatty Liver Disease in Liver Biopsies Obtained from Obese Patients during Gastric Bypass Surgery

ER Jacobson, DJ Janiec, L Spaulding, H Blaszyk. University of Vermont College of Medicine, Burlington, VT; Walter Reed Army Medical Center, Washington, DC.

Background: Sampling error regarding disease grade and stage has been ascribed to needle liver biopsies in patients with chronic liver disease. Although several studies evaluating sampling error in liver biopsies exist, none have investigated this phenomenon in patients with non-alcoholic fatty liver disease (NAFLD). This study aims to determine the rate and extent of sampling error in liver biopsies obtained from patients undergoing Roux-en-Y gastric bypass surgery (RYGBP) for morbid obesity.

Design: Ten morbidly obese patients underwent simultaneous liver biopsies from the right and left hepatic lobes during an open examination preceding RYGBP. The biopsies were subsequently randomly evaluated and then blindly re-evaluated by a liver pathologist. Percentage of fat and degrees of inflammatory activity and fibrosis were determined and semi-quantitatively scored for each sample using a four-tiered grading and staging system.

Results: Four patients (40%) had a difference of one grade and five patients (50%) had a difference of at least one stage between the right and left lobes. No two-grade differences were found in any of the patients and only one patient had a two-stage difference. Differences in grading and staging were seen predominantly in paired samples with significantly different biopsy sizes and number of portal tracts. Blinded histologic re-evaluation did not result in grading or staging scores that differed by more than one in any of the biopsies.

Conclusions: Liver biopsy samples taken from the right and left hepatic lobes differed in histopathologic grading or staging in 50% of the NAFLD patients, however, differences of more than one stage or grade were uncommon. Obtaining an adequately sized biopsy (> 1.5 cm in length with > 10 portal tracts) greatly reduces sampling error. Although obtaining two simultaneous liver biopsies may reduce sampling error, cost and risk-benefit issues pertaining to additional liver biopsies should be considered.

1296 Diffuse Biliary Casts Causing Hepatic Allograft Failure: Clinicopathological Perspective

S Jakate, J Scudiere, A Savo, F Dodson. Rush University Medical Center, Chicago, IL.

Background: Diffuse biliary cast formation in hepatic allograft is an uncommon and poorly understood phenomenon that often leads to graft failure and re-transplantation. Described in up to 18% of orthotopic liver transplants (OLT) in the older literature (pre-1979), limited attention to bile cast syndrome is accorded in modern literature probably due to its much lower incidence. Several causative mechanisms are suspected which include ischemia, acute cellular rejection, infection and biliary obstruction. We reviewed clinicopathological findings in 6 patients with hepatic allograft failure due to diffuse bile casts to look for causes and associated conditions.

Design: Between 1997 and mid-2004, 473 OLT were performed in our institution of which 52 (11%) were re-transplants due to allograft failure. 6 of these graft failures (12% of all failed grafts, and 1% of total transplants) were solely due to diffuse bile casts. The following aspects from these 6 cases were reviewed: original disease that caused liver failure, histological evidence of acute cellular rejection, ischemia or cholestasis in the pre-failure biopsies from the graft, sepsis, radiological detection of bile casts by ultrasound and/or CT, duration of graft survival, donor liver type and period of ischemia and recurrence of bile casts in the new graft.

Results: Native diseases were HCV (3/6), HBV (1/6), PBC (1/6) and confluent necrosis (1/6). Biopsies 1 to 6 weeks before graft failure showed cholestasis with increasingly larger bile plugs in all 6 cases, cellular rejection in only 2/6 cases and no sign of zone 3 ischemic change in any case. None had sepsis clinically. Radiologically (ultrasound and/or CT), none showed evidence of bile cast formation. Graft failure occurred in 17 to 315 days (mean 172 days) after transplant. All grafts were from heart-beating donors with <10 hours of cold ischemia. And there was no recurrence of this phenomenon in the new grafts (follow-up 2 months to 7 years).

Conclusions: Diffuse bile cast formation is an uncommon cause of allograft failure. The causative mechanisms and clinicopathological associations remain unknown. It occurs at an average of six months after transplant and shows no definite relationship with native liver disease, donor liver ischemia, graft ischemia or cellular rejection and does not predispose to similar cast formation in the new grafts. Imaging studies such as ultrasound and CT fail to detect the bile casts. Enlarging bile plugs in the graft biopsies may be the best way of predicting impending failure due to bile casts.

1297 Liver Cell Steatosis and Apoptosis in Experimental Fatty Liver Disease. A Mechanism towards Increased Liver Injury

C Kalogeropoulou, I Tsota, P Zabakis, T Kourelis, T Petsas, AC Tsamandas. Univ. of Patras, Patras, Greece.

Background: Liver cell steatosis seems to have a generally benign prognosis, either because most hepatocytes are not significantly damaged, or mechanisms that replace injured hepatocytes are induced. Apoptosis has been linked to liver cell depletion and ensuing liver fibrosis. This study assesses the effect of liver cell steatosis and apoptosis on the disease severity, in experimental non-alcoholic (NAFLD) and alcoholic (AFLD) fatty liver disease.

Design: The study included 50 male C57Bl/6 wild type mice aged 7-8 weeks: 25 mice were ob/ob (group A-NAFLD) and 25 their lean littermates (group B-AFLD). Ten mice were used as controls. In group A, mice received standard mouse chow ad libitum. In group B, mice were fed with liquid diets containing ethanol, for 5 w. Ethanol concentration was gradually increased by 1%, every 3 days, until reaching 4% ethanol (vol/vol). Controls were fed with equal volumes of similar liquid diet in which dextrin substituted ethanol. All mice were sacrificed at 5 w. SGPT values were measured in blood samples. Steatosis (% of hepatocytes affected) was graded as follows: 0 (<5%), 1 (5%-30%), 2 (31%-70%), 3 (>70%). Liver tissues were evaluated for **I)** Bax, Bcl-2, TNFα, and caspase-3 mRNA (RT-PCR) and protein (Western blot), **II)** liver stellate cell activation (immunostain for αSMA) and **III)** apoptosis (TUNEL method). Results were expressed following morphometric analysis.
Results: Mice of groups A and B, displayed higher SGPT values compared to controls (p<0.001 respectively). A direct correlation between liver cell apoptosis and degree of steatosis was recorded (*group A*: r =0.58, p <0.01, *group B*: r =0.73, p <0.01). Increased steatosis was associated with: **I)** decreased Bcl-2 mRNA levels (*group A*: r =-0.34 p<0.05, *group B*: r =-0.61 p<0 .01), **II)** increased Bax/Bcl-2 mRNA and protein ratio (*group A*: r=0.63 and 0.74 p<0.01, *group B*: r=0.59 and 0.38 p<0.01 and p<0.05), **III)** active caspase-3 (*group A*: r=0.64, *group B*: r=0.71-p<0.01). In group B (AFLD) a direct correlation was revealed between **I)** apoptosis and stellate cell activation (r =0.46, p<0.05) and **II)** TNFα levels and active caspase-3 (r=0.68, p<0.01).
Conclusions: In cases of experimental fatty liver disease, lievr cell steatosis may contribute to hepatocytic injury. Further research is warranted in order to clarify the molecular pathways responsible for the proapoptotic effect of steatosis and whether this increase in apoptosis contributes directly to progression of liver injury in cases of fatty liver disease.

1298 Increased Bax/Bcl-2 Ratio Upregulates Caspase-3 and Increases Apoptosis in an Experimental Model of Acute Liver Failure
C Kalogeropoulou, I Tsota, P Zabakis, T Kourelis, T Petsas, AC Tsamandas. Univ. of Patras, Greece.
Background: Apoptosis has been linked to liver cell depletion however, its regulating mechanisms have not been fully elucidated. Bax/Bcl-2 ratio has been considered as the best regulator of apoptosis. This study investigates the alterations of Bax/Bcl-2 ratio in relation to changes in the apoptosis co-ordination enzyme, caspase-3, in an experimental model of acute liver failure.
Design: The study comprised 120 Wistar rats that received simultaneously allyl-alcohol (intraperitoneally 0.05ml/kg) and carbon tetrachloride (rhinogastric 1.9ml/kg). Rats were sacrificed at 2, 4, 6, 12, 24, 48, 81, and 153 hr, after chemicals institution. SGPT values were measured in blood samples. Liver tissues were evaluated for **a)** Bax and Bcl-2 mRNA (semiquantitative real time PCR assay), **b)** Bax and Bcl-2 protein levels (Western blot), and distribution (immunohistochemistry), **c)** caspase-3 activity (substrate cleavage assay), **d)** immunohistochemical expression of antigens CK7, HEPAR, CD68, αSMA and **e)** apoptosis (TUNEL method). Results were expressed following image analysis and the bax/bcl-2 ratio was calculated.
Results: The death rate of animals was 80% within 48 hrs after chemical institution. Liver sections developed combined periportal and pericentral necrosis; it developed at 2 hr and the peak was at 48 hr. Liver regeneration originated from zone 2 and accomplished (at 153 hr) mainly by non-necrotic mature hepatocyte proliferation; most of them were HEPAR(+) and less CK7(+). Bax mRNA was significantly increased and Bcl-2 mRNA decreased towards 48 hr (+252% and -61%). Similar results were recorded for bax and Bcl-2 proteins (+342% and -25% by 48hr). Bax/Bcl-2 ratio reached the peak at 48 hr and thereafter decreased. Apoptosis reached the peak 48 hr. Apoptotic bodies were sequestrated in the adjacent hepatocytes and sinusoidal cells. Double stain with TUNEL and antigen CD68 or αSMA, revealed that apoptotic bodies were phagocytosed by Kupffer cells or incorporated in stellate cells respectively. The Bax/Bcl-2 ratios were correlated with *up-regulated caspase-3 activity* (r=0.734 and 0.610-p<0.01), *apoptosis* (r=0.553 and 0.362 p<0.01 and p<0.05), and *SGPT values* (r=0.574 and r=0.603, p<0.01)
Conclusions: This study provides evidence that the changes in the Bax/Bcl-2 ratio may contribute to caspase-3 activation and increase of liver apoptosis in experimental model of acute liver failure. These results may have prognostic and therapeutic implications in acute liver failure.

1299 Resistance of Fatty Acyl-CoA Oxidase Null Mice to Methionine-Choline Deficient Diet-Induced Steatohepatitis
P Kashireddy, R Gupta, MS Rao. Feinberg School of Medicine, Northwestern University, Chicago, IL.
Background: Fatty acyl-CoA oxidase (AOX) is the first and rate-limiting enzyme of the peroxisomal β-oxidation system. Mice with disrupted AOX gene (AOX null mice) develop marked steatohepatitis during the first 2-4 months of life, followed by decreased fatty change. Wild type mice fed methionine-choline deficient diet (MCDD) for 4 weeks also develops marked steatohepatitis. The histology of steatohepatitis that develop in young AOX null mice (AOXNM) and MCDD mice are comparable. However the effect of MCDD in AOXNM has not been studied. In this study, we investigated the possibility of enhanced liver cell damage by MCDD in AOXNM through synergistic mechanisms.
Design: Male AOXNM aged 5-6 months were fed MCDD (8 mice) or control diet (4 mice) for 4 weeks. In addition, male wild type mice of same age were also fed MCDD or control diet (4 mice in each group) for 4 weeks. At the time of sacrifice blood was collected for estimation of serum alanine transaminase (ALT) and triglycerides. Portions of liver were processed for light microscopy and the remainder was snap-frozen for triglyceride (TG) estimation.

Results: H&E-stained sections of liver from wild type mice fed MCDD showed marked steatohepatitis, whereas livers from mice fed control diet were normal. Livers from AOXNM fed normal diet showed mild fatty change and groups of hepatocytes with marked peroxisome proliferation. Histology of livers from AOXNM maintained on MCDD was comparable to AOXNM fed normal diet and lacked steatohepatitis. In wild type mice fed MCDD, serum ALT levels (139±10U/L) and liver triglyceride levels (368±16mg/g) increased several fold over the controls (ALT 57±6 and TG 17±1). Whereas, serum TG levels in MCDD fed wild type mice were 34±2, compared to 106±3 in wild type fed control diet. In AOXNM fed MCDD the liver TG levels were markedly lower compared to wild type mice fed MCDD (53 mg/g liver in AOX versus 368 mg/g liver in wild type). TG levels in the liver of AOXNM fed control diet was higher than in wild type controls (53 versus 17mg/g). Interestingly the serum ALT levels in wild type and AOXNM fed MCDD and AOXNM on control diet was comparable.
Conclusions: The results of this study show that AOXNM are resistant to MCDD-induced steatohepatitis. This resistance of AOXNM to MCDD is most likely due to increased levels of peroxisome proliferator activated receptor α (PPARα) in livers caused by accumulation of long chain fatty acids. Increased PPARα upregulate the fatty acid oxidation system resulting in decreased hepatic fatty acid content.

1300 Telomere Shortening in Hepatocellular Carcinomas Arising in Cirrhotic Livers in Patients Infected with Hepatitis C Virus
P Kashireddy, DM Weinrach, KL Wang, MS Rao. The Feinberg School of Medicine, Northwestern University, Chicago, IL.
Background: Telomere shortening is considered as one of the molecular causes of genetic instability, a common finding in many types of malignant neoplasms. It is also shown that telomere shortening plays an important role in initiation and progression phases of tumor development. Oxidative DNA damage appears to be one of the causes of telomere shortening. Oxidative stress is implicated in causation of several human diseases including cancer. Increased incidence of hepatocellular carcinomas (HCC) in United States has been attributed to chronic hepatitis C (HCV) infection. The pathogenesis of HCV-associated HCC is not understood. One of the postulated mechanisms is oxidative stress resulting from unrelenting inflammation. The purpose of this study is to evaluate telomere shortening in HCC developing in HCV-associated cirrhosis to determine whether telomere shortening contributes to either development of cirrhosis or HCC.
Design: This study included 5 explants from patients that underwent liver transplant for end-stage liver disease caused by chronic HCV infection. All these livers showed cirrhosis and HCC. Formalin-fixed and paraffin embedded sections containing HCC and cirrhotic regenerative nodules were hybridized with a Cy3-labeled telomere-specific peptide nucleic acid probe, and counterstained with 4-6-diamidino-2-phenylindole. In addition, sections from 5 normal livers were also processed for Telomere Fluorescent in Situ Hybridization (TELI-FISH). Visualization and photography were performed using Zeiss-axiophot epifluorescence microscope. Images were taken at x100 magnification and photographs were prepared with the use of photoshop 5.0. Telomere signals were counted in 15 to 20 nuclei in HCC, regenerative nodules and normal liver in each case.
Results: Telomere fluorescent signals were easily identified as discrete bright red spots within each nucleus. The mean number of telomere signals in normal liver, regenerative nodules and HCC were 9.0 (range 8-10), 10.2 (range 9 to 12.8), and 1.2 (range 0-2.2), respectively. Telomere signals were significantly less in HCC.
Conclusions: The results of this are interesting in two respects: 1) There is no difference in the telomere signals between control livers and regenerative nodules suggesting telomere shortening is not associated with cirrhosis development in HCV infected patients; and 2) Telomere shortening in HCC but not in regenerative nodules also indicates that telomere dysfunction is a late event in the development of HCC.

1301 Villous-Intestinal Differentiation and Progression to Colloid Carcinoma, Characterstic of a Major Subset of IPMNs, Are Not Features of Mucinous Cystic Neoplasms
I Khalifeh, O Basturk, G Zamboni, DS Klimstra, W Frankel, RH Hruban, J Cheng, NV Adsay. Wayne State University, MI; University of Verona, Italy; Memorial Sloan-Kettering Cancer Center, NY; Ohio State University, OH; Johns Hopkins University, MD.
Background: A distinct subtype of intraductal papillary mucinous neoplasm (IPMN) characterized by intestinal differentiation and diffuse expression of the intestinal markers MUC2 and CDX2 has recently been recognized. The invasive carcinomas (IC) arising from these intestinal-type IPMNs are mostly of colloid (CC) type. This has led to the hypothesis of an intestinal pathway of carcinogenesis in IPMNs. The presence or absence of an intestinal pathway in mucinous cystic neoplasms of the pancreas has not been examined.
Design: All MCNs (defined to have ovarian-type stroma) in the authors files were reviewed to identify those with florid papillary nodules (PN) and/or IC. Morphologic and immunophenotypic characteristics of the PNs and the type of IC were investigated.
Results: *Pattern of PNs.* PNs were identified in 13 cases and were composed of complex papillae lined by 1-3 cell-layers of cuboidal-columnar cells with prominent nucleoli. In addition, in 3 of these, there were also smaller polypoid intraluminal growths composed of tubular units lined by foveolar-like epithelium. In some foci, the epithelium resembled intestinal absorptive cells or that of gallbladder; however, none had a villous adenoma pattern. Immunohistochemically, rare MUC2+ goblet cells (<1%) were identified in 5/13 cases studied, in accordance with the findings of Luttges and Kloppel. Similarly, scanty nuclear labeling with CDX2 (<1%) was noted in 2/13. MUC1 was expressed diffusely in 10/12. *Type of IC.* All 8 ICs identified were of the tubular type. No CC type IC was identified.

Conclusions: Diffuse intestinal differentiation characterized by MUC2/CDX2 expressing villous-intestinal nodules seen in many IPMNs is not a feature of MCNs. In contrast, the papillary nodules in MCNs commonly express MUC1. Colloid type invasive carcinoma, which constitutes >60% of invasive carcinomas in IPMNs, is not seen in association with MCNs, if defined to exhibit ovarian-type stroma. These findings provide an additional argument for the distinction of these two entities, as well as for the importance of using ovarian-type stroma as a required criterion for MCN.

1302 The Distinction of Mixed Mucinous Carcinomas of Ampullo-Pancreatobiliary Region from Colloid Carcinoma: A Clinocopathologic Analysis of 25 Cases

F Khanani, O Basturk, S Khayyata, JD Cheng, A Andea, L Fathallah, NV Adsay. Wayne State University, MI.

Background: In the breast where mucinous carcinomas have been well characterized, it has been documented that "mixed mucinous" (MM) carcinomas have significantly worse prognosis than colloid carcinomas (CC). This issue has yet to be resolved in the ampullo-pancreatobiliary (A-PB) region.

Design: All invasive ca with prominent extracellular mucin formation identified in the authors' institution were analyzed. Colloid pattern was defined strictly as in the breast (pools of mucin that contain scanty, detached ca cells, most of which are floating within the mucin), and tumors that comprised >90% of this pattern was designated as CC. Tumors with areas in which more cells were clinging to the mucin-stroma interface, and those with non-mucinous cellular infiltration into the stroma were classified as MM. MM ca in which the non-mucinous component had intestinal features were classified as MM-int, and those with ordinary ductal ca pattern as MM-du.

Results: 8 cases were classified as CC, 7 as MM-Int and 10 as MM-Du. The main clinical and pathologic characteristics are documented in Table 1.

Conclusions: MM ca of the A-PB region are distinct from CCs both immunophenotypically and clinically. MUC2 expression may be seen in any mucin-forming tumor of this region including some MM-ductal ca (in contrast with the non-mucinous examples of this tumor that typically lack MUC2). MUC1 expression, on the other hand, is a reliable discriminator of MMs from CC (100% vs 0%). In contrast, lack of CDX2 expression distinguishes MM-Du. Overall, the survival rate of CC is much better than that of MM. MM-Du cases behave like ordinary ductal ca. MM-Int group appeared to have intermediary behavior with a median and 5-y surv 28 mos and 50% (122 and 71% in CC); however, the difference did not reach statistical significance. Of note, in 4 MM-Int non-invasive neoplasm constituted the majority of the tumor.

TYPE	CC (n=8)	MMIT (n=7)	MMDT (n=10)
MEAN AGE YRS	64	60	69
MEAN SIZE TM (CM)	5.2	5.5	3.5
MEAN SIZE OF INV TM (CM)	4.5	2.5	3.5
SEX M/F	5/3	6/1	5/5
LN + CASES	3/7	4/7	6/7
MEADIAN SURVIVAL IN MONTHS	122	28	7
MUC1	0%	100%	100%
MUC2	100%	80%	50%
CDX2	76%	60%	0%

Survival Functions
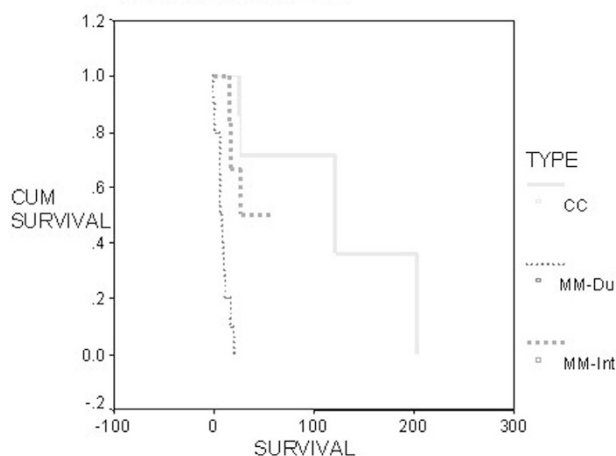
1303 Invasive Micropapillary Carcinoma of the Ampullo-Pancreatobiliary Region

SH Khayyata, O Basturk, F Khanani, H Nassar, J Cheng, NV Adsay. Wayne State University, MI.

Background: Originally described as a distinctive type of invasive carcinoma in the breast, the micropapillary pattern (MP) is being increasingly recognized as a separate entity in other organs including the urinary bladder; however, it has not yet been documented in the pancreas (PAN) or peri-ampullary (P-AM) region.

Design: 313 PAN and 38 P-AM carcinomas were reviewed to investigate MP in this location

Results: 7 P-AM AND 5 PAN cases (3 %) were composed predominantly (>50%) of MP ca. In addition, in 3 P-AM carcinomas of the NOS type, there were rare foci of lymphovascular invasion with MP-like features in the mucosa and the submucosa, which were not regarded as MP ca. *Pathology:* MP ca were characterized by small, round-to-ovoid micropapillary clusters (without fibrovascular cores), which were lying within clefts. The micropapillary units were closely packed, with much less intervening stroma than is typically seen in carcinomas of this region. The cells had a fair amount of acidophilic cytoplasm, and moderate degree of nuclear atypia. In 9 cases, there was abundant inflammation composed of PMNs, which were both intraepithelial, focally forming microabcesses, and stromal. PMNs were focal in 3 cases in which MP component was less abundant. The concentration of the PMNs in and around the tumor cells, along with the lack of any specific history or pathologic evidence of prior instrumentation indicated that the presence of PMNs was a primary process. *Immunohistochemistry:* The neoplastic cells expressed galectin-3 and e-cadherin (molecules implicated in abnormalities of tumor cell-stroma adhesion) in 8/8 and 6/8 cases, respectively. Reversal of cell-polarity was observed by MUC1 in all 8 cases tested, which showed labeling in the stroma-facing surfaces of the MP clusters, also confirming that the "clefts" are not merely processing artefact, but indeed a true biologic alteration. *Clinical:* M/F=9/3 ; mean age 66; and mean tm size 3.3 cm. LN metastasis was detected in 7/11 cases. Median survival was 8 months (all were resected), which qualifies the group to be graded as G3 (poorly differentiated).

Conclusions: Invasive MP ca described as a distinct entity in the breast and urinary bladder does also occur in the P-AM/PAN, and constitute 3 % of the tumors in this region. MP in this location, however, is commonly associated with abundant neutrophilic infiltrates. MP ca appears to be more common in P-AM than in PAN. Further studies are warranted to determine the mechanisms of MP development, and the neutrophilic chemotaxis specific to this tumor.

1304 Allelotype Analysis of Extrahepatic and Intrahepatic Cholangiocarcinoma

AM Krasinskas, L Wang, A Bakker, JL Hunt. University of Pittsburgh Medical Center, Pittsburgh, PA.

Background: The molecular pathogenesis of extrahepatic cholangiocarcinoma (ECC) has not been well characterized. Allelic imbalance has been studied in intrahepatic cholangiocarcinoma (ICC) and comparisons have been made to allelic imbalance in hepatocellular carcinoma. Since ECC is associated with chronic inflammatory biliary diseases, it may have a different pathogenesis than ICC. This study compares patterns of allelic imbalance between ICC and ECC at loci that have been implicated in biliary tumor carcinogenesis.

Design: 16 cholangiocarcinomas (8 ECC and 8 ICC) were obtained from archived specimens over a 22-month period. Clinicopathologic data were obtained from the surgical pathology reports. DNA was extracted after microdissection from formalin-fixed normal and tumor tissue. PCR was performed using fluorescently labeled primers for polymorphic microsatellite makers at the following loci: APC at 5q23 (D5S.1384, D5S.659), p53 at 17p13 (D17S.516, D17S.768, D17S.1884), DCC at 18q21 (D18S.364, D18S.487, D18S.1119), p21 at 1q36 (D1S.407) and p16 at 9p21 (D9S.251). Capillary electrophoresis was used to obtain the peak heights from the alleles in informative cases, and these were compared in a ratio between the tumor and normal sample. Ratios that were <0.7 were indicative of allelic imbalance (loss of heterozygosity). Fractional allelic loss (FAL) was calculated as the number of loci with allelic imbalance/total number of informative loci.

Results: The mean tumor size was 3.5 cm for ECC and 7.5 cm for ICC. All tumors were moderately differentiated and there were no differences between TNM classifications. Similar FALs for individual loci were seen in both ECC and ICC on 1q (both 67%), 5q (64%, 60%), 9p (both 67%) and 17p (50% and 63%)(overall, p≤0.68). Allelic imbalance of 18q was less frequent in ECC compared to ICC (22% and 52%, p≤0.08). Overall FAL for ECC ranged from 0 to 63% (mean 46%) and for ICC ranged from 29% to 100% (mean 60%)(p≤0.28).

Conclusions: Both ECC and ICC exhibit frequent allelic imbalance. ECC tends to exhibit less frequent allelic imbalance of 18q (DCC) and lower overall FAL than ICC. These data suggest a potential difference in tumorigenesis between ECC and ICC.

1305 Prevalence and Significance of Central Venulitis in Adult Liver Allografts

AM Krasinskas, SC Abraham. University of Pittsburgh Medical Center, Pittsburgh, PA; Mayo Clinic, Rochester, MN.

Background: In the post-liver transplant (OLT) setting, central venulitis (CV) can be associated with portal-based acute rejection (AR), de novo autoimmune hepatitis (AIH) or can occur in isolation (ICV). Because protocol allograft biopsies are not performed in many centers, the prevalence and significance of CV (particularly in adults) has not been well defined. We studied adult OLT patients with protocol biopsies and long-term histologic and clinical follow-up, which allowed us to estimate the prevalence and study the natural history of CV.

Design: The study population included 100 consecutive adult OLT patients who met the following criteria: 1) OLT was not performed for primary disease that could recur in zone 3, such as hepatitis C or AIH; 2) protocol liver biopsies were taken; and 3) long-term (≥3 yrs) histologic follow-up was available. CV was defined as centrilobular hepatocyte dropout and hemorrhage with mononuclear inflammation. All allograft biopsies were reviewed for CV and, when present, the following features were scored: 1) portal AR; 2) zone 3 fibrosis; 3) ductopenia; and 4) de novo AIH.

Results: Mean age at OLT was 51 yrs (range, 17-71 yrs); 67 were males and 33 females. A total of 572 allograft biopsies were reviewed (mean, 5.7 per patient) and had been obtained from 4 days to 7.25 yrs post-OLT (mean, 1.4 yrs). CV was seen in 36 (36%) patients: 8 had CV+AR, 15 had ICV with AR at an earlier time point, and 13 had ICV without ever having AR. ICV tended to occur later (mean, 492 days) than

CV+AR (mean, 279 days), p≤.06. In our population, ICV was generally not treated with increased immunosuppression but CV+AR was. On follow-up, 71% of repeat biopsies following CV+AR showed resolved AR and persistent CV; in 7 patients AR subsequently recurred. Nine (25%) patients with CV developed zone 3 fibrosis (including 5 with bridging), 3 (8%) developed ductopenia, and 3 (8%) developed de novo AIH. These adverse outcomes were more common in severe CV than mild CV (p≤.05). One patient with ductopenia required re-transplantation at 3 months, but all 36 were alive at clinical follow-up within the past year.

Conclusions: Central venulitis occurs in 36% of adult OLT patients and tends to persist after AR has resolved. ICV occurs in 28% of cases and tends to occur later than CV+AR. In a significant minority of patients, CV is associated with zone 3 fibrosis (25%) (including bridging fibrosis in 14%), ductopenia (8%) and de novo AIH (8%). Although CV does not appear to impact patient survival, it may contribute to increased morbidity.

1306 Clinicopathologic Findings and Outcome for 12 Liver Transplants with Unusual Donor Diseases

M Krishna, S Pungpapong, SC Abraham, AP Keaveny, RC Dickson, RE Nakhleh. Mayo Clinic, Jacksonville, FL; Mayo Clinic, Rochester, MN.

Background: This report describes 12 liver transplant (LT) cases with uncommon donor liver disease, a majority of which were undetected prior to LT. The cases consisted of donor amyloidosis (AM), schistosomiasis (SCH), iron overload (IO) and alpha-1-antitrypsin deficiency (A1AT).

Design: All LT cases with donor AM, SCH, IO and A1AT were identified. Slides and patient charts were reviewed with the aim of identifying posttransplant findings, clinical course and outcome.

Results: There were 6 cases of donor AM (5 vascular, transthyretin/hereditary; 1 sinusoidal and portal interstitial, type unknown), 3 with SCH, 2 with IO and 1 with homozygous A1AT. Four of 6 donor livers with AM were used as part of domino transplantation; in all other cases the donor disease was unrecognized prior to transplant. The findings were present in the donor biopsies performed at the time of LT in all cases, and absent in explants. There were 9 male and 3 female allograft recipients with ages ranging from 29-71 years. Indications for LT were endstage HCV (4 cases;1 with EtOH, 1 with HCC), EtOH cirrhosis (2 cases, 1 with HCC), cryptogenic cirrhosis (2), and 1 case each of PBC, PSC with cholangiocarcinoma (CC), choledochal cyst/CC, and allograft loss due to biliary necrosis/chronic rejection, respectively. Follow-up biopsies were performed in 11 cases at 1-508 weeks post-LT. Of the 6 cases with AM 2 suffered graft loss due to hepatic artery thrombosis and stenosis at 1 and 18 weeks respectively, both with vascular transthyretin AM, the first case also having interlobular arteritis. One patient died at 53 weeks due to recurrent HCC. The remaining 3 patients had stable graft function at 3-59 weeks. All cases of SCH were confirmed with donor serology, treated with praziquantel after LT, and had stable graft function at 8-72 weeks. IO was persistent in the 2 recipients at 8 and 112 weeks; the latter case also had stage 3 recurrent HCV and underwent multiple phlebotomies beginning at 116 weeks. The 1 case of donor A1AT had stable graft function, but died at 740 weeks due to nontransplant-related cause.

Conclusions: (1) The role of donor vascular transthyretin amyloidosis in hepatic arterial complications is unclear, and needs further study. (2) With treatment donor liver SCH does not appear to impact LT outcome. (3) Donor IO tends to persist and may exacerbate the progression of fibrosis. (4) Donor A1AT may not impact outcome post LT.

1307 Ovarian-Type Stroma in Hepatobiliary Mucinous Cystadenoma and Pancreatic Mucinous Cystic Neoplasms: An Immunohistochemical Study

MM Lam, PE Swanson, MP Upton, MM Yeh. University of Washington, Seattle, WA.

Background: Hepatobiliary mucinous cystadenomas (HBCs) and pancreatic mucinous cystic neoplasms (PMCNs) arise almost exclusively in women, and their pattern of cell differentiation is similar to ovarian MCNs. HBCs and PMCNs comprise mucin-producing epithelial cells lining an ovarian-type stroma that expresses estrogen receptor (ER) and progesterone receptor (PR). Inhibin, secreted by sex cord stromal cells, has been described in pancreatic and ovarian MCNs, but not in HBCs. Furthermore, over-expression of hepatocyte growth factor (HGF) and its receptor, c-met, is involved in a variety of tumors, including ovarian cancers derived from surface epithelium. In this study, we compared the immunohistochemical expression of HGF, c-met, inhibin, ER and PR in PMCNs and HBCs to further understand their morphology and pathogenesis.

Design: Archived cases of 8 HBCs, 10 PMCNs and 6 simple liver cysts were studied immunohistochemically with antibodies to HGF, c-met, inhibin, ER and PR. Stromal density was semi-quantitatively graded from 0 to 3. The percentages of ER and PR positive stromal cells, staining intensity of HGF and c-met in epithelial cells, and inhibin reactivity in stromal cells were semi-quantitatively graded from 0 to 4.

Results: All of our cases of HBCs and PMCNs were found in women (mean ages of 46 vs 55, respectively, p>0.05). All HBCs had abundant stroma, while PMCN stromal density was more variable (3 vs 1.8, respectively, p<0.05).

Immunohistochemical Results (Mean Score)

	ER	PR	Inhibin	HGF	c-met
Hepatobry Mucinous Cystadenoma (HBCs); n=8	3.5	3.5	2.8	1	3.9
Pancreatic MCNs (PMCNs); n=10	1.2	0.9	1.4	0.6	3.7
Simple Liver Cysts; n=6	0	0	0	0.3	2.7

Stromal cells in HBCs had greater ER/PR staining and more consistent focal strong reactivity to inhibin when compared to PMCNs (p<0.05 in all three). Simple liver cysts lacked ovarian-type stroma and were negative for ER, PR and inhibin. HGF expression was not significantly different among the epithelia of HBCs, PMCNs and simple liver cysts, but c-met expression in the epithelium of HBCs and PMCNs was significantly stronger than in simple liver cysts (p<0.05).

Conclusions: HBCs and PMCNs are histologically similar, but careful comparison reveals significant differences in stromal density and reactivity to ER, PR and inhibin, indicating different microenvironments. Additionally, c-met is up-regulated in HBCs and PMCNs compared to simple liver cysts, suggesting that this receptor is activated in the pathogenesis of HBCs and PMCNs.

1308 Overexpression of beta-Catenin Is Associated with the Progression of Human Hepatocarcinogenesis Independent of GSK-3 beta

J Liang, M Losada, L Barisoni, L Chiriboga, H Yee, B West. New York University Medical Center, New York, NY.

Background: Overexpression of ß-catenin has been demonstrated in colon carcinomas, melanomas and human hepatocellular carcinoma (HCC). ß-catenin is regulated by protein complexes, including glycogen synthase kinase-3 ß (GSK-3 ß). When ß - catenin is phosphorylated by GSK-3 ß, it is targeted for ubiquitination and proteasome-mediated degradation. On the other hand, phosphorylation of GSK-3 ß (phospho-GSK-3 ß) results in inactivation of GSK-3ß and stabilization of ß-catenin. ß-catenin binds to transcription factors, translocates to the nucleus and activates the transcription of a variety of target genes. There is conflicting data on the association of phospho-GSK-3 ß with the development of HCC in recent studies. In this study, we analyzed the expression of ß-catenin and GSK-3ß in low-grade and high-grade dysplastic nodules (LDN, HDN) and HCC.

Design: A total of 33 liver specimens were selected, including 10 LDN, 4 HDN and19 HCC. Formalin-fixed, paraffin-embedded sections were immunostained with antibodies to ß-catenin, GSK-3 ß, phospho-GSK-3 ß (Ser9) and CK19. Immunoreactivity was scored based on intensity (0=none, 1= weak, 2=strong) and distribution (0=none, 1=focal, 2= diffuse).

Results: The immunoscores of ß-catenin are summarized in Table 1.
1): There is increased cytoplasmic but decreased membranous expression of ß-catenin in HCC both in intensity and distribution compared with LDN and HDN. There is no significant difference in ß-catenin expression between LDN and HDN. There is no convincing ß-catenin nuclear staining. 2). Expression of either GSK-3 ß or phospho-GSK-3 ß is not detected in hepatocytes in any lesions. 3). In contrast to normal bile ducts, CK19-stained proliferative bile ducts are also stained strongly with both GSK-3 ß and phospho-GSK-3 ß in a diffuse cytoplasmic staining pattern.

Conclusions: 1). Assuming the validity of a progression model of hepatocarcinogenesis: LDN-HDN-HCC, overexpression of beta-catenin is associated with the progression of human hepatocarcinogenesis independent of GSK-3 beta. 2). GSK-3 ß can be used as a marker for identification of proliferative bile ducts.

Table 1: Immunoscores of ß-catenin in LDN, HDN and HCC

	Membranous staining		Cytoplasmic staining	
	Intensity	Distribution	Intensity	Distribution
LDN (n=10)	1.1	1.6	0.8	1.1
HDN (n=4)	1.2	1.5	0.9	1.2
HCC (n=19)	0.7	1.2	1.7	1.8

1309 Expression of Pancreatic Duodenal Transcription Factor 1 (PDX-1) and CDX-2 in Mucinous Cystadenocarcinomas of the Pancreas and Ovary

X Lin, C Deng, JF Silverman, M Tung, YL Liu. Allegheny General Hospital, Pittsburgh, PA.

Background: Pancreatic mucinous cystadenocarcinomas (MCA) is an uncommon malignancy histologically similar to ovarian MCA due to the presence of mucinous epithelium and surrounding ovarian type stroma. PDX-1, a pancreatic-duodenal transcription factor, has recently been reported to be expressed in the pancreatic endocrine neoplasms and adenocarcinomas. CDX-2, an intestinal transcription factor, has also been reported to be expressed in some of pancreatic adenocarcinomas. However, the diagnostic value of PDX-1 and CDX-2 expression in pancreatic mucinous cystadenocarcinoma has not been studied.

Design: 12 pancreatic MCAs and 22 ovary MCAs were retrieved from the hospital computer system. Immunostaining for PDX-1 and CDX-2 together with cytokeratins CK7 and CK20 were performed on an automated immunostainer with appropriate positive and negative controls. The statistical analysis was performed with Chi-square test.

Results:

Immunohistochemical results of PDX-1, CDX-2, CK7 and CK20 in MCAs

Primary	No.	PDX-1	CDX-2	CK7	CK20
Pancreas	12	100.0%*	66.7%*	83.3%	100.0%*
Ovary	22	54.5%	9.1%	100.0%	54.5%

*: P < 0.01.

Conclusions: PDX-1 and CDX-2 positivity is more frequently seen in pancreatic MCAs than in histological similar ovarian MCAs. However, expression of PDX-1 in all pancreatic MCAs and ovarian MCAs with positive CK20 suggest that some ovarian MCAs may share a similar histogenesis with pancreatic MCAs. In the working-up of metastatic MCA of unknown origin, negative staining for PDX-1 and CK20 are more consistent with ovarian MCAs.

1310 The Effect of Sindbis Viral Vectors on the N-Nitroso-Bis(2-Oxopropyl)Amine(BOP) Induced Hamster Pancreatic Ductal Adenocarcinoma and Cholangiocarcinoma

Q Liu, AB West, S Merali, B Levin, D Meruelo, A Pellicer. NYU School of Medicine, New York, NY.

Background: Sindbis viral vectors have the ability to infect mammalian tumor cells through a laminin receptor, which is substantially upregulated in numerous human tumors including pancreatic cancer.

Design: This study was done to evaluate the suitability of a BOP induced hamster pancreatic cancer model for cancer gene therapy with Sindbis viral vectors. 20 female Syrian golden hamsters were used. 18 of the hamsters were injected s.c. 70 mg BOP/per kg of body weight, followed by 3 injection of 20 mg BOP/per kg with 3 cycles of choline-deficient diet, DL-ethionine and L-methionine in 10 weeks. 2 hamsters were not injected with BOP and used as negative controls. 10 weeks after initiation, plasma levels of S-adenosyl-L-methionine (AdoMet, SAM) were determined. 9 BOP injected hamsters received daily i.p. injections of Sindbis vectors for 8 weeks and the other 9 BOP injected hamsters were given PBS buffer. Blood was drawn at 4 weeks after the Sindbis and PBS injection started. The hamsters were sacrificed at 8 weeks after the Sindbis and PBS injection and organs including pancreas and liver were harvested for histology and molecular studies.

Results: The levels of AdoMet were increased in all hamsters at 10 week after BOP initiation (5.1-10.9 µM, normal: <5 µM). The levels of AdoMet slightly decreased in BOP injected hamsters treated with Sindbis vector at four weeks after the injection (5.12 vs 6.55 µM). At autopsy, no pancreatic tumors were identified in pancreas on gross examination. However, microscopic examination revealed pancreatic ductal adenocarcinomas/Pancreatic intraepithelial neoplasia III(PanIN III) in 3 out of 9 BOP injected hamsters treated with Sindbis vector compared to 7 out of 9 BOP injected hamsters treated with PBS. The livers of BOP injected animals were extensively cirrhotic on both macroscopic and microscopic examination. Cholangiocarcinomas were found in 7 out of 9 BOP injected hamsters treated with Sindbis vector and 8 out of 9 BOP injected hamsters treated with PBS.

Conclusions: Sindbis viral vectors appeared to decrease the manifestation of BOP induced pancreatic ductal adenocarcinomas but not that of BOP induced cholangiocarcinomas. Immunohistochemistry and molecular studies would be used to determine the laminin receptor levels in hamster pancreas and liver, which may explain the difference between pancreas and liver in response to the treatment with Sindbis viral vectors.

1311 The Tubulin Beta-4 Polypeptide (TUBB4), a Marker of Resistance to Taxanes, Is Overexpressed in Pancreatic Intraepithelial Neoplasia and Pancreatic Ductal Adenocarcinoma

A Maitra, D Cao, K Lee, A Itami, RH Hruban, M Ouellette. The Johns Hopkins Hospital, Baltimore, MD; Eppley Institute for Research in Cancer, Omaha, NE.

Background: Alteration in beta-tubulin isotype selection has emerged as an important mechanism of taxane resistance in breast, prostate, lung and ovarian cancers. Expression of the tubulin beta-4 polypeptide (TUBB4; also known as class III beta-tubulin) has been associated with resistance to paclitaxel and taxotere, two commonly used microtubule-stabilizing anticancer agents. Pancreatic ductal adenocarcinomas (PDA) demonstrate limited responsiveness to paclitaxel, and the recent availability of an immunohistochemical assay can permit identification of TUBB4-negative cases as potential candidates for therapy with this agent. In this study, we analyzed TUBB4 expression in a series of archival PDAs; in addition, we examined TUBB4 labeling in Pancreatic Intraepithelial Neoplasia (PanIN), in order to determine whether abnormal microtubule dynamics are a feature of precursor lesions of PDA.

Design: Tissue microarrays (TMAs) were generated from archival specimens of 49 PanINs (PanIN1 19, PanIN2 22 and PanIN3 8) and 60 PDAs. Each adenocarcinoma was represented with up to 4 cores on TMAs, to exclude tissue heterogeneity. Immunolabeling with anti-TUBB4 was scored as negative (expression in < 5% lesional cells), focal (5-25% expression) and diffusely positive (>25% expression).

Results: No TUBB4 labeling was evident in non-neoplastic pancreatic ductal epithelium, including both inter- and intra-lobar ductal epithelium. In contrast, the vast majority (47/60 or 78%) of PDAs demonstrated either diffuse (43/60) or focal (4/60) TUBB4 overexpression. TUBB4 was also progressively overexpressed in the histologic spectrum of non-invasive precursor lesions, including 3/16 (19%) PanIN-1, 5/17 (29%) PanIN-2, and 5/8 (63%) PanIN-3 lesions.

Conclusions: TUBB4 is overexpressed in most PDAs, possibly accounting for the suboptimal response to microtubule-stabilizing agents. Nevertheless, TUBB4 immunohistochemical labeling can help identify subsets of patients who might benefit from such therapy. The upregulation of TUBB4 in non-invasive precursor lesions of PDA suggests that microtubule dysfunction is an early feature in the multistage pathogenesis of this cancer.

1312 Steatosis in Human Immunodeficiency Virus and Hepatitis C Virus Co-Infected Patients

MP Murray, KM Marks, AH Talal, RM Gulick, MJ Glesby, LM Petrovic. Weill Medical College Cornell University, New York, NY.

Background: Hepatic steatosis is a common finding in liver biopsies from patients with hepatitis C virus (HCV)-related liver disease. The prevalence, severity and impact of steatosis are poorly understood in HIV/HCV co-infected patients. Whether steatosis is associated with more extensive liver fibrosis, host factors such as diabetes, body mass index (BMI), and antiretroviral therapy (ART) is currently the topic of great interest.

Design: Liver biopsies from HIV/HCV patients (n=106) were evaluated and graded for inflammation, steatosis/steatohepatitis, and staged for fibrosis. The inflammation and fibrosis were graded/staged based on the modified Scheuer's grading/staging system for chronic hepatitis. Steatosis/steatohepatitis were assessed based on the criteria proposed by Brunt et al. Patient records were retrospectively reviewed to elucidate risk factors for steatosis.

Results: Steatosis was present in 56% of biopsies, with grade 2-3/3 in 7%. The overall fibrosis stage was higher in patients with steatosis compared to the group without steatosis (p=0.06). Steatosis was also associated with more advanced pericellular fibrosis (p=0.03). Necroinflammatory grade was not associated with the presence of steatosis. The median duration since HIV diagnosis was 10 yrs; median

CD4 was 413 cells/ul at time of biopsy. 58% had an AIDS diagnosis, 88% had history of ART and 67% were on ART at biopsy. Of pts with available HCV genotypes, 92 (87%) were 1a or b, 5 were 2a or 2b, and 4 were 3a. Of 104 pts with available HCV viral loads, 63 (59%) had >1,000,000 copies/ml. Median BMI was 26.0 and was similar in men and women; 10 (10%)of patients were diabetic. On univariate analysis, steatosis was positively associated with BMI (odds ratio [OR]=1.12 per kg/m2, 95% confidence interval [CI]=[1.002-1.25], p=0.04), nadir CD4 count (OR=1.13 per 50 cells/ul, CI=[1.00-1.27], p=0.04), and log HIV RNA (OR=1.49, CI=[0.99-2.24], p=0.05). Alcohol use and duration of ART use were not associated with the presence of steatosis. On multivariate analysis, steatosis was associated with HDL (OR=0.75, CI=[0.56-1.00], p=0.05), and BMI (OR=1.15, CI=[1.00-1.32], p=0.04).

Conclusions: Our results suggest that in HIV/HCV co-infected patients, steatosis is common, and when present is associated with more advanced fibrosis, including pericellular fibrosis. Steatosis was also associated with higher BMI.

1313 Double Immunohistochemical Staining with MUC4/P53 Is Useful in the Distinction of Pancreatic Adenocarcinoma from Chronic Pancreatitis- A Tissue Microarray Based Study

JW Nash, A Bhardwaj, P Wen, C Barbacioru, S Jones, WL Frankel. Ohio State University, Columbus, OH.

Background: Several immunohistochemical stains have been proposed as useful in the distinction of pancreatic adenocarcinoma (PA) from chronic pancreatitis (CP) such as maspin, MUC4, p53 and Smad4. We compared these stains and determined if a double stain with MUC4/p53 improved the specificity and sensitivity for the distinction of PA from CP.

Design: Seventy-two cases of PA and 18 cases of CP were retrieved from the archival files. Carcinomas were graded as well, moderately, or poorly differentiated using WHO criteria. Tissue cores from formalin-fixed, paraffin embedded donor blocks (2 cores per block) were arrayed to create a tissue microarray of cores measuring 2.0 mm each. Sections were stained with antibodies against maspin, MUC4, p53, and Smad4. Additionally, a two color, double stain for MUC4 and p53 was developed and evaluated. Five percent or greater staining in either of the cores was interpreted as positive, and the intensity (0,1,2,3) and percentage of tumor cells staining were evaluated by 2 pathologists. Sensitivity, specificity and correlation with tumor differentiation were determined.

Results: The sensitivity for distinction of PA from CP was 90% with maspin, 77% with MUC4, 63% with Smad4, and 60% with p53; while the specificity was 88% with p53 and Smad4, 78% with MUC4 and 67% with maspin. A two color, double stain was developed using MUC4 and p53 since these antibodies showed staining limited to either the cytoplasm or nucleus, respectively, avoiding interference of interpretation between the stains. When MUC4 and p53 were combined, and positive staining for either considered a positive result, the sensitivity for detecting PA increased to 95% but specificity fell slightly to 73%. When immunoreactivity for both antibodies was necessary for a positive, the sensitivity fell to 39% but the specificity was 100%. No correlation was found between intensity or extent of staining with any of the stains and degree of tumor differentiation.

Conclusions: The single most sensitive immunohistochemical stain for the distinction of PA from CP was maspin, while the most specific stains were p53 and Smad4. Sensitivity with the double stain for MUC4/p53 was greater than any of the individual stains while specificity remained high. The double immunohistochemical stain for MUC4/p53 can be a useful diagnostic tool in conjunction with the H&E stained section for the diagnosis of PA particularly when limited tumor is available for the performance of multiple stains.

1314 Hepatitis C Recurrence and Acute Cellular Rejection Following Orthotopic Liver Transplantation (OLTX): A Histopathologic Preliminary Report on the "Hepatitis C 3" Trial

GJ Netto, C Fasola, M Abecassis, the Hepatitis 3 Trial Group. Baylor University Med Ctr, Dallas; Emory University; Northwestern University.

Background: The primary objectives of the Hepatitis C 3 trial are to compare the rates of hepatitis C (HCV) recurrence, acute cellular rejection (ACR), and treatment failure (death, graft loss or >1 dose of corticosteroid for presumptive rejection) among three immunosuppressive Rx regimens.

Design: The trial is an open-label, prospective, randomized multicenter study involving adult patients receiving OLTX for end stage HCV liver disease randomized to three Rx Arms : arm 1: tacrolimus (TAC) and steroids (Pred); arm 2: TAC, mycophenolate mofetil (MMF) and Pred; and arm 3: TAC, MMF and daclizumab (steroid free arm). A total of 312 pts from 17 institutions will be randomized at a ratio of 1:1: 2. Per protocol, liver biopsies are obtained at days 1, 90, 365 and 730. All biopsies are reviewed by a central pathologist. All hepatitis C recurrences and rejections were biopsy documented. HCV recurrence is evaluated according to Batts and Ludwig schema (Batts et al. Am J Surg Pathol 1995: p1409). ACR is evaluated using the 1997 Banff schema (Demetris et al. Hepatology 1997: p658). Primary composite end points are defined as a recurrent HCV of stage ≥ 2 during the first year or grade ≥3 at any point post transplantation and or an ACR of Banff global grade ≥2 with RAI score ≥4 . The current abstract summarizes the histologic findings of 276 biopsies obtained from 125 pts with a F/U range of (6-382 days) post OLTX..

Results: HCV recurrence: Histologic HCV recurrence as defined above was established in 46/125 pts (36.8%). 23 (50%) of HCV recurrences were diagnosed on or before day 90 post OLTX (18.4 % three months recurrence rate). The shortest and longest durations to HCV recurrence were 40 and 371 days post OLTX respectively.
ACR: Histologic ACR as defined above was established in 12/125 pts (9.6%). Only one pt had two episodes of ACR with the second episode being severe (Banff global grade 3). The RAI scores range was 4-7. The majority of ACR's occurred in the first month (70 %) with the earliest and latest ACR occurring on days 3 and 70 respectively.

Conclusions: At three months post OLTX, 36.8 % HCV recurrence rate and 9.6% ACR incidence is histologically demonstrated in 125 pts with complete data and histology reported to the study center in the Hepatitis C 3 trial. Pts accrual has been completed in March 2004. An updated report on histologic findings in all pts completing 12 months F/U will be presented.

1315 Evaluation of Interobserver Agreement in Hepatitis C Grading/Staging and ACR Grading: The "HCV 3" Multiinstitutional Trial Experience

GJ Netto, G Klintmalm, The Hepatitis C 3 Trial Group. Baylor University Medical Ctr., Dallas, TX.

Background: Primary objectives of the Hepatitis C (HCV) 3 trial are to compare the rates of hepatitis C recurrence, acute cellular rejection (ACR), and Rx failure among three immunosuppressive regimens. By design, clinical management decisions are based on local pathologist's interpretations of liver Bx's. Therefore, demonstrating acceptable degree of interobservers agreement between local and central pathologist is crucial.

Design: HCV 3 Trial: The trial is an open-label, prospective, randomized multicenter (17 institutions) study involving 312 pts undergoing OLTX for end stage HCV. Pts are randomized to 3 Rx Arms. Liver Bx's are obtained at days 1, 90, 365 and 730. For final data analysis, all Bx's are reviewed by a Cpath. HCV recurrence is evaluated according to Batts and Ludwig schema (Batts et al. Am J Surg Pathol 95). ACR is evaluated using the 1997 Banff schema (Demetris et al. Hepatology 97). Primary composite end points are defined as a recurrent HCV of stage≥ 2 during the first year or grade ≥3 at any point or an ACR of Banff global grade≥ 2 with RAI score≥ 4 . Interobserver Agreement: H&E sections (two sets of identical recuts) from 11 liver biopsies (5 ACR and 6 HCV) were sent by the central pathologist to 16 local pathologists from 12 institutions. For each slide, pathologists (including central pathologist) completed an ACR/HCV worksheet designed for HCV 3 trial data collection illustrating the Banff/Batts & Ludwig critiria. Statistical analysis was performed on raw ACR/HCV data as well as on ACR/HCV data grouped according to the clinically significant "primary endpoints" cut-off's.

Results: Statistically significant agreement was found among all participating pathologists. Agreement was stronger for HCV grading/staging compared to ACR grading. Agreement was relatively stronger when data were grouped based on end point cut off's.

Variable (Raw)	Kendall C.C.	Kappa	p value
HCV Grade	0.72	0.30	0.0001
HCV Stage	0.85	0.33	0.0001
ACR global	0.56	0.37	0.0001
ACR RAI	0.57	0.15	0.0001

Variable (End Points Grouping)	Kappa	p value
HCV Grade	0.76	0.0001
HCV Stage	0.76	0.0001
ACR global	0.62	0.0001
ACR RAI	0.62	0.0001

Conclusions: An acceptable Interobserver agreement in grading and staging of HCV and in grading ACR is found among 17 hepatopathologists participating in HCV 3 trial.

1316 Copper Stain in Chronic Biliary Disease: An Aid To Diagnosis?

H Qureshi, SC Abraham, TC Smyrk. Mayo Clinic, Rochester, MN.

Background: Stainable copper accumulates in the hepatocytes of patients with chronic biliary disease, and can be detected with a histochemical stain. We studied biopsies from patients with chronic biliary disease and controls in order to assess the relationship stainable copper, diagnosis, and stage of disease.

Design: Pathology files were searched for cases demonstrating all stages of primary biliary cirrhosis (PBC), primary sclerosing cholangitis (PSC), sarcoidosis, chronic hepatitis C and steatohepatitis. A series of biopsies showing acute panacinar cholestatic hepatitis was also identified. We applied a rhodanine stain to all biopsies, and scored stainable copper as follows: no copper = 0; copper in rare periportal hepatocytes = 1, patchy periportal staining = 2; circumferential periportal staining = 3; staining in non-periportal hepatocytes = 4. All H and E slides were reviewed to confirm diagnosis and stage of disease.

Results: Stainable copper was detected in the chronic biliary diseases with the prevalence and mean score shown in Table 1. Copper was not detected on 18 cases of steatohepatitis or 8 cases of acute panacinar cholestatic hepatitis. Three of 15 biopsies with sarcoidosis had stainable copper; all had duct damage and at least stage 2 disease. Two of 21 biopsies with chronic hepatitis C had stainable copper; both were cirrhotic.

Conclusions: Copper accumulates in the liver of patients with chroinic biliary disease. Both the prevalence and extent of positive staining increase with increasing stage of disease, reaching 100% in stage 4 disease. While the prevalence of stainable copper is lower in stage 1 disease (30% for PBC and 47% for PSC), a positive result adds support for the diagnosis.

Table 1: Prevalence and (mean score) of copper

Stage	PBC	PSC
1	6/20 (0.4)	8/17 (0.8)
2	14/16 (1.3)	10/16 (1.0)
3	9/9 (2.2)	21/24 (2.7)
4	6/6 (3.2)	15/15 (3.3)

1317 Stellate Cell Activation in Liver Biopsies with Hepatitis C Compared with Hepatitis C/Diabetes Mellitus

M Rivera, F Ahmed, LM Petrovic. NYPH-Weill Cornell Medical Center, New York, NY.

Background: Hepatits C virus (HCV) infection is a major cause of chronic liver disease. Steatosis is a common finding both in HCV and in diabetes mellitus (DM). Hepatic stellate cell activation, manifested by the expression of smooth muscle actin (SMA), is a major factor responsible for fibrosis and its progression in chronic liver disease. The aim of this study was to assess and compare the degree of stellate cell activation in liver biopsies of patients with HCV alone and in patients with HCV/DM.

Design: A total of 69 liver biopsies were evaluated: HCV (n=39), and HCV/DM (n=30). All biopsies were immunostained with the antibody for smooth muscle actin (SMA). A grading system on a scale of 0-3 was applied reflecting the percentage of stellate cell activation which occurred in each zone of the hepatic acinus. Statistical analysis (t-test and Wilcoxon rank-sum test) was implemented to determine if stellate cell activation differed at a given stage of fibrosis, grade of inflammation and steatosis in comparing the aforementioned groups.

Results: The mean stage of fibrosis for the HCV/DM and HCV group were 2.8 and 1.6 respectively (p<.0001). The mean grade of inflammation for the HCV/DM group and HCV group were 1.9 and 1.5 respectively (p=0.03). The mean grade of steatosis for the HCV/DM and HCV group were 1.1 and 0.5 respectively (p=0.01). The average grade of stellate cell activation for all zones for the HCV/DM group and HCV group was 1.3 and 1.2 respectively (p=.39). However, in both diagnostic groups combined, a significant stellate cell activation was observed in the zone 1 of the acinus and portal tracts for higher stages (>2) vs lower stages (≤2) of fibrosis (p<.0001). In addition, a statistically significant increase in stellate cell activation was observed in zone 1 for the HCV/DM group (mean=1.5) as compared to the HCV group (mean=1.2) regardless of stage of fibrosis (p=.02).

Conclusions: The results suggest that the activated stellate cells are predominantly present in zone 1 of the acinus, which correlates with advanced stages (>2) of fibrosis. Zone 1 stellate cell activation is significantly increased in the HCV/DM group as compared to the HCV group.

1318 Lymphatic Vessel Density and VEGF-C Expression Correlate with Malignant Behavior in Human Pancreatic Endocrine Tumors

L Rubbia-Brandt, B Terris, E Giostra, B Dousset, P Morel, MS Pepper. Geneva University Hospital, Geneva, Switzerland; Hopital Cochin, Paris, France.

Background: Metastatic dissemination of tumor cells to regional lymph nodes is a common early feature of many human cancers including pancreatic adenocarcinoma. In contrast, lymph node metastasis is more variably observed in pancreatic endocrine tumors.

Design: The objective of this study was to assess the lymphatic system of human pancreatic endocrine tumors and to correlate this to clinical behavior. Immunohistochemistry was performed using antibodies to two recently identified markers of lymphatic endothelium, namely LYVE-1 and podoplanin, and to the lymphangiogenic factor, vascular endothelial growth factor-C (VEGF-C).

Results: As has previously been reported, we observed that in the normal pancreas, islets of Langerhans are devoid of intra-islet lymphatics, but that lymphatics are present in connective tissue in association with ducts and blood vessels. We found that both benign and malignant pancreatic endocrine tumors contain intra-tumoral lymphatic vessels. Lymphatic vessel density was related to the size of the tumor in benign tumors, and to the presence of liver metastasis but not to lymph node metastasis in malignant tumors. VEGF-C was expressed in tumor cells: 4/19 (21 %) of benign tumors were positive while of 6/9 (67%) of borderline tumors and 9/11 (82%) of carcinomas were positive.

Conclusions: These findings strongly suggest that lymphangiogenesis occurs in pancreatic endocrine tumors and that lymphatic invasion and the development of metastases are associated with VEGF-C expression.

1319 Maspin Is Overexpressed in the Majority of Pancreatic Ductal Adenocarcinomas and Pancreatic Intraepithelial Neoplasia (PanIN) Lesions: A Potential Biomarker for Early Detection

S Salaria, M Cronin, E Kim, Q Zhang, A Maitra, C Neumann, RH Hruban, MG Goggins, JL Abbruzzese, L Ho. Johns Hopkins University, Baltimore, MD; U.T. M. D. Anderson Cancer Center, Houston, TX.

Background: Maspin, a serine protease inhibitor, is downregulated in breast and prostate cancers. However, we recently identified Maspin as a differentially *over*expressed gene in pancreatic adenocarcinomas using suppression subtraction hybridization. The pattern of Maspin expression in the multistage progression of pancreas cancer has not been systematically examined. Therefore, Maspin immunolabeling was performed in a large series of archival pancreatic adenocarcinomas and Pancreatic Intraepithelial Neoplasia (PanIN) using a high-throughput tissue microarray (TMA) approach.

Design: TMAs were constructed from 300 archival pancreatic cancer specimens and matched non-neoplastic pancreatic tissues. Multiple (2-4) cores were represented from each cancer to exclude effects of heterogeneous antigen expression. A PanIN TMA comprised of 37 lesions of all histologic grades was also constructed. Monoclonal anti-Maspin was used for immunohistochemical labeling, and a four-tiered scoring scheme based on intensity was adopted: negative (0), 1+, 2+, and 3+. In cases with heterogeneous expression, the predominant staining pattern was assigned. PanIN cores were scored as positive (+) or negative (-) only. Maspin scores were correlated with a variety of clinicopathological parameters, including tumor size, differentiation, stage, and patient survival.

Results: Of the 300 primary pancreatic cancer specimens, Maspin expression was 3+ in 101 (34%), 2+ in 105 (35%), and 1+ in 73 (24%); 21 (7%) cases lacked Maspin expression. Of the 37 PanIN lesions, 22 (60%) were positive, and 15 (40%) lacked Maspin expression. By histologic grade, 13/27 (48%) low-grade PanIN (1A and 1B) and 9/10 (90%) high-grade PanIN (2 and 3) expressed Maspin. Non-neoplastic pancreatic parenchyma, including ductal epithelium, acini, and islets, did not demonstrate Maspin expression. Maspin expression in the 300 pancreatic cancers demonstrated no significant correlation with tumor size, differentiation, metastases, or survival.

Conclusions: Maspin is overexpressed in the vast majority of infiltrating adenocarcinomas of the pancreas but not in normal pancreatic tissues. Maspin expression in non-invasive precursor lesions of pancreatic cancer signifies its importance as a potential early detection biomarker for patients at risk for developing this deadly disease.

1320 Immunohistochemical Labeling for Deoxycytidine Kinase (dCK) in Pancreatic Cancer Correlates with Response to Gemcitabine

V Sebastiani, S Witzel, F Ricci, D Laheru, C Iacobuzio-Donahue. The Johns Hopkins Hospital, Baltimore, MD.

Background: Deoxycytidine kinase (dCK) is an enzyme involved in the phosphorylation of 2'-deoxycytidine to its active form, as well as the phosphorylation of many deoxynucleoside analogues, such as gemcitabine, used in anticancer chemotherapy. Deficiency of dCK protein, due to a mutation or a deletion of the gene, has been reported as a mechanism of resistance to these molecules and failure of chemotherapy. The aim of our study was to evaluate dCK immunohistochemical expression in human pancreatic cancers, and to correlate that expression with the genetic status of the gene.

Design: Thirty-six cases of surgically resected, Gemcitabine-naïve pancreatic cancer were collected. IHC for dCK was performed using polyclonal anti-human dCK antibody at a 1:200 dilution following standard techniques. The slides were scored blindly by two of the authors (V.S. and C.I.D.) with agreement in all cases. For nineteen patients for which the primary carcinoma was immunostained, the complete treatment history was also obtained. Clinical responses and immunostaining patterns were compared using a Fisher exact test.

Results: Thirty-one cases were conventional infiltrating duct adenocarcinoma, 2 were acinar cell carcinomas, 1 was mucin producing carcinomas, 1 mucinous cystic adenocarcinoma and 1 microcystic cystoadenocarcinoma. dCK protein was always detectable within the cytoplasm of normal acinar cells and islets, as well as in the nuclei of normal lymphocytes and stromal cells. Among infiltrating carcinomas, dCK was expressed in 29 (80.5 %) cases. Ten cases (34.5%) showed nuclear staining only, 4 cases (13.8%) cytoplasmic staining only, and 15 cases (51.7%) showed both patterns. Seven cases (19)% were negative for dCK protein within the neoplastic epithelium. Strong intensity was detected in 15 of the 29 positive cases (51.7%). For 19 patients, dCK immunostaining patterns were correlated with the observed clinical response, including CA19-9 levels pre and post treatment. Complete lack of dCK immunostaining was correlated with failure of Gemcitabine treatment and disease progression, whereas strong positive dCK showed a trend with stable disease (p<0.1).

Conclusions: dCK is expressed in the majority of pancreatic cancers and shows different patterns of cellular localization (cytoplasm versus nucleus) and a range of expression intensities that may have biologic significance. The pretreatment measurements of dCK protein levels in paraffin-embedded tissues might be of useful predictive value in the clinical setting.

1321 Analysis of MSI and Cdx2 Expression in Adenocarcinomas of the Ampulla of Vater

F Sessa, F Franzi, C Zampatti, D Furlan, C Capella. University of Insubria, Varese, Italy; Ospedale di Busto Arsizio, Busto Arsizio, Varese, Italy.

Background: Microsatellite instability (MSI), an indicator of mutation of mismatch repair genes, has been reported in a variety of malignant tumors. The role of MSI in the development of adenocarcinomas (AC) arising from the ampulla of Vater (AV) has not yet been well established because only a few studies have been done on this topic.

Design: Seventy nine surgically resected (Whipple procedure) invasive AC, 44 from the AV and 35 from head of pancreas (HP) were immunostained for hMLH1, hMSH2 and Cdx2 using avidin-biotin-complex method, with positive and negative control. The MSI status of AC of AV was established by a fluorescent pentaplex PCR at Bat-26, Bat-25, NR-21, NR-22, NR-24 mononucleotide markers using an automated DNA sequencer (Applied Biosystems 310).

Results: According to Cubilla and Fitzgerald (1980) we classified the AC of AV as periampullary (11/44), intra-ampullary (26/44) and mixed (7/44). Twenty eight were of intestinal type (Cdx2 positive) and 16 were of pancreatobiliary type (Cdx2 negative). Cdx2 was detected in 12/26 (46%) intra-ampullary ACs and in 16/18 (89%) of the other types with a p=0,0089. MSI was detected in 6 cases; 1 with hMLH1 and hMSH2 nuclear positivity and 5 without hMLH1 nuclear positivity; all cases were Cdx2 positive and classified as of the intestinal type. Three out of six MSI AV-AC were intra-ampullary, 2 were periampullary AC, and 1 was of mixed type. Histologically one case had mucinous pattern, 3 were ACs with a minor mucinous component and 2 were poorly differentiated, medullary-type AC. No MSI was found in the HP ductal carcinomas and Cdx2 was detected only in 2 of them.

Conclusions: This study indicates that MSI is involved in the development of subset of ampullary carcinoma of intestinal type showing the same histologic features of MSI colorectal cancer(mucinous pattern or rich peritumoral lymphocitic infiltrate). Periampullary and mixed AC of the AV are from intestinal mucosa. Pancreatobiliary AC of the AV, like pancreatic cancer do not express MSI. Cdx2 can be useful to distinguish AC of AV of the intestinal type from HP carcinoma.

1322 The Expression of PDGF-C in Non-Alcoholic Steatohepatitis: A Trend of Increase as Fibrosis Progresses and a Pattern of Centrilobular Accentuation

AJ Shaw, JS Campbell, N Fausto, J Dai, MM Yeh. University of Washington, Seattle, WA.

Background: Non-alcoholic steatohepatitis (NASH) can progress to fibrosis, cirrhosis and hepatocellular carcinoma. However, the exact mechanisms leading to fibrosis remain largely unknown. Platelet-derived growth factor (PDGF) especially PDGF-B produced by activated hepatic stellate cell (HSC) is well known to perpetuate liver fibrosis. PDGF-C is a novel member of the PDGF family that has been implicated in the development of fibrosis in a few organs, including cardiac fibrosis. We examine the expression of PGDF-C in NASH and its relationship to activated HSC.

Design: 46 consecutive NASH cases were retrieved from our archive during a period from 2000 to 2001. All were core biopsy specimens. Routine stains including H/E, trichrome, and PAS with diastase were reviewed. The liver biopsies were graded and staged using the Brunt criteria. Double immunohistochemical stains for PGDF-C and smooth muscle actin (SMA) were performed to evaluate for the cells expressing PGCF-C and the presence of activated HSC. The SMA and PDGF stains were semiquantitatively scored from 0 to 3.

Results: The staining of PDGF-C is mainly seen in the cytoplasm of sinusoidal endothelial cells and there is no staining in normal liver. The staining of SMA is noted in the activated HSC. Double staining of PDGF-C and SMA are noted in some activated HSC. The scores of single PDGF-C as well as SMA stainings are significantly greater in the centrilobular than in periportal regions, when compared at the same stage or across stages (p<0.05). The scores of PDGF-C staining show a trend of increase as the stages increase, both in central and periportal regions (p<0.05, respectively). The expression of PDGF-C in periportal region shows a trend of increase when the grades increase (p<0.05). The scores of PDGF-C staining in periportal region increase when the amount of fat increases (p<0.05).

Conclusions: The expression of PDGF-C and SMA shows a centrilobular accentuation, reflecting the typical pattern of injury and fibrosis seen in NASH. There is a trend of increase in PDGF-C expression as fibrosis progresses. These findings suggest PDGF-C may play an important role in the progression of hepatic fibrosis in NASH.

Mean scores of immunohistochemical staining

Stage	SMA portal	SMA central	PDGF-C portal	PDGF-C central	Double portal	Double central
0	0.71	1.4	0.29	0.64	0	0.29
1	0.42	1.3	0.47	0.94	0.28	0.53
2	0.77	1.6	0.73	1.3	0.19	0.5
3/4	0.3	0.7	0.8	1.6	0.15	1.1

1323 Detection of Lymphatic Invasion in Pancreatic Cancers Based on Immunohistochemistry of D2-40

Y Shimizu, S Ban, T Mitsuhashi, F Ogawa, T Hirose, M Shimizu. Saitama Medical School, Iruma, Saitama, Japan.

Background: Lymphatic invasion is an important microscopic finding when examining surgical specimens of pancreatic cancer. Recently, a new monoclonal antibody D2-40 has been reported as a marker of lymphatic endothelium. Several studies have been done for the evaluation of lymphatic invasion in various cancer cases; however, none of them have paid specific attention to cases of pancreatic cancer. In this present study, we performed immunohistochemical staining with D2-40 in cases of pancreatic cancers to evaluate its usefulness to detect lymphatic invasion.

Design: Forty cases of invasive pancreatic cancer (25 cases with lymph node (LN) metastases, 15 without LN metastases) were investigated. A representative section was selected in each case, and the detection rate of lymphatic invasion was compared between routine hematoxylin and eosin (HE)-stained slides and immunohistochemical-stained slides using D2-40 (Signet Laboratories Inc.). Slides were stained with both 3,3'-diaminobenzidine (DAB) and alkaline phosphatase (APase)-Fast Red as the chromogen, and the immunostaining results were also compared.

Results: By using immunohistochemical staining, 10 out of 40 cases (25%) were noted to have lymphatic invasion. These included 7 of 25 cases with lymph node metastases and 3 of 15 cases with negative lymph node involvement. On the other hand, lymphatic invasion was observed in only 4 cases by HE-stained slides alone. These 4 cases showed lymph node metastases as well. As for the chromogen, the APase-Fast Red detection method was superior to the DAB detection method. In other words, the former enabled clearer visualization of the lymphatic endothelium than the latter in this study.

Conclusions: Our findings indicate that D2-40 is useful to detect lymphatic invasion in cases of pancreatic cancers, especially by using the APase-Fast Red rather than DAB as the chromogen. As shown above, lymphatic invasion may be overlooked when only HE stain is used, even for positive LN cases.

1324 Lipid-Rich Pancreatic Endocrine Neoplasms (PENs): Characterization of a Clinicopathologically Distinct Variant

RS Singh, O Basturk, G Zamboni, DS Klimstra, R Chetty, S La Rosa, JD Cheng, CV Capella, NV Adsay. Wayne State University, MI; Verona University, Italy; Memorial Slaoan-Kettering Cancer Center, NY; University of Insubria, Italy; University of Toronto, Canada.

Background: Most PENs show the typical endocrine morphology; however, a lipid-rich pattern, which is typically a diagnostic problem in biopsies, has been reported mostly as individual cases. Some have been included in the rare clear-cell variant, associated with von Hippel-Lindau (VHL). The histogenesis, clinicopathologic characteristics and significance of this lipid-rich pattern have not been unraveled.

Design: 11 PENs characterized by foamy/microvesicular cytoplasm were analyzed.

Results: _Histopathology:_ The cells had abundant foamy/microvesicular cytoplasm. In some cases, the nuclei were obscured by the vesicles, and the endocrine chromatin pattern was not as evident. The growth pattern was relatively diffuse with vague compartmentalization of the cells by a delicate vasculature; prominent nesting was noted in only 4 cases. Pathology reports indicated substantial diagnostic challenge in these cases: On biopsies, 1 case was misdiagnosed as adrenocortical neoplasm, 2nd as RCC and a 3rd as solid-pseudopapillary tumor. All were chromogranin and synaptophysin positive. _EM:_ (in 3 cases) confirmed the cytoplasmic vesicles to be lipid vacuoles. Neuroendocrine granules were evident. _Clinical:_ As in ordinary PENs, there appeared to be 2 distinct subsets: _Familial/Syndromic_ group (1 VHL, 1 MEN-1 and 1 glucagonoma) was seen mainly in younger adults (mean age: 43), whereas the _non-syndromic/nonfamilial_ cases (n=8) were mostly in elderly males (mean age: 65 vs 58 in ordinary PENs). _Pathogenesis:_ IHChemically, markers implicated in VHL-associated neoplasia including HIF1-α, inhibin and melan-A (in clear cell PENs) and MUC6 (in serous adenomas) were mostly negative in this group (1/10, 0/10, 0/10 and 0/10, respectively).

Conclusions: Lipid-rich pattern reminiscent of adrenal cortex identifies a clinicopathologically distinct subset of PENs. It presents a diagnostic challenge for surgical pathologists, especially in biopsies. EM supports the name lipid-rich for this variant. The accumulation of lipid in syndromic patients (usually younger age) maybe an intrinsic biologic defect, whereas in the non-syndromic cases (mostly elderly males) the process may be senescence-related. The findings also suggest that the pathogenesis of lipid-rich tumors may be different than the VHL-associated clear cell variants of PENs.

1325 Prevalence of Pancreatic Intraepithelial Neoplasia in Non-Ductal Type Neoplasms of the Pancreas

EB Stelow, DJ Chute, CA Moskaluk. University of Virginia, Charlottesville, VA.
Background: Pancreatic intraepithelial neoplasia (PanIN) is currently considered a precursor lesion for the development pancreatic ductal adenocarcinoma. Precursor lesions for other pancreatic neoplasms, however, remain obscure. We undertook this study to investigate the prevalence of PanIN in less common forms of pancreatic neoplasia to (1) assess whether the identification of PanIN might assist with the diagnosis of particular tumors and (2) possibly shed light on the etiology of these less common neoplasms.
Design: The surgical pathology files at the University of Virginia (UVa) from 7/1/91 to 8/1/04 were searched for all cases of pancreatic mucinous cystic neoplasms (MCNs), serous cystadenomas (SCs), solid pseudopapillary tumors (SPTs), acinar cell carcinomas (ACCs), and pancreatic endocrine neoplasms (PENs). All slides from these cases were reviewed and assessed for PanIN and sub-typed according to the current PanIN classification system.
Results: From 7/1/91 to 8/1/04 there were 14 MCNs, 12 SCs, 3 SPTs, 2 ACCs, and 23 PENs reviewed at UVa. Of the MCNs, 13 (93%) showed PanIN (grade 1a/b (6); grade 2 (6); grade 3 (1)). Of the SCs, 10 (83%) showed PanIN (grade 1a/b (2); grade 2 (7); grade 3 (1)). Of the SPTs, 2 (67%) showed PanIN (grade 1a/b (1); grade 2(1)). Of the ACCs, 2 (100%) showed PanIN (grade 1a/b (1); grade 3 (1)). Of the PENs, 16 (70%) showed PanIN (grade 1a/b (3); grade 2 (10); grade 3 (3)). No tumor type showed a statistically higher prevalence of PanIN.
Conclusions: Despite the fact that PanIN is considered a precursor lesion for the development of pancreatic ductal adenocarcinoma, it is found in a high percentage of pancreata that harbor other primary pancreatic neoplasms. When identified, it should, therefore, not be used to assist in the diagnosis of a specific pancreatic neoplasm. Whether it plays any role in the development of pancreatic neoplasms other than pancreatic ductal adenocarcinoma will require further investigation as no particular tumor type appears to be more associated with its presence.

1326 Reticulin, Copper, and CD34 Staining in the Diagnosis of Focal Nodular Hyperplasia

ZL Tabatabai, LD Ferrell. University of California San Francisco, San Francisco, CA.
Background: The diagnosis of focal nodular hyperplasia (FNH) and its differentiation from cirrhosis (cir) with features of chronic biliary tract disease (CBD) can be difficult, particularly in small biopsy samples. We undertook this study to assess the utility of reticulin (retic), copper, and CD34 staining in the diagnosis of FNH and its distinction from cirrhosis with features of CBD.
Design: Formalin-fixed, paraffin-embedded tissues of native livers from 10 cases of chronic obstructive biliary tract disease (5 each of primary biliary cirrhosis and primary sclerosing cholangitis), 10 cases of chronic hepatitis C cirrhosis (hepC cir), and 14 cases of FNH were stained with Retic, Copper, CD34, and H&E. The stains were examined and analyzed in a blinded fashion by two pathologists. The Retic stain was assessed for cell plate thickening and pseudoacinar pattern. The Copper stain was evaluated for staining of hepatocytes at periphery of nodules and the percentage of staining (0%, 1-25%, 25-50%, >50%), as well as associated cholestasis on the corresponding H&E. The CD34 stain was assessed for the presence or absence of periportal staining and periportal staining with intranodular extension.
Results: Cell plates were lined by Retic with at least focal thickening of 4-6 cells in 100% of all cases. A pseudoacinar pattern was also present at least focally in 100% of all cases. Copper staining was positive in 50%, 90%, and 100% of cases of FNH, hepC cir, and CBD cases, respectively. Of the positive cases, no FNH cases showed >25% staining, whereas 33% of hepC cir and 80% of CBD cases showed >25% staining. Of the cases that were positive, histologic cholestasis was absent in 86%, 11%, and 10% of FNH, hepC cir, and CBD cases, respectively. CD34 showed periportal staining with intraportal extension in 100%, 60%, and 0% of FNH, HepC cir, and CBD cases, respectively, and showed only periportal staining in 40% and 100% of HepC cir and CBD cases, respectively.

Conclusions: Thickened plates and pseudoacinar patterns may be seen on Retic stain in FNH, hepC cir, and CBD and may present a pitfall in diagnosis for well-differentiated hepatocellular carcinoma, particularly in small biopsy samples. Although copper staining may be seen in FNH, it is less commonly associated with cholestasis and shows less staining when compared to cirrhosis of CBD. CD34 staining pattern differences may be related to lack of remodeling of blood flow patterns due to the predominant portal-based damage in CBD and may be useful in distinguishing FNH from cirrhosis of CBD, but not from hepC cir.

1327 Correlation of Laboratory Values, Genotypes and Liver Histology in Hepatitis C

SS Talwalkar, L Zhang, J Snyder, C Maclein, MB Ray. Univ. of Louisville, Louisville, KY.
Background: More than one million new cases of hepatitis C virus (HCV) are reported annually. Among the 6 genotypes, the most common, type I, has been associated with the highest mortalities, chronicity and drug resistance. However, the relationship between liver function tests, genotypes and liver histology has not been studied. We try to evaluate if any corelation exists.
Design: 73 patients with a diagnosis of hepatitis C were included in the study. Liver functions tests, hepatitis C viral loads (VL) and genotypes (G) were obtained from the patient records. Mean liver enzymes (MLE): AST, ALT, Alk.PO4 were calculated. The cohort was then divided based on the G, which were compared with MLE (Table 1) followed by seperation into two groups based on VL. The liver biopsies, done simultaneously, from all these patients were graded and based on portal/lobular inflammation and stage of fibrosis, without any prior knowledge of the laboratory data.
Results: Of 73 cases, 64 were G I, 4 G II, 4 G III and 1 G IV. MLE for G I were significantly higher compared to other Gs (p<0.05) (Table 1). 35 of 73 had VL > 500,000 with mild to moderate elevation of mean AST (58-74 U/L) and ALT (70-82 U/L). 25 of these 35 cases had stage 3-4 fibrosis. 18 of the 25 cases with advanced fibrosis had VL > 500,000; their portal and lobular grade was 1-2 and mean AST and ALT were 63 ± 9.5 and 56 ± 10.2. All of these cases were genotype I (Table 2). Predominant lymphocytic infiltrates in the peri-portal areas, without piecemeal/bridging necrosis, with occasional lymphoid follicles were seen in 13 of these 18 patients which was distinctly absent in all the cases with VL < 500,000 and/or with stage 1-2 fibrosis
Conclusions: Type I is associated with higher VL and higher MLEs compared to other genotypes. VL > 500,000 increase the risk of progression to cirrhosis but do not significantly affect the liver functions. Follow-up of these patients with repeat biopsies and liver functions is required for accurate staging of disease progression and response to treatment.

Table 1:Correlation of HCV genotypes with Mean Liver Enzymes (MLEs)

Mean Liver Enzymes	Genotype I	Genotype II	Genotype III	Genotype IV
AST (10-47 U/L)	105	62	57	62
ALT (20-60 U/L)	89	37	43	45
Alk.PO4 (38-126 U/L)	115	80	87	99

Table 2: Correlation of Viral loads, MLEs and Histologic Grading

Viral Loads (IU/ml)	Mean AST	Mean ALT	Mean Alk.PO4	Stage 3-4 (n=25)
<500,000	90 ± 10.6	62 ± 8.6	105 ± 12.7	7
>500,000	63 ± 9.5	56 ± 10.2	83 ± 10.1	18

1328 α –Methylacyl Coenzyme A Racemase (P504S Antibody) Expression in Hepatocellular Carcinoma

K Taylor, D Lawson, G Cotsonis, A Fields, C Cohen. Emory University School of Medicine, Atlanta, GA; Emory University School of Public Health, Atlanta, GA.
Background: α -Methylacyl CoA racemase (AMACR-P504S) is a mitochondrial and peroxisomal enzyme involved in the metabolism of branched-chain fatty acid and bile acid intermediates. AMACR overexpression has been demonstrated in prostatic carcinoma and high grade prostatic intraepithelial neoplasia as well as in lung (14%), colon (45-70%), breast (3-15%), and endometrial (7%) carcinomas. Expression of AMACR may be of prognostic significance and therapeutic relevance. Because of its involvement in the metabolism of bile acid intermediates, we investigated AMACR expression in hepatocellular carcinoma (HCC), correlating results with prognostic factors and outcome.
Design: 89 HCC, using tissue microarray (TMA) technology, were immunostained for AMACR using rabbit monoclonal AMACR antibody (1/40) (Zeta Corp) and HRP labeled polymer conjugated secondary antibody (Envision, Dako Corp). Visually, expression was evaluated in the cytoplasm as intensity (0-3+) and percentage of positive cells scored on a 4-tiered system with less than 10%=negative, 11-25%=1, 26-50%=2, 51-75%=3, and 76-100%=4. The TMA was also evaluated by a computer-assisted imaging technique, the Automated Cellular Imaging System (ACIS) (San Juan Capistrano, CA), with results given as intensity, percentage, and score. Prognostic parameters and follow up were obtained with IRB approval.
Results: Frequency of AMACR expression in HCC was 72% (58/82). There was a statistically significant correlation between the visual and image cytometric quantitation (p value <0.0001). No statistical correlation was noted of AMACR expression (assessed visually and by automation), with prognostic parameters (nuclear grade, stage, histologic grade, mitotic rate, cirrhosis, tumor necrosis, metastatic disease), or outcome (local recurrence, overall and disease-free survival) with a mean follow up of 27.19 months (range 1.5-83 months). AMACR expression was noted in 21/51 (29%) normal/cirrhotic livers.
Conclusions: ACIS provides an easy, quick and objective means to quantitate AMACR overexpression in HCC and TMA's. Results correlate significantly with visual scoring. The 72% frequency of AMACR expression in HCC is comparable to the 81% reported. However, the lack of a statistically significant correlation between prognostic parameters and outcome suggests that, while AMACR is present in a high percentage of HCC, it does not appear to directly have an affect on outcome.

1329 Activated Caspase 3 Expression in Hepatocellular Carcinoma

K Taylor, D Lawson, G Cotsonis, A Fields, C Cohen. Emory University School of Medicine, Atlanta, GA; Emory University School of Public Health, Atlanta, GA.
Background: Caspase 3 is a downstream effector cysteine protease in the apoptotic pathway. It has previously been shown to be expressed in 52% of hepatocellular carcinoma (HCC) by immunohistochemistry. Nuclear survivin, present in 42% HCC, correlated with poor prognostic survival parameters. We studied Caspase 3 expression in HCC and related it to survivin overexpression, prognostic parameters, and outcome.
Design: Paraffin-embedded sections of 88 HCC specimens, using tissue (TMA) microarray technology, were immunostained for activated Caspase 3 after prior steam antigen retrieval using polyclonal activated Caspase 3 (1/100) (Cell Signaling, Beverly, MA) and HRP labeled polymer conjugated secondary antibody (Envision, Dako Corp, Carpinteria, CA). Tonsillar tissue was used as the positive control. Immunostaining was evaluated in the cytoplasm and nucleus of HCC and Kupffer cells, according to intensity (0-3+) and percentage of cells stained. Prognostic parameters and follow up were obtained with IRB approval. Mean follow up time was 27.19 months (range 1.5-83 months).
Results: Caspase 3 was present in 80 of 88 (91%) HCC, nuclear positive in 17 of 88 (19%) and cytoplasm positive in 39 of 88 (44%). In addition, Caspase was present in 55 of 88 (62%) Kupffer cells. In our previous study, survivin was present in 30 of 72 (42%) HCC and cytoplasmic survivin in 60 of 72 (83%). Nuclear Caspase 3 expression significantly correlated with cytoplasmic survivin expression (p=0.0306). Caspase 3 nuclear intensity significantly correlated with nuclear grade (p=0.0145) and tended to correlate with histologic grade (p=0.0769). Neither nuclear nor cytoplasmic Caspase expression correlated with clinicopathologic/prognostic parameters (gender, cirrhosis, histologic type, microvascular invasion, necrosis, stage, lymph node staging) or outcome (local recurrence, metastatic disease, overall or disease free survival).
Conclusions: Surprisingly, activated Caspase 3 correlates with poor prognostic parameters (survivin expression, histologic grade, nuclear grade). Unlike survivin, which suppresses apoptosis and is associated with worse outcome (short disease free survival), caspase 3 has no relation to outcome. As a reflection of apoptosis, Caspase 3 is expected to be associated with improved survival. This association is not confirmed in our data.

1330 Hepatic Angiomyolipomas Share a Similar Gene Expression Profile with Hepatic Stellate Cells

M Torbenson, R Kannangai, M Rojkind, J Sicklick, AM Diehl. Johns Hopkins, Baltimore, MD; George Washington University, Washington, DC; Duke University Medical Center, Durham, NC.
Background: Angiomyolipomas of the liver are rare neoplasms composed of large epithelioid cells with intermixed fat and blood vessels. Hepatic Angiomyolipomas have no clear normal-cell counterpart in the liver. However, angiomyolipomas have some similarities to liver stellate cells as both express neural crest derived markers such as HMB 45. Stellate cells in the liver can be quiescent, activated, or have a myofibroblastic phenotype depending on their state of activation.
Design: To further explore the similarities between hepatic AML and stellate cells, gene expression of a hepatic angiomyolipoma was studied by cDNA microarray analysis. Real time PCR was used to confirm gene expression. Quiescent and activated stellate cells were obtained from mice fed normal and half choline deficient diets. To examine stellate cells with a myofibroblastic phenotype, stellate cell lines CFSC-8B and CFSC-5H were used. Gene expression of known markers of activated stellate cells was compared between the angiomyolipoma, activated primary mouse stellate cells, and rat stellate cell lines. Next, 5 novel genes from the AML were selected because they were not previously known to be markers of stellate cells and expression was measured by real time PCR in the activated mouse stellate cells and in myofibroblastic stellate cell lines. Finally, expression levels of 10 novel genes were determined in 5 cirrhotic and 5 non-cirrhotic human livers.
Results: In the hepatic AML, gene expression microarray studies and subsequent confirmation by real time PCR demonstrated over expression of known markers of activated stellate cells including TGF-beta, smooth muscle actin, and collagen. In addition, 3/5 novel markers that were identified in the AML, including RRAD, CTSK, and NIBAN, were also found to be over expressed in activated (compared to quiescent or myofibroblastic) stellate cells. Of 10 novel genes over-expressed in AML, 9 were also over-expressed in cirrhotic human livers vs. non-cirrhotic livers.
Conclusions: Hepatic angiomyolipomas share a similar gene expression profile and may differentiate towards activated stellate cells.

1331 EGFR Is Phosphorylated at Ty845 in Hepatocellular Carcinoma

M Torbenson, R Kannangai, F Sahin. Johns Hopkins, Baltimore, MD.
Background: Epidermal growth factor receptor (EGFR) is frequently over-expressed in carcinomas from many organ systems including a significant proportion of hepatocellular carcinomas (HCC). Recent clinical trials of inhibitors of EGFR have been disappointing despite their clear efficacy in cell line and animal studies. The reasons for failure are unclear but may be partly related to our limited understanding of EGFR signaling in tumors. EGFR is known to be activated by phosphorylation at different tyrosine (Tyr) sites, leading to subsequent activation of different pathways. Cell line and animal studies have shown non-neoplastic hepatocytes signal primarily through STAT-3 and MAPK. Other benign tissues also signal through STAT-5 and AKT. Essentially nothing is known about EGFR signaling in primary HCC.
Design: We investigated the site of EGFR phosphorylation by western blot in 18 HCCs. Subsequent pathway activation was investigated by tissue arrays in 79 HCCs using antibodies that recognize phosphorylated (or activated) proteins.
Results: 14/18 HCCs had detectable EFGR by western blotting and 13/14 showed phosphorylation at Tyr845. Phosphorylation at Tyr845 is known to be mediated by

Src and to subsequently signal through STAT-1. In contrast, no EGFR phosphorylation was detected at Tyr998, Tyr1045, or Tyr1068, which signal through other pathways including STAT-3 and MAPK. Tissue array studies correlated well with these findings demonstrating no correlation between EFGR over expression (27% of cases) and STAT-3 nuclear positivity (15%), AKT (4%), MAPK (3%), or STAT-5 (3%) positivity, all p > 0.05.
Conclusions: In HCC, EGFR is phosphorylated at Tyr845 and signals primarily through the STAT-1 pathway, in contrast to normal and regenerating liver which signals primarily through the STAT-3 (stimulatory) and AKT (inhibitory) pathways

1332 The Role of Matrix Metalloproteinases and Their Inhibitors in the Metastatic Potential of Primary Hepatic Tumors

M Tretiakova, Z Gao, W Liu, C Gong, J Hart. University of Chicago, Chicago, IL; University of Calgary, Calgary, AB, Canada.
Background: The clinical behavior in terms of risk of local invasion, metastasis and mortality rate differ among cholangiocarcinoma, hepatocellular carcinoma arising from cirrhotic liver and hepatocellular carcinoma arising from non-cirrhotic liver. This study was designed to explore the expression of E-Cadherin (E-C), matrix metalloproteinases (MMPs), and the tissue inhibitors of metalloproteinase (TIMPs) in tumor and surrounding liver tissue in these groups.
Design: Tissue arrays were constructed utilizing tissues from 6 normal livers (NL), tumor and adjacent background non-neoplastic liver from 24 hepatocellular carcinomas arising from cirrhotic liver (HCC-C, CL), 13 hepatocellular carcinomas arising from non-cirrhotic liver (HCC-NC, NCL), and 6 cholangiocarcinoma (CCA, CCA-L). They were stained immunuohistochemically with antibodies against MMP1, MMP2, MMP3, MMP6, MMP7, MMP9, TIMP1, TIMP2, TIMP3 and E-C. The intensity of staining was scored manually by two pathologists as well as automatically using the Chromavision Automated Cellular Imaging System (ACIS).
Results:

	NL	CL	NCL	CCA-L	HCC-C	HCC-NC	CCA
MMP1	0.5	2.8	2.0	2.5	1.5	1.7	0.0
MMP2	2.5	2.7	2.9	3.0	2.4	2.6	0.2
MMP3	1.0	1.4	0.9	2.0	0.0	0.2	0.0
MMP6	3.0	2.4	2.9	1.5	2.1	2.8	1.5
MMP7	3.0	2.8	2.8	3.0	2.2	1.9	2.0
MMP9	2.7	2.1	2.3	2.5	1.5	1.2	1.7
E-C	2.3	0.9	1.5	1.0	1.2	2.5	1.8
TIMP1	3.0	1.6	2.7	2.5	1.4	2.1	1.2
TIMP2	1.5	0.9	0.6	1.0	0.1	0.1	0.7
TIMP3	2.3	1.2	1.8	0.0	0.0	0.0	0.0

Conclusions: In comparison to NCL and NL, the CL showed significant lower expression of E-C, TIMP1 and TIMP3. The CCA-L demonstrated a significantly higher level of MMP3, and lower level of E-C and TIMP3. The expression of these proteins represents a more favorable environment for tumor invasion and metastasis in HCC-C and CCA. HCC-NC has the highest E-Cadherin expression which is consistent with the very low risk of metastases in these tumors. In contrast, CCA has the highest level of TIMP2 expression, consistent with its high risk of metastasis.

1333 The Potential Effect of Liver Cell Steatosis and Apoptosis on the Progression of the Disease in Cases of Chronic Hepatitis B and C

AC Tsamandas, K Thomopoulos, G Theocharis, I Syrrokosta, D Dimitropoulou, T Petsas, C Karatza, C Gogos. Univ. of Patras, Greece.
Background: In cases of chronic hepatitis C, steatosis is an increasingly recognized factor influencing the progression of fibrosis. On the other hand, apoptosis has been linked to liver cell depletion and ensuing liver fibrosis. This study investigates the presence of liver cell steatosis and apoptosis and their relation with disease severity, in cases of chronic hepatitis B (HBV) and C (HCV).
Design: The study included 210 serial liver biopsies from 210 patients with HBV (n=101) and HCV (n=109). HAI score ranged from 3/18-13/18, and fibrosis stage from 1-6 (17HBV/32HCV). Steatosis (% of hepatocytes affected) was graded as follows: 0 (<5%), 1 (5%-30%), 2 (31%-70%), 3 (>70%). Liver tissues were evaluated for **I)** Bax, Bcl-2, TNFα, and caspase-3 mRNA (RT-PCR) and protein (Western blot), **II)** myofibroblasts activation (immunostain for αSMA) and **III)** apoptosis (TUNEL method). Results were expressed following morphometric analysis.
Results: In both groups (HBV+HCV), cases with steatosis had higher HAI score (p<0.001) and higher fibrosis stage (p<0.001) than those without steatosis. A direct correlation between liver cell apoptosis and steatosis was recorded (*HBV*: r =0.56, p<0.01, *HCV*: r =0.61, p<0.01). Cox analysis revealed that only hepatic steatosis was an independent predictor of apoptosis (OR, 1.33; CI, 1.06–1.66, p=0.015). Increased steatosis was associated with: **I)** decreased Bcl-2 mRNA levels (*HBV*: r =-0.29 p=0.03, *HCV*: r =-0.53 p=0.006), **II)** increased Bax/Bcl-2 mRNA and protein ratio (*HBV*: r=0.59 and 0.55 p<0.01, *HCV*: r=0.66 and 0.41 p<0.01 and p<0.05) and **III)** active caspase-3 (*HBV*: r=0.58, *HCV*: r=0.79-p<0.01). In the presence of steatosis, increasing apoptosis was associated with activation of myofibroblasts and advanced fibrosis (*HBV*: r =0.37 and r=0.41, p<0.05, *HCV*: r =0.45 and r=0.32, p<0.05). However the later correlations could not be demonstrated in the absence of steatosis, implying that superimposed steatosis makes liver with HBV or HCV more vulnerable to injury. In HCV cases, TNFα levels were correlated with active caspase-3 (r=0.64, p=0 .004).
Conclusions: This study shows that liver cell steatosis and apoptosis contribute to the disease progression in cases of chronic hepatitis B and C. Further research is warranted in order to clarify the molecular pathways responsible for the proapoptotic effect of steatosis and whether this increase in apoptosis contributes directly to fibrogenesis.

1334 Hepatic Progenitor Cell Activation in Human Chronic Liver Diseases and the Relation to Hepatocellular Carcinoma Development

AC Tsamandas, D Dimitropoulou, I Syrrokosta, T Kourelis, D Bonikos, C Gogos. Univ. of Patras, Greece.

Background: This study investigates the potential role of hepatic progenitor cells (HPC) activation and their relation to HCC future development in patients with chronic liver disease (CLD).
Design: The study included 52 liver biopsies obtained from 52 patients with CLD assigned in 2 groups (26 each). Group A: chronic hepatitis B (HBV-A1-n=9), chronic hepatitis C (HCV-A2-n=5), genetic hemochromatosis (GH-A3-n=5), and alcoholic liver disease (ALD-A4-n=7). These 26 patients developed HCC (confirmed by liver biopsy) in a 1-5 (median 3) year period after the time of the initial biopsy. None of these 26 patients had HCC at the first time. Group B: 26 biopsies: HBV (B1-n=9), HCV (B2-n=5), GH (B3-n=5) and ALD (B4-n=7). Patients of group B did not develop HCC at the same time period. Liver biopsies were matched for inflammation grade and fibrosis stage: subgroup A1 to B1, A2-B2, A3-B3, A4-B4. Paraffin sections were subjected to **a)** immunohistochemistry using anti-CK7, anti-LCA and anti-CD34 antibodies and **b)** in-situ hybridization for alpha fetoprotein mRNA detection. Cells with morphologic features of HPC (Roskams T et al Hepatology 39:1739, 2004) that were CK7+/AFP+ **and** LCA(-)/CD34(-) were scored. In addition, we performed gene analysis for AFPmRNA, on microdissected tissue samples removed from liver sections. Microdissection targets included areas with HPC expression, as this was described above. Microdissected tissue was amplified with PCR.
Results: The table lists the results for CK7 and AFPmRNA expression. Similar results were obtained from AFP gene analysis. The numbers of HPC were directly correlated with **i)** inflammation degree (p<0.01) and **ii)** fibrosis stage (p<0.01).

Table: CK7 and AFPmRNA expression in 52 CLD cases

		CK7	AFPmRNA
HBV	A1	59.2±2.3*	55.8±1.5¤
	B1	31.4±3.2*	29.3±1.1¤
HCV	A2	56.7±1.8**	50.3±1.4•
	B2	27.2±2.1**	24.3±1.7•
GH	A3	60.3±3.4ℵ	54.7±2.3•
	B3	32.1±1.8ℵ	29.3±1.1•
ALD	A4	64.2±4.1∂	61.3±1.5∞
	B4	34.3±3.2∂	31.2±2.4∞

*, **, ℵ, ∂, ¤, •, ∞:p<0.01

Conclusions: The study shows that HPC are frequently present in CLD cases and their numbers are directly related to the severity of the disease. The fact that biopsies of group A (cases that developed HCC in the future) showed significantly higher HPC numbers, supports the hypothesis that HPC proliferation is associated with increased risk for hepatocellular carcinoma. Further studies are needed to determine if the increased expression of HPC in CLD cases predicts the risk for future development of HCC in such cases.

1335 p62 as a Reliable Marker for Mallory Bodies in Nonalcoholic Steatohepatitis (NASH)

G-H Wang, A Mehrotra, JP Ong, ZM Younossi, Z Goodman. Armed Forces Institute of Pathology, Washington, DC; Inova Fairfax Hospital, Falls Church, VA.

Background: The finding of Mallory bodies (MB) in a liver biopsy is of great value in the diagnosis of NASH. The presence of MB and/or zone 3 pericellular fibrosis, although not essential for diagnosis, help to distinguish NASH from steatosis. MB often can be identified in H&E stains, but they may be difficult to find. In such cases immunostains may be helpful. Stains for cytokeratin and ubiquitin have been used for a number of years. Recently, p62, a ubiquitin binding protein and functional component in TNF-a and IL-1 signaling cascade, was found to be a major constituent of MB. The present study was to determine the value of immunostaining for p62 in recognition of MB and as an adjunct in the diagnosis of NASH.
Design: Liver biopsies from 103 patients undergoing bariatric surgery were obtained for studies of fatty liver disease. These were classified histologically as NASH (n=28) or steatosis (n=75) based on H&E and Masson trichrome stains. Another 17 cases previously diagnosed as NASH and 10 cases of steatosis from the files of AFIP were also included for a total of 130 biopsies – 45 NASH and 85 steatosis. Each biopsy was stained with anti-p62 (RDI) and anti-ubiquitin (Dako). The cases were then reclassified as NASH or steatosis with non-specific inflammation based on the identification of MB decorated by p62 and/or ubiquitin antibodies.
Results: Both ubiquitin and p62 decorated MB, when present. Small MB not identifiable by H&E could be visualized. There was also background staining of hepatocyte cytoplasm and nuclei that was more prevalent with ubiquitin than p62. Kupffer cells and portal lymphocytes were frequently decorated by p62. Fifteen of the 45 NASH biopsies (33%) had MB recognizable on H&E stain. Immunostaining for p62 detected MB in an additional 3, while 2 of the 3 were also positive for ubiquitin. All 3 had already been classified as NASH based on the presence of steatosis, ballooning degeneration and zone 3 pericellular fibrosis. None of the 85 cases of steatosis was reclassified as NASH after immunostaining.
Conclusions: Immunostaining for MB with antiserum to p62 generally has good agreement with results of H&E and ubiquitin, but p62 stained MB are often easier to recognized because ubiquitin tends to be diffusely present to a greater extent in the hepatocyte cytoplasm and nuclei. A stepwise approach H&E and trichrome stains, followed by immunostaining of the doubtful samples, may increase the diagnostic yield for NASH.

1336 Expression of BNIP3, a Pro-Apoptotic Protein, Is Suppressed during Hepatic Carcinogenesis

R Wilcox, K Tracy, B Dibling, M Tretiakova, K Macleod, J Hart. University of Chicago.

Background: Data from cell kinetic studies suggest that suppression of apoptosis may be more important than increased cell proliferation during the process of hepatic carcinogenesis. However, the molecular mechanisms involved in the anti-apoptotic process have not been elucidated. BNIP3 is a hypoxia-induced, pro-apoptotic member of the BCL-2 gene family that is strongly expressed during hepatic morphogenesis. The expression of BNIP3 protein was chosen because it is suppressed by retinoblastoma (Rb) protein.* We have shown in previous cDNA microarray studies that Rb expression is up-regulated during hepatic carcinogenesis (Am J Pathol 2003; 162:991-1000).
Design: Paraffin embedded samples from normal liver tissue (n=4), cirrhotic liver (n=11), macroregenerative nodules (n=56), hepatocellular carcinoma (n=52) and cholangiocarcinoma (n=2) were collected. Three tissue microarray blocks constructed with 1.5mm cores were subjected to immunohistochemical study using a 1:50 dilution of monoclonal mouse antibody to BNIP3 (Abcam) incubated for one hour at room temperature following antigen unmasking in citrate buffer. Intensity of reactivity was scored on a 0-3 scale.
Results: Granular cytoplasmic reactivity was present diffusely in hepatocytes. There was no reactivity in bile duct epithelium, endothelium, Kupffer cells, inflammatory cells or stroma. There was a stepwise decrease in staining intensity from normal (X = 2.5) and cirrhotic (X = 2.64) liver to macroregenerative nodule (X = 2.20) to hepatocellular carcinoma (X = 1.87). The difference in mean intensity of reactivity in cirrhotic samples (X=2.64 ± 0.51) versus hepatocellular carcinoma (X=1.87 ±0.66) was statistically significant (p<0.01). There was no reactivity in cholangiocarcinoma.
Conclusions: The incremental decrease in BNIP3 suggests that suppression of apoptosis is an important aspect in the development of hepatocellular carcinoma. Furthermore, the seemingly paradoxical finding of increased expression of Rb, a tumor suppressor gene, during hepatic carcinogenesis, might be explained by its role in suppressing BNIP3.
*Dibling BC, Tracy K, Spike BT, Van den Hout C, KF MacLeod. The RB tumor suppressor protects cells from hypoxia-induced necrosis through repression of BNip3. *In preparation* (2004).

1337 Can Alpha-Methylacyl-COA Racemase (AMACR/P504s) Be Utilized to Easily Differentiate Hepatocellular Carcinoma (HCC) from Cirrhosis?

SJ Wu, S Cotler, A Kajdacsy-Balla, G Guzman. Univ. of Illinois at Chicago, Chicago, IL.

Background: Immunohistochemistry with anti-AMACR/P504S was recently found to be useful for detecting adenocarcinoma of prostate, HCC, and renal cell carcinoma. AMACR was noted to be expressed in normal tissues from the nervous system, colon, kidney, breast, and pancreas, blood elements, and hepatocytes. Distinction between HCC and cirrhosis may be fraught with difficulty. Our aim was to determine whether AMACR (P504S) is differentially expressed in HCC and cirrhosis.
Design: The study material consisted of paraffin blocks of primary HCCs and adjacent cirrhotic liver from 20 patients who underwent liver transplantation. Immunohistochemical stain with Anti-AMACR was performed. Positive AMACR staining was defined as cytoplasmic or parabasal granular staining which can be easily observed at low power magnification (<100×). We compared the cytoplasmic distribution, pattern, and intensity of AMACR immunostain in HCC and the cirrhotic liver.
Results: 20 out of 20 HCC (100%) stained positively for AMACR. In 16 out of 20, the AMACR positivity comprised a majority of the tumor (75%), while the remaining 4 out of 20 showed ≤ 25% staining. Lack of staining with AMACR was observed in the clear cell type of HCC. Areas of fibrosis, bile duct epithelium, inflammatory cells, vessels, and fat were negative for AMACR stain. The staining features for HCC were distinctively different when compared to that seen in cirrhosis. Cytologically HCC displayed a strong clumpy granular diffuse or parabasal staining whereas the cirrhotic liver showed a weak diffuse finely granular cytoplasmic positivity. These patterns were easily discernible even at low power magnification. Architecturally, the pseudoglandular or trabecular types of HCC showed a characteristic pattern with AMACR immunostain. In these variants of HCC, the cluster or ribbon-like arrangement of cells imparted a "flower bouquet" distribution of the granules. In the cirrhotic liver, the narrow liver cell plates were highlighted by the negative staining of sinusoidal/fibrous components, allowing for immediate recognition of it's benign architecture. The dysplastic hepatocytes showed clumpy granular positivity, similar to that seen in malignant hepatocytes, although these lacked the architecture of HCC.
Conclusions: We conclude that AMACR (P504S) may be effectively utilized to separate HCC versus cirrhosis through a distinctive difference in the pattern of staining of benign and malignant hepatocytes.

1338 Arterialization of Central Zones in Alcoholic Cirrhosis

A Yabes, LD Ferrell. Univ of California, San Francisco, CA.

Background: Fibrosis of the centrizonal region is a typical feature of alcoholic cirrhosis. We have anecdotally noted small arteries within centrizonal scars that can lead to mistaken identification of scarred central zones as portal tracts, and so result in errors in diagnosis of the etiology of the cirrhosis. In this study, we aim to confirm the location and determine the frequency of this under-recognized finding.
Design: 17 explanted livers with history and histology of alcoholic cirrhosis were reviewed by H&E stain for centrizonal arteries. Cases showing this possible feature

were then studied with orcein to identify the dark, densely-stained elastic fibers of the original portal zones and to identify any copper deposits, CD34 to identify endothelium, and SMA and calponin to identify muscular components of the vessel walls.

Results: By H&E, 12 of the 17 livers (71%) showed arteries in probable centrizonal regions. Orcein identified original portal zones by the presence of darker, denser elastic fibers (3-4+ staining) in portal tract connective tissue in all cases. Interlobular bile ducts were noted near the hepatic arteries in the portal zones. In contrast, scarred centrizonal regions showed only 1-2+ orcein staining of small, delicate fibers. Ducts were not routinely present near the artery in the centrizonal region and no copper deposits were noted in adjacent hepatocytes to suggest ductopenic portal zones. However, ductular metaplasia was present typically near the edges of the scarred central zone. SMA and calponin demonstrated smooth muscle and CD34 confirmed an endothelial lining in these vessels. CD34 also showed sinusoidal staining of variable degrees, a phenomenon known as "capillarization", or "arterialization", of sinusoids. 50% of cases showed diffuse and patchy CD34 staining in nodules, while 42% had only patchy staining, and 8% had minimal staining. The most diffuse staining occurred in the smaller nodules.

Conclusions: Centrizonal arterialization is a common, but under-recognized, feature in alcoholic cirrhosis which may lead to errors in correctly identifying original portal tracts. The problem is compounded by bile ductular metaplasia adjacent to the centrizonal scars to further mimic portal zones. Orcein stain could be useful to differentiate portal zones from scars in this setting. We propose that our finding of increased sinusoidal capillarization of nodules supports the concept that this additional arterial blood flow from the centrizonal region contributes to the abnormal hemodynamics and metabolic function of the nodules of alcoholic cirrhosis.

1339 Tissue Transglutaminase II: A Biomarker of Pancreatic Ductal Adenocarcinoma

G-Y Yang, HP Dilworth, R Ashfaq, RH Hruban, A Maitra. Johns Hopkins Medical Institutions, Baltimore, MD; UT Southwestern Medical Center, Dallas, TX.

Background: Multiple global gene expression platforms (cDNA, oligonucleotide, and SAGE) have demonstrated that transglutaminase 2 (TGase) transcripts are overexpressed in infiltrating pancreatic ductal adenocarcinomas. Biochemically, TGase mediates the transamidation of a post-translational modification of proteins incorporated with a GTP-binding protein. TGase is known to be associated with cell migration, extracellular matrix assembly, cell apoptosis, and differentiation. TGase protein is only minimally expressed in non-neoplastic pancreatic epithelial cells, but the expression of TGase in infiltrating cancer and precursor lesions (Pancreatic Intraepithelial Neoplasia or PanIN) has never been systematically documented. In the present study, the expression pattern of TGase was systemically analyzed immunohistochemically in pancreatic adenocarcinoma and in PanIN lesions.

Design: Sixty-nine cases of pancreatic ductal adenocarcinoma with different grades of PanIN lesions were analyzed. Paraffin sections were labeled with a polyclonal antibody to TGase (Biomeda, CA) using heat-treated antigen retrieval and appropriate positive and negative controls. The avidin-biotin-peroxidase method was used in all labeling. Cases were scored as positive if cytoplasmic labeling was seen.

Results: 54 of 69 (78%) primary infiltrating pancreatic ductal adenocarcinoma exhibited positive labeling. 19 of 50 (38%) PanIN lesions showed positive labeling; while, all of 19 positive labeling PanIN lesions were PanIN-3. Furthermore, 19/24 (80%) PanIN-3 lesions were positive. PanIN-1b and -2 were all negative. In PanIN-3, the focal positive labeling was mainly identified in the lesions adjacent to invasive carcinoma. In addition, angiogenic endothelial cells surrounding carcinomas also exhibited positive labeling, but not in endothelial cells remote to tumor. All non-neoplastic pancreatic tissues were negative.

Conclusions: Transglutaminase II immunostaining profiles of non-neoplastic, PanIN and malignant pancreatic lesions appear to be significantly different, and suggest that TGase may be a malignant and an early invasive biomarker for pancreatic carcinoma and PanIN-3 lesions. In addition, this marker may aid in studying tumor angiogenesis. Our results suggest that transglutaminase II may prove to be a valuable ancillary test in the evaluation of pancreatic carcinogenesis.

1340 Correlation between Hereditary Hemochromatosis Genotypes and Phenotypes

MM Yearsley, I Aguilera, WL Frankel, TW Prior. The Ohio State University Medical Center, Columbus, OH.

Background: A small percentage of patients heterozygotes for the HFE gene accumulate sufficient hepatic iron to meet accepted criteria for expressed hereditary hemochromatosis. The aim of this study was to review the genotypes on the non-282 HFE homozygous patients evaluated for Hereditary Hemochromatosis at our molecular laboratory and to establish if there is any clinical and histological differences among genotypes.

Design: We retrospectively reviewed the clinical and laboratory information of 126 cases received for hereditary hemochromatosis screening at the molecular laboratory, without knowledge of the genotype. Molecular screening was performed by polymerase chain reaction. 11 liver biopsies were available for review. All biosies were staged and graded for chronic hepatitis according to Batts and Ludwig. Iron stains were reviewed and hepatocyte iron deposition was graded 0-4.

Results: Genotypes were present, as follows: H63D/wild type (wt), 23 cases (18.2%); C282Y/wt, 18 cases (14.2%); C282Y/H63D, 7 cases (5.5%); H63D/H63D, 2 cases (1.5%); C282Y/C282Y, 3 cases (2.3%) and wt/wt, 73 cases (57.9%). All groups were predominantly composed of caucasian males. Increased iron, transferrin and iron saturation, as well as increased AST were seen more frequently in H63D/wt and C282Y/C282Y than in the other groups. Higher stage of fibrosis was noted in the liver biopsies

of C282Y/C282Y, C282Y/wt and C282Y/H63D groups than in the H63D/wt group, except for one case with concomitant Alpha-1-antitrypsin deficiency. Inflammatory activity (grade) was similar in all groups. Iron deposition was seen in hepatocytes in all groups, and there were no significant differences.

Conclusions: Abnormal iron studies and liver function tests are seen in non-C282Y homozygous patients; however, biochemical differences cannot be used to separate the various genotype groups. Iron overload and liver fibrosis are seen in homozygotes as well as heterozygotes, but appear to be lower in the H63D/wt group. The role of exogenous factors such as Alpha-1-antitrypsin deficiency and alcohol consumption should be considered as genetic modifiers. Additional larger studies are recommended to further evaluate these findings.

Liver biopsy findings in genotype groups

Genotype	Number of cases	Average Grade	Average Stage	Average Hepatocyte iron
C282Y/wt	5	3.2	2.6	2
H63D/wt	4	1.5	1	1.5
C282Y/H63D	1	1	3	2
C282Y/C282Y	1	2	3	2

### 1341 Monocyte Recruitment and Modulation of Angiogenesis in Hepatocellular Carcinoma

LM Yerian, MW Lingen. Cleveland Clinic Foundation, Cleveland, OH; University of Chicago, Chicago, IL.

Background: Angiogenesis is a critical, early, and poorly understood event during hepatocellular carcinogenesis. Chronic inflammation is a predisposing factor for the development of hepatocellular carcinoma (HCC), and inflammation is known to incite angiogenesis in wound-healing and in tumors of other organs. The role of inflammation in angiogenesis in HCC is not known. Our previous studies demonstrated that CD68 positive macrophage populations are increased in dysplastic nodules (DN) and HCC when compared to adjacent cirrhotic liver in patients with chronic hepatitis C. We hypothesized that HCC can recruit monocytes which stimulate angiogenesis.

Design: Normal peripheral blood monocytes were isolated and cultured. Using a modified Boyden chamber, monocyte migration in response to serum-free conditioned media (CM) from a HCC cell line (PLC/PRF/5) was assessed. Monocytes were cultured in isolation and in a transwell co-culture system with the HCC cell line. CM was collected. Endothelial cell migration assays were performed with CM from monocytes and from monocytes co-cultured with the HCC cell line to assess for proteins that stimulate angiogenesis.

Results: Monocyte migration was stimulated in response to HCC CM.

Figure 1. HCC media induces monocyte migration
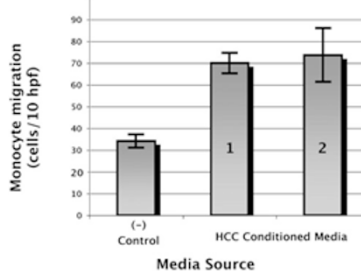
CM collected from pure monocyte cultures did not stimulate endothelial cell migration. CM collected from monocytes co-cultured with the HCC cell-line, on the other hand, strongly stimulated endothelial cell migration.

Figure 2. Co-cultured monocytes induce endothelial cell migration
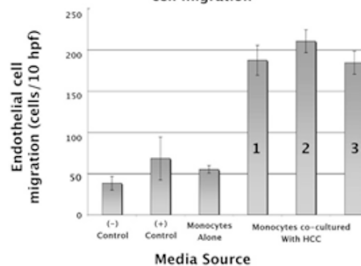
Conclusions: Proteins produced by HCC are capable of inducing migration of monocytes. These findings suggest that the prominent macrophage populations previously identified by immunohistochemical staining are recruited by the HCC. Furthermore, monocytes co-cultured with HCC produced potent stimulators of angiogenesis. Identification of the specific proteins responsible for stimulation of angiogenesis may provide a new therapeutic modality.

1342 Expression of MUC1, MUC2, MUC5AC and CDX2 in Carcinomas of the Gallbladder and Extrahepatic Bile Duct

H Zhang, O Basturk, M Othman, JD Cheng, S H. Khayyata, A Maitra, R Hruban, NV Adsay. Wayne State University, MI; The John Hopkins University, MD.

Background: Alteration or aberrant expression of MUC and CDX2 genes has been found in a variety of malignant neoplasms and is believed to play important roles in the tumorigenesis in these organs. The expression profile of these MUC genes in carcinomas of the gallbladder (GB) and extrahepatic bile ducts (EHB) is rarely studied, and no data has been published on CDX2 expression in these neoplasms.

Design: The expression profile of MUC1, MUC2, MUC5AC and CDX2 were investigated immunohistochemically in a total of 33 cases of carcinomas arising from GB (20 cases) or EHB (13 cases). Labeling of more than 10% of the cells was regarded as expression, as previously done in other studies.

Results: MUC1 was commonly expressed in both invasive (88%) and in-situ (60%) carcinoma of the GB and EHB. MUC5AC was expressed in approximately half of the cases (50% invasive and 67% in-situ carcinoma). In contrast, expression of MUC2 and CDX2 was rare in invasive carcinoma (2/26 for each), and slightly higher in the in-situ carcinoma (30 and 22%, respectively). These MUC2/CDX2 expressing in-situ lesions displayed intestinal morphology; however, the invasive carcinomas appeared to be ordinary carcinomas (without obvious intestinal features). No MUC1, MUC2, MUC5AC or CDX2 expression was detected in the 2 cases of small cell carcinoma.

Conclusions: MUC and CDX2 expression profiles in GB and EHB carcinomas are similar to that of pancreatic ductal adenocarcinoma, supporting the close kinship between these foregut carcinomas. MUC1, the so-called mammary type mucin, which has been implicated in tumor aggressiveness, is expressed in most cases, in keeping with the rapidly fatal outcome of these tumors. In contrast, MUC2 and CDX2, "key molecules in intestinal programming" with well-established tumor suppressor activity, are present in less than 10% of the cases. The unusual cases that express these two markers do not appear to be morphologically different. On the other hand, MUC2/CDX2 expression is slightly more common in the in-situ lesions, which typically exhibit intestinal morphology, in keeping with the intestinal metaplasia sometimes observed to precede biliary carcinomas.

1343 Histologic Evaluation of Steatohepatitis and Fibrosis (Stage) in Hepatitis C

L Zhang, S Talwalkar, C McClain, MB Ray. U of L, Louisville, KY.

Background: Hepatitis C virus is a major cause of chronic liver disease in the world. Although viral loads, genotypes and coinfections with hepatitis B or HIV play a critical role in chronicity, the relationship of steatohepatitis with increased liver fibrosis is not well understood. Recent studies demonstrated that superimposed non-alcoholic steatohepatitis (NASH) might influence fibrosis in hepatitis C(hep C). The present study evaluates degree of steatohepatitis in hep C patients with/without risk factors of NASH and correlates the results with the degree of liver fibrosis (stage).

Design: Liver biopsies from 75 patients (average age of 46.3) with hep C were included in the study. Twenty-one of 75 (28%) patients had single or multiple risk factors (diabetes mellitus, hyperlipidemia, obesity, metabolic syndrome or medications) for NASH. Three of the 21 (14.3%) had an additional history of alcoholism. Five histologic parameters were evaluated on a semi-quantitative scale and expressed in numerical scores (0-10): % of fatty change (0=0, 1-33=1, 34-67=2 and >67=3), lipogranulomas (absent=0, present=1), glycogenated nuclei (GN) (absent=0, occasional=1, several=2, many=3), ballooning degeneration (BD) of hepatocytes (absent=0, present=1) & Mallory bodies (absent=0, occasional=1, several=2). Fibrosis was scored (0-4) based on standard grading criteria.

Results: Of the 21 patients with risk factors for NASH, 16 (14+2, 76.2%) had higher steatohepatitis scores (>3) compared to 25 (21+4) patients with only hep C (25 of 54, 46.3%). Twelve of these 21 (59%) had higher stage of fibrosis (scores 3-4) versus only 19 of 54 (33%) without NASH (Table1). Overall, in both groups of patients, of the 5 histologic parameters only GN & BD are correlated directly with higher stage of fibrosis (scores 3-4) (P<0.05) (Table 2).

Conclusions: 1). Hep C patients with risk factors for NASH are more prone to develop cirrhosis. 2) GN and BD of hepatocytes in hep C are related to fibrogenesis independent of risk factors for NASH

Scoring of Steatohepatitis & Staging of Fibrosis in Hep C Patients +/- Risks for NASH

Steatohepatitis scores	Hep C (n=54)	Hep C + Risks for NASH(n=21)
0-2	29/54(53.7%)	5/21(23.8%)
3-5	21/54(38.9%)	14/21(66.7%)
6-10	4/54(7.4%)	2/21(9.5%)
Fibrosis 0-2	35/54(64.8%)	9/21(42.5%)
Fibrosis 3-4	19/54(33.2%)	12/21(58.5%)

Direct Correlation between GN & BD with Fibrosis

Scores	Stage 0-2	Stage 3-4
GN = 0 (n=35)	23/35(65.7%)	12/35(34.3%)
GN = 1(n=29)	17/29(58.6%)	12/29(41.4%)
GN = 2-3(n=11)	4/11(36.4%)	7/11(63.6%)
BD = 0 (n=61)	40/61(65.6%)	21/61(34.4%)
BD = 1(n=14)	4/14(28.5%)	10/14(71.4%)

Neuropathology

1344 Hemispheric Extraventricular Glioneurocytoma: A Clinicopathological Review with Immunohistochemical Profile

D El Demellawy, M Sur, J Provias. McMaster University, Hamilton, ON, Canada.

Background: Tumors expressing concomitant neuronal and glial differentiation in the same tumor cells are classified under the umbrella of glioneurocytic tumors (GNC). Tumors in this category are not recognized in the WHO classification 2000. There are no definite morphologic criteria to assess grade and prognosis of these tumors.

Design: We evaluated 10 cases of GNC diagnosed in our department from 2003-2004 with emphasis on clinico-pathological features, immunohistochemical profile and prognosis.

Results: The 10 cases of GNC showed a male to female ratio of 2:3 with age range of 23-59 years. The most common complaint was seizure. 9 cases had a tumor in the frontal lobe and one in the temporal lobe. 8 cases had hypodense, non-enhancing lesions, one of which showed a cystic component and one showed calcification. Two cases showed enhancing hyperintense lesions on T2 imaging. All cases were morphologically low grade tumors. Endovascular proliferation was present in 5 cases which was not interpreted as high grade and may be analogous to what is seen in pilocytic astrocytoma. 3 cases also showed ganglionic differentiation and 5 cases had minigemistocytic morphology. Immunohistochemically, all cases showed varying degrees of positivity for glial and neuronal markers in the same tumor cells. Synaptophysin and NSE were most sensitive in identifying neurocytic differentiation. Calretinin was a good marker for mature ganglion cells and cells showing early neuronal differentiation but not undifferentiated neurocytes. CD56 was a sensitive but non-specific marker for glial differentiation similar to S-100 and GFAP. Vimentin, CD57, neurofilament, alpha-synuclein and beta-tubulin were non-contributory.

Conclusions: GNC are a distinct entity and not rare tumors. From our study it shows that these tumors are composed of single cells with divergent glial and neurocytic differentiation. Immunohistochemistry is an essential tool to show co-expression of glial and neurocytic differentiation. Our findings show that synaptophysin and calretinin are the best markers for neurocytic differentiation and GFAP, S-100 and CD56 for glial differentiation. Some of the GNC may show atypical features such as increased mitosis and endovascular proliferation but prognostic and grading implications are still unclear. Specific morphologic criteria for grading and prognosis needs long term follow up of larger series of such tumors.

1345 Changes in the Internal Granular Cell Layer of the Cerebellum in Progressive Multifocal Leukoencephalopathy in 3 Patients with AIDS

H Ghaffar, RJ Hicks, LA Moral. Baystate Medical Center/Tufts University School of Medicine, Springfield, MA.

Background: Progressive multifocal leukoencephalopathy (PML) is a disease of the central nervous system caused by infection with JC polyomavirus (JCV) in immunosupressed hosts. Demyelination, viral inclusions and astrocyte pleomorphism are characteristically seen in PML, the former resulting from lytic JCV infection of oligodendrocytes and the latter reflecting restrictive JCV infection of astrocytes. Cellular alterations in the internal granular cell layer (IGCL) of the cerebellum have also been described, and productive infection of granule cell neurons by JCV was recently demonstrated in a HIV-positive patient with PML. Here we study the histopathologic changes in the cerebellar IGCL of 3 PML cases and assess the utility of in situ hybridization (ISH) and immunohistochemistry (IHC) in identifying JCV-infected cells at this level.

Design: Formalin-fixed tissue samples from 3 HIV-positive patients with neurologic dysfunction and imaging studies demonstrating demyelination in the cerebellum were assessed, 1 at autopsy and 2 by open biopsy. PML was confirmed histologically in all 3 cases. JCV ISH was performed using a hybridized biotinylated DNA probe. Single and double-label IHC were performed using antibodies specific for the VP-1 capsid of the JC virus and MAP-2.

Results: Morphologic, ISH and IHC changes of PML were present in the cerebellar white matter of all 3 cases. Marked neuronal loss in the IGCL of the cerebellum was featured in 2 cases. In 1 case, the cellularity of the IGCL was unaltered but enlarged ovoid nuclei with glassy chromatin were focally noted. There was no significant difference between JCV ISH and IHC staining of the IGCL. In 2 cases, JCV ISH and single-label IHC were positive in a moderate to high number of cells that appeared to represent granule cell neurons, and double-label IHC revealed VP-1 immunoreactivity in MAP-2 positive cells. In 1 case with pronounced neuronal loss, JCV ISH and IHC were negative in the IGCL.

Conclusions: Our results support that JCV can infect IGCL neurons and suggest that this may lead to neuronal loss. Enlarged ovoid nuclei with glassy chromatin in the IGCL are the result of JCV infection. ISH and double-label IHC are similarly useful in demonstrating infection of cerebellar granule cell neurons, including morphologically normal ones. In cases with severe neuronal depletion, enlarged nuclei with glassy chromatin are not found in the IGCL and ISH or IHC for JCV may be negative.

1346 Immunoreactivity for Claudin-1 Can Help Distinguish Meningiomas from Potential Histologic Mimics

HP Hahn, EA Bundock, JL Hornick. Brigham & Women's Hospital, Harvard Medical School, Boston, MA.

Background: The diversity of histologic variants of meningioma can occasionally make the distinction between meningiomas and other tumors difficult. Ultrastructural studies have shown that a distinguishing feature of meningothelial cells and meningiomas is the presence of cell adhesion complexes similar to epithelial desmosomes. Claudin-1 is a recently identified component of tight junctions, whose expression is believed to be important in maintaining the blood-brain barrier. The